9-1983

Modeling Erosion on Long Steep Slopes with Emphasis on the Rilling Process

Digital Object Identifier: https://doi.org/10.13023/kwrri.rr.148

Michael C. Hirschi
University of Kentucky

Billy J. Barfield
University of Kentucky

Ian D. Moore
University of Kentucky

Research Report No. 148

MODELING EROSION ON LONG STEEP SLOPES WITH EMPHASIS ON THE RILLING PROCESS

by

Michael C. Hirschi
Research Specialist

Billy J. Barfield
Professor
Principal Investigator

and

Ian D. Moore
Assistant Professor
Co-Principal Investigator

Department of Agricultural Engineering
University of Kentucky
Lexington, Kentucky

Project Number: B-072-KY (Completion Report)
Agreement Number: 14-34-0001-0224 (FY 1980)
Period of Project: October 1979-September 1983

Water Resources Research Institute
University of Kentucky
Lexington, Kentucky

The work upon which this report is based was supported in part by funds provided by the United States Department of the Interior, Washington, D.C., as authorized by the Water Research and Development Act of 1978. Public Law 95-467.

September 1983

DISCLAIMER

Contents of this report do not necessarily reflect the views and policies of the United States Department of the Interior, Washington, D.C., nor does mention of trade names or commercial products constitute their endorsement or recommendation for use by the United States government.

ABSTRACT

A model of soil erosion, known as KYERMO, is presented which emphasizes those processes which are important on steep slopes. Particular emphasis is placed on modeling rill development and geometry since this is the least understood process in erosion mechanics. The model requires an input rill pattern.

Rainfall inputs to the model require the use of breakpoint rainfall and kinetic energy. Surface storage is calculated based on random roughness data of Linden (1979). Infiltration is modeled by use of the two layer Green-Ampt-Mein-Larson model as proposed by Moore and Eigel (1981). Runoff is related to rainfall excess and surface storage by the exponential relationship of Tholin and Keifer (1960).

Erosion is modeled separately as rill and interrill erosion. Interrill erosion is modeled by evaluating raindrop splash and interrill transport capacity. Raindrop splash is predicted by using the Bubenzer and Jones (1971) equation which requires kinetic energy, rainfall intensity, and percent clay. Interrill transport capacity is modeled by either the Yalin (1963) or Yang (1973) equation depending on user preference. The rate of delivery of soil to a rill is a minimum of either the transport rate or splash rate.

Rill detachment capacity is calculated using the shear excess equation of Foster (1982). Transport capacity is calculated from either the Yalin (1963) or Yang (1973) depending on user preference. The distribution of detachment around the rill boundary is calculated as a function of the shear distribution. Shear is distributed by using a modification of the

area method of Lundgren and Jonsson (1964). Rill wall sloughing is calculated by using the procedure of Wu et al. (1982) which uses a critical wall angle. Flow routing in rills is calculated by using the kinematic routing procedures of Brakensiek (1966).

Data is presented showing that predictions made with model components are reasonable. A limited sensitivity analysis with the model shows that predictions follow the trends that one would expect.

DESCRIPTORS: Erosion*, Sediment Erosion*, Erosion Rates, Slope Stability, Model Studies, Slopes*; Slope Degradation, Rill Erosion*, Rain, Rills.

IDENTIFIERS: Long Steep Slopes; Rilling Process, Modeling Erosion.

ACKNOWLEDGEMENTS

The authors are grateful for the support and cooperation of Kentucky Utilities Company in providing space and support to conduct the research. The authors also gratefully acknowledge the support of Lloyd Dunn and Jim Wilson in developing instrumentation for measuring erosion on field plots. Appreciation is also expressed to Dr. Donald Colliver for assisting in the development of instrumentation systems.

TABLE OF CONTENTS

TABLE OF CONTENTS (Continued)

TABLE OF CONTENTS (Continued)

LIST OF TABLES

LIST OF FIGURES

LIST OF FIGURES (Continued)

LIST OF FIGURES (Continued)

CHAPTER 1 INTRODUCTION

Upland erosion, although heavily researched in the last 40 years, is still only a partially understood process. The key to understanding erosion is to understand the individual processes that cause erosion and the interactions between those processes.

The erosion model developed in this study utilized the basic conceptual model shown in Figure 1.1 and the moisture balance shown in Figure 1.2. Each block of the figures represents a given set of relationships that calculate the quantities involved. The framework was developed in this manner so that new relationships developed by subsequent research can simply be inserted into the model, causing flux rather than obsolescence.

The major emphasis in the development of this model was toward the rilling process. It was believed that a more thorough understanding of this process would allow erosion models to be more accurate and more applicable to special circumstances, such as steep and/or long slopes. A secondary emphasis was on the use of relationships with physical meaning and measureable parameters, thus allowing the user to examine the effects of steeper, longer, or otherwise different slopes and conditions from those in the data base.

Public awareness of the current and potential problems due to soil erosion will push government and industry to deal with the problem. It is hoped that this model can further the understanding of soil erosion and assist in its reduction.

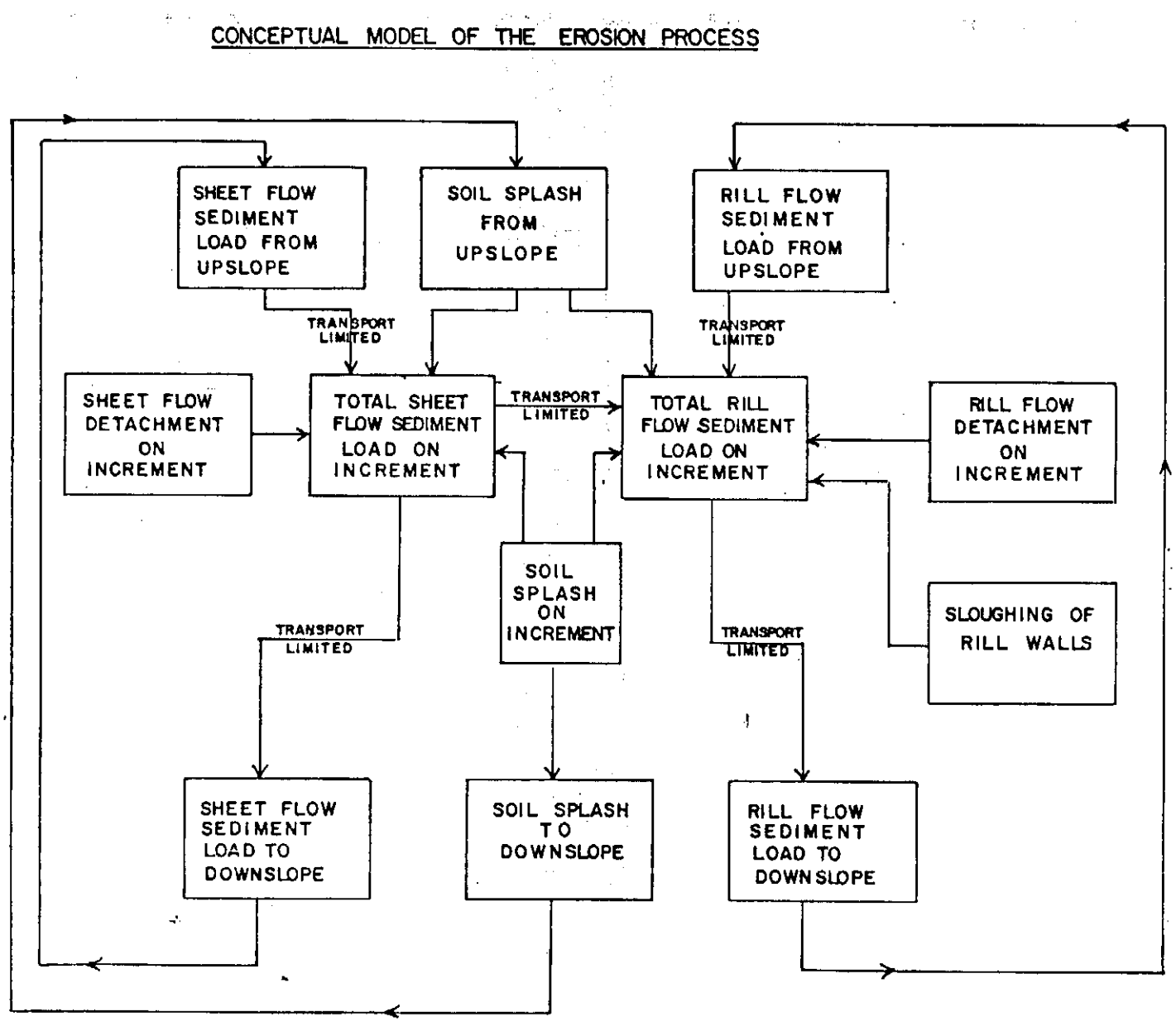

Figure 1.1 Conceptual model of the erosion process

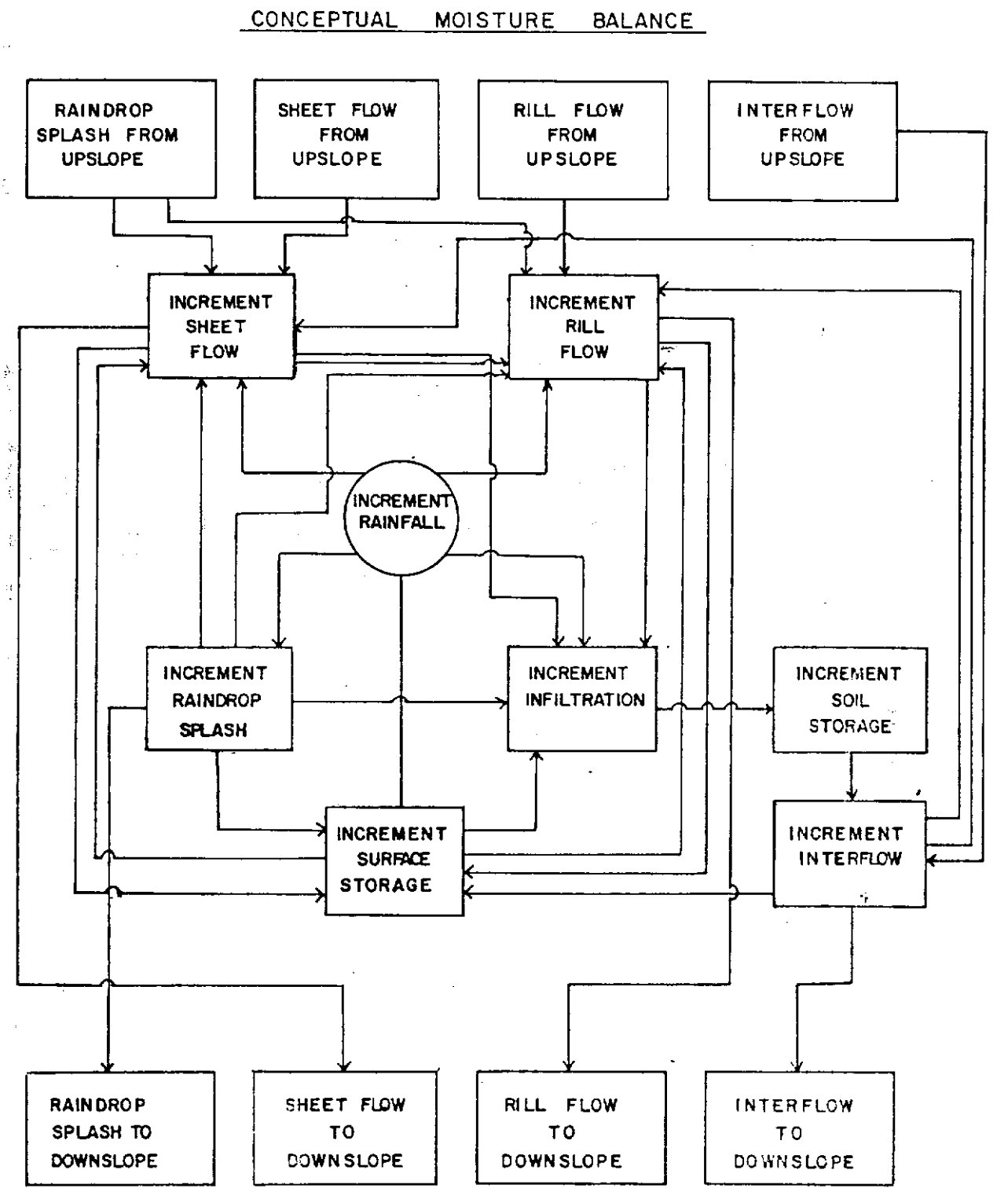

Figure 1.2 Conceptual moisture balance model

CHAPTER 2 RAINFALL CHARACTERISTICS

Water sources for upland erosion are primarily rainfall and snowmelt. Since the modeling effort in the report is limited to erosion resulting from rainfall, only rainfall characteristics will be discussed. Three major areas are discussed: 1) rainfall characteristics, 2) raindrop detachment of soil particles, and 3) raindrop splash transport of water and soil particles.

Characteristics Important to Erosion

Rainfall has certain characteristics which are important to the erosion process. These include: 1) rainfall intensity, 2) temporal and spatial distribution of rainfall intensity and volume, 3) raindrop size distribution at different intensities, and 4) kinetic energy of the raindrops during a storm. Because upland erosion is considered a "field-sized" phenomenon, the spatial variation in rainfall is not considered herein.

Natural rainfall is spatially and temporally highly variable. The major conditions specified to group rainstorms together are location, duration, and return interval. For erosion work, fairly short, rare events are of primary interest, i.e. a 5 year return interval storm with a duration of 1 hour, since most of the erosive energy occurs in these short duration storms. For example, in Lexington, Kentucky, the average annual erosivity index, a measure of the potential energy for erosion, is 178 whereas the erosivity index for a one year storm in Lexington is 30. One could thus conclude, since erosion is proportional to the erosivity index, that an annual storm will produce approximately 1/6 as much erosion as would be expected in a typical year. Typically, one observes that most of the erosive rainfall occurs in a few storms in a given year (Foster et al., 1982). The characteristic of these larger storms need to be known in order to model the erosion process.

Time Distribution of Rainfall Intensity

Rainfall intensity is an important parameter, not only because it affects runoff rates, but because other characteristics such as drop size and kinetic energy also vary with intensity. Rainfall intensities for natural storms are extremely variable, even within a given storm. Historical data on average intensities, durations, and return intervals are usually given in the form of depth-duration-frequency information charts developed from data by Hershfield (1961) and Frederick et al. (1977) and others. For example, rainfall volumes and intensities are given in Table 2.1 for Lexington, Kentucky, for return periods and durations typically of interest for erosion modeling. The rare events correspond to intensities of one in/hr or greater, which also correspond to storms with a high erosive potential.

The combination of storms of smaller return periods might also be of interest, since a low intensity storm occuring in a soil with a high soil moisture content might be more erosive than a higher intensity storm occurring on a dry soil. Soil effects will be discussed in detail in a later section.

Rainfall intensity is highly variable within a given storm, with the distribution of intensity varying widely from storm to storm. The characterization of this distribution is important since the timing of peak intensity can have a significant effect on runoff volume. A method frequently used to characterize storms for hydraulic design purposes is known as the Depth Duration Frequency (DDF) Method (Barfield et al., 1981). In this method, storms are characterized so that the intensities corresponding to any duration will have a consistent return period. An example of a DDF storm is given in Figure 2.1. The SCS type storms are simply derivatives of the DDF method.

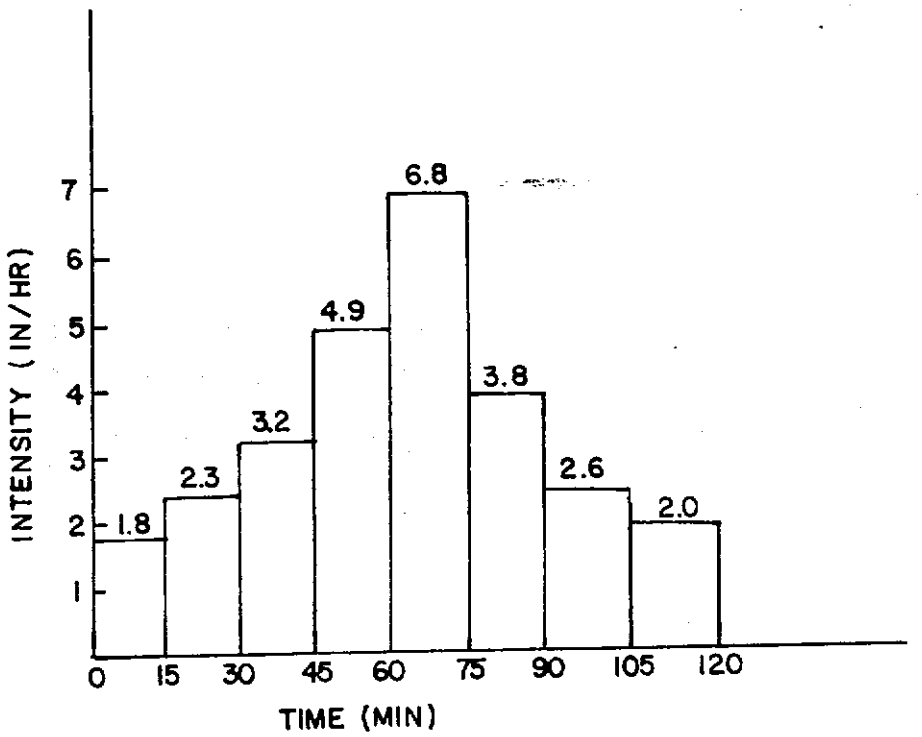

Figure 2.1 Synthetic 100 year, 2 hr storm pattern developed using DDF method for Lexington, KY

Table 2.1 Average Rainfall Intensity (in/hr) and Rainfall Volume (in) for Various Durations and Return Intervals for Lexington, Kentucky (From Barfield, Warner & Haan, 1981)

	Return Interval (Years)				
Duration	2	10	25	50	100
			Intensity		
15 min	3.3	4.7	5.4	6.2	6.8
30 min	2.3	3.3	3.9	4.3	4.9
45 min	1.8	2.6	3.0	3.4	3.8
60 min	1.5	2.3	2.5	2.8	3.2
120 min	0.9	1.3	1.4	1.6	1.8
			Volume		
15 min	0.8	1.2	1.4	1.6	1.7
30 min	1.2	1.7	2.0	2.2	2.5
45 min	1.4	2.0	2.3	2.6	2.9
60 min	1.5	2.3	2.5	2.8	3.2
120 min	1.8	2.6	2.8	3.2	3.6

The DDF and SCS Type storms are synthetic storms developed for design purposes only. The probability of obtaining an actual storm with this distribution is unknown. Huff (1967) presented procedures for evaluating the distribution of intensities within natural storms. In his analysis of storms in Illinois, separate distributions were developed for storms with maximum intensities in the first, second, third and fourth quarter of the storm as shown in Figure 2.2. The frequency of each quartile storm is shown in Table 2.2. Even with this division by quartiles, a wide range of rainfall volumes will result as shown by the range of cumulative percent of precipitation versus cumulative percent of storm. Rainfall intensity is equal to the slope of the curves in Figure 2.2, therefore, one can conclude that a wide range of intensities exists for a given time within a quartile storm. Thus, since the rainfall intensity distribution has a significant effect on runoff

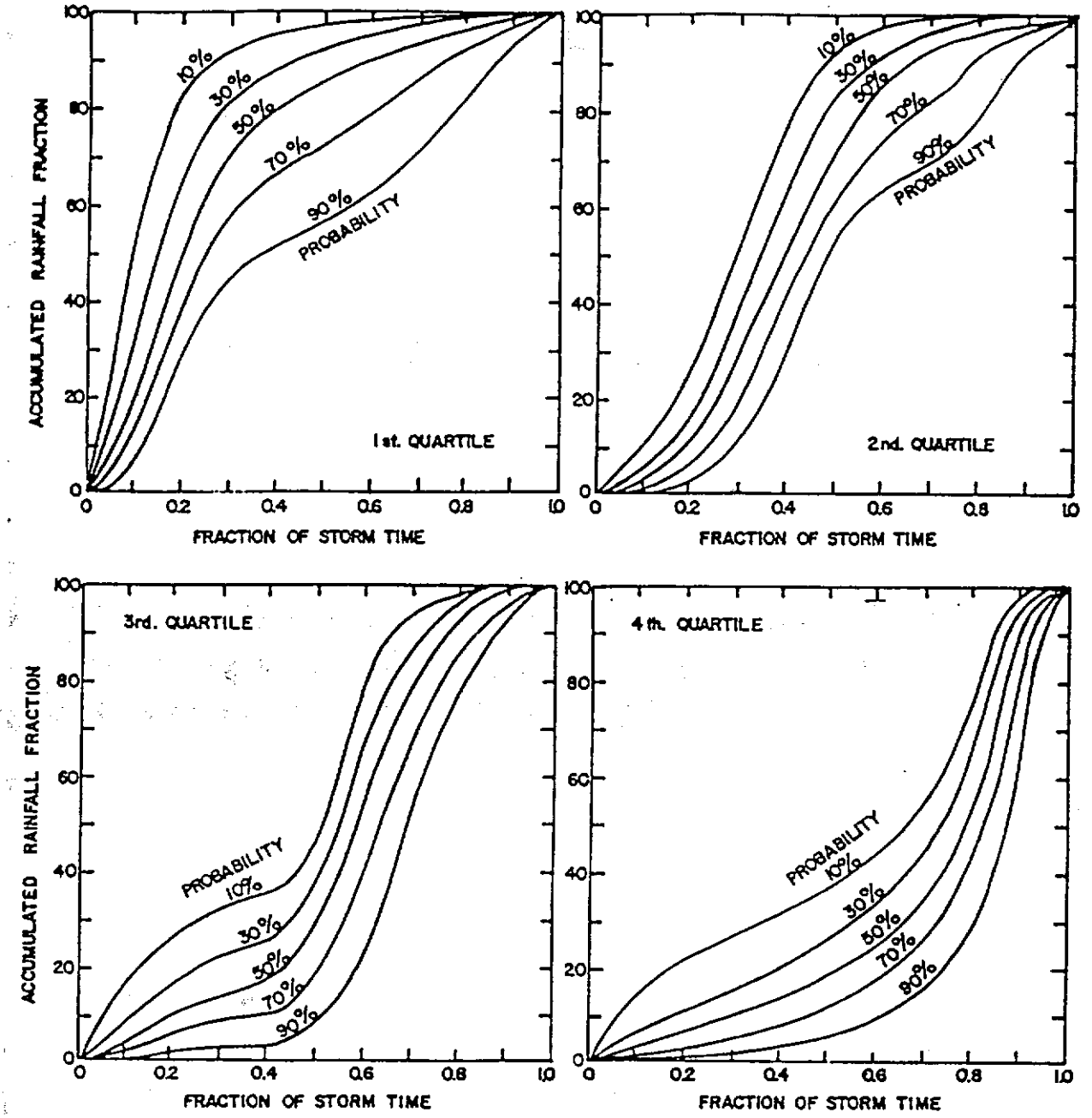

Figure 2.2 Huff's storm distributions (adapted from Huff, 1967)

Table 2.2 Frequency of Quartile Storms and Storm Duration within Each Quartile (Adapted from Huff, 1967)

Quartile	Frequency of Storms in Quartile (%)	Duration of Storms in Each Quartile (%) <12 hr	12-24 hr	>24 hr
First	20	45	29	26
Second	36	50	33	17
Third	19	35	42	23
Fourth	15	22	26	52
Percentage of Storms	100	42	33	25

and consequently on erosion it will be desirable for a physically based model of erosion to accept any arbitrary time distribution of intensity.

Rainfall Drop Size Distribution

Numerous studies have shown that the soil detachment by impact of raindrops is proportional to the kinetic energy and the intensity of rainfall (Free, 1960; Wischmeier and Smith, 1958; Foster et al., 1977b; Bubenzer and Jones 1971; and others). Kinetic energy for a storm depends strongly on the drop size distribution since kinetic energy for a given raindrop size is given by the product of mass times one half the square of the fall velocity and since both mass and fall velocity increase with increasing drop diameter. A knowledge of the drop size distribution is therefore important.

The characterization of drop size distribuitons has been performed in only limited areas of the U.S. Carter et al. (1974) presented raindrop characteristics for the south-central U.S. based on data collected at Baton Rouge Louisiana, (181 samples) and Holly Springs, Mississippi (315 samples). By using the flour pellet method of Bentley Carter et al. (1904) size was determined as a function of rainfall intensity or:

$$d_{50} = 1.63 + 1.33i - 0.33i^2 + 0.3i^3 \qquad (2.1)$$

where d_{50} is the median drop diameter in millimeters and i is the average

rainfall intensity in inches/hour. Carter et al. (1974) contend that a cyclical effect exists due to drop interactions. At medium intensities, drops break up due to air friction resulting in a lowered d_{50} value, but as the intensity increases further, drops collide and join, resulting in an elevated d_{50} value.

McGregor and Mutchler (1977) also evaluated the drop size distribution at Holly Springs, Mississippi, as a function of rainfall intensity. McGregor and Mutchler used a different form for their regression equation, but found the same general trend, or:

$$d_{50} = 2.76 + 11.40\ e^{-1.04i} - 13.16\ e^{-1.17i} \qquad (2.2)$$

where d_{50} is the median drop diameter in millimeters and i is the rainfall intensity in inches/hour.

The classic paper on drop size and intensity is that of Laws and Parsons (1943). Based on data from Washington, D.C., they proposed that:

$$d_{50} = 2.23\ i^{0.182} \qquad (2.3)$$

The intensities examined by Laws and Parsons were less than 4 in/hr so equation 2.3 is not necessarily applicable at higher intensities. A comparison of Equations 2.1, 2.2 and 2.3 is given in Figure 2.3.

The curves shown in Figure 2.3 can lead to the misleading conclusion that the average drop diameter is uniquely correlated to rainfall intensity. In fact other parameters come strongly into play. In Figure 2.4, the data base is shown that was used to develop the McGregor and Mutchler (1977) curves for Mississippi. From this data base, it is obvious that the range in average diameters for a given intensity is well over 100% of the average diameter. The implications of this variation will be discussed in a subsequent section.

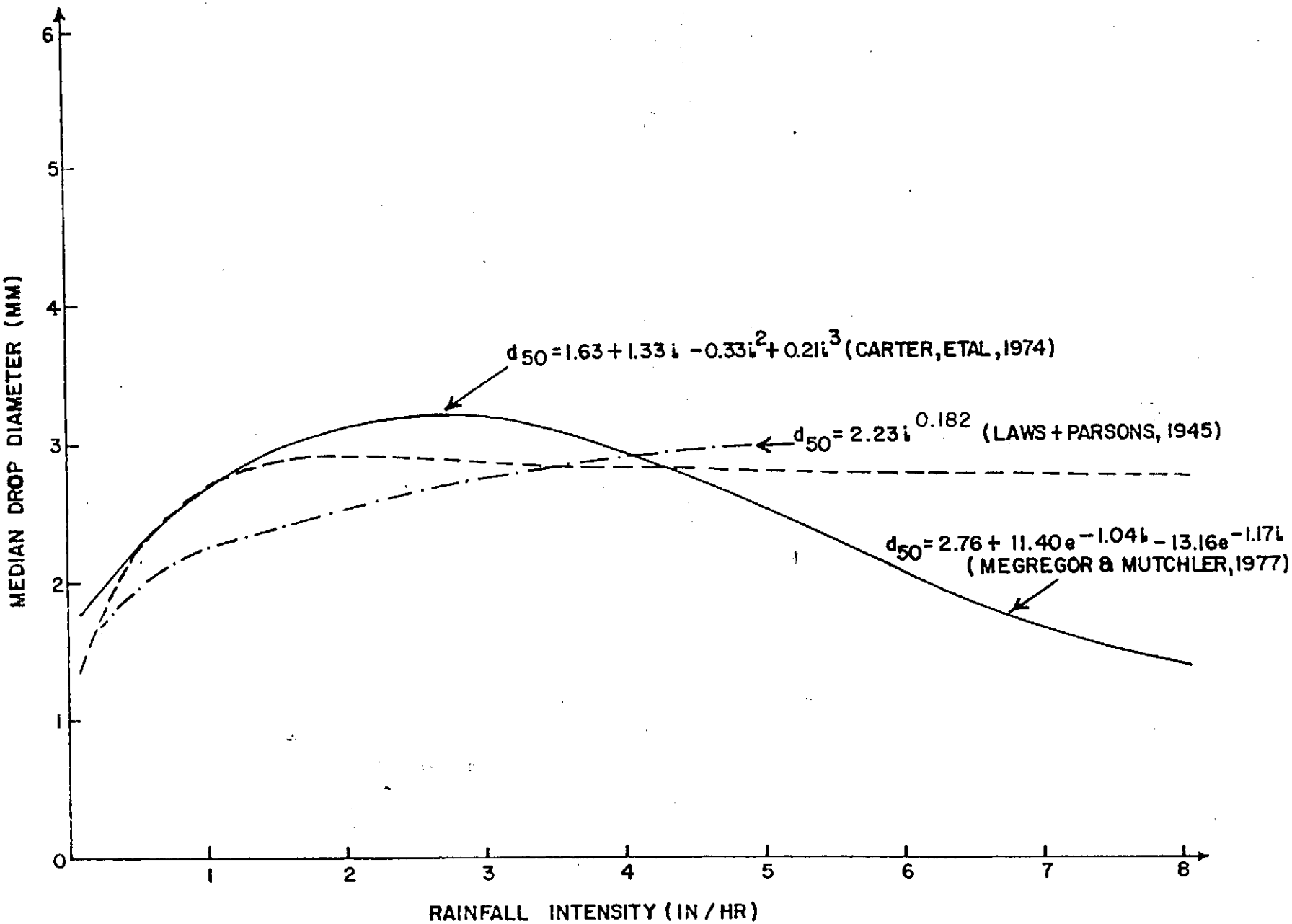

Figure 2.3 The relationship between rainfall intensity and average drop size from several researchers

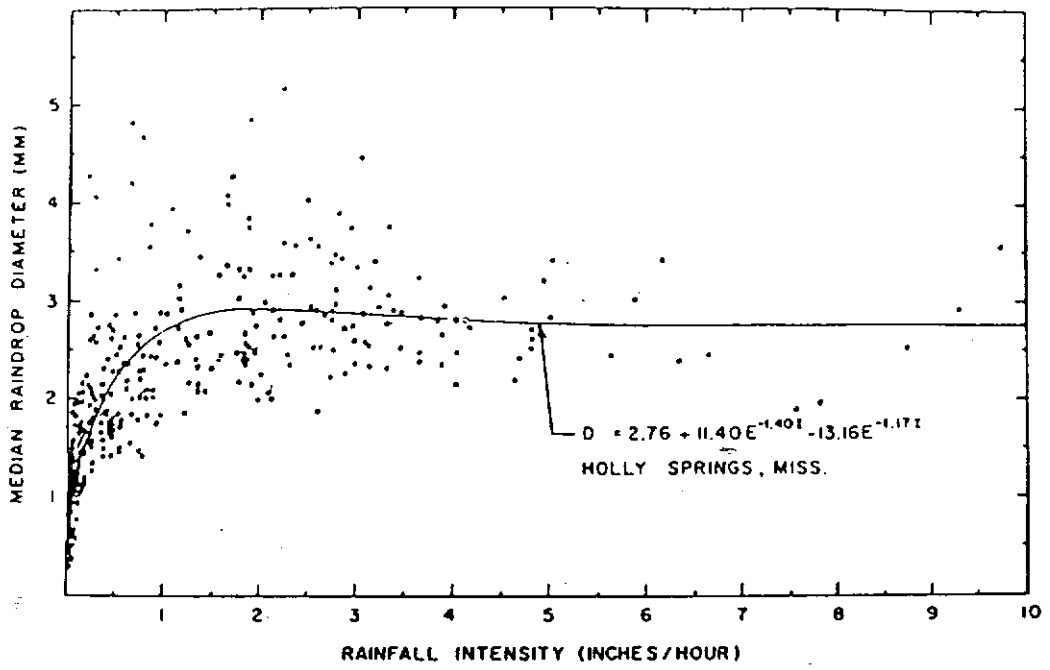

Figure 2.4 Relationship of median raindrop size and rainfall intensity computed from 315 raindrop samples collected in Holly Springs, Mississippi (after McGregor and Mutchler, 1977)

Knowledge of the median drop size is valuable, but a full drop size distribution for different intensities is needed in order to calculate kinetic energy. Data are available for a few intensities for Urbana, Illinois; Washington, D.C.; the South Central U.S.; and Pullman, Washington. Figure 2.5 is a plot of average data for Washington, D.C. at selected intensities from Laws and Parsons (1943). The Laws and Parsons data for Washington, D.C. show that average drop size increases with increasing intensity and that the drop sizes are approximately normally distributed. The Washington, D.C. data were taken at intensities of 6 in/hr and lower. At higher intensities, the drop size apparently decreases with intensity as shown by Carter et al. (1974), Hudson (1981) and others with the drop size distribution becoming skewed toward smaller drops.

Rainfall Kinetic Energy

A drop size distribution for rainfall can be converted to a kinetic energy per unit of rainfall under some simplifying assumptions, i.e.:

(1) Spherical shaped particles.

(2) Turbulent free air with zero vertical velocity.

(3) Particles have reached their steady state (terminal) velocity.

Using these assumptions, Laws (1941) and Gunn and Kinser (1949) developed predictors of the terminal velocity of raindrops falling in still air as shown in Figure 2.6. Using these results, McGregor and Mutchler (1977) and Carter et al. (1974) translated their drop size distributions into kinetic energy values and developed the average curves shown in Figure 2.7. These relationships show that the kinetic energy size increases with intensity up to an intensity of 1.5 to 2.0 inches per hour and then becomes nearly constant or decreases slightly.

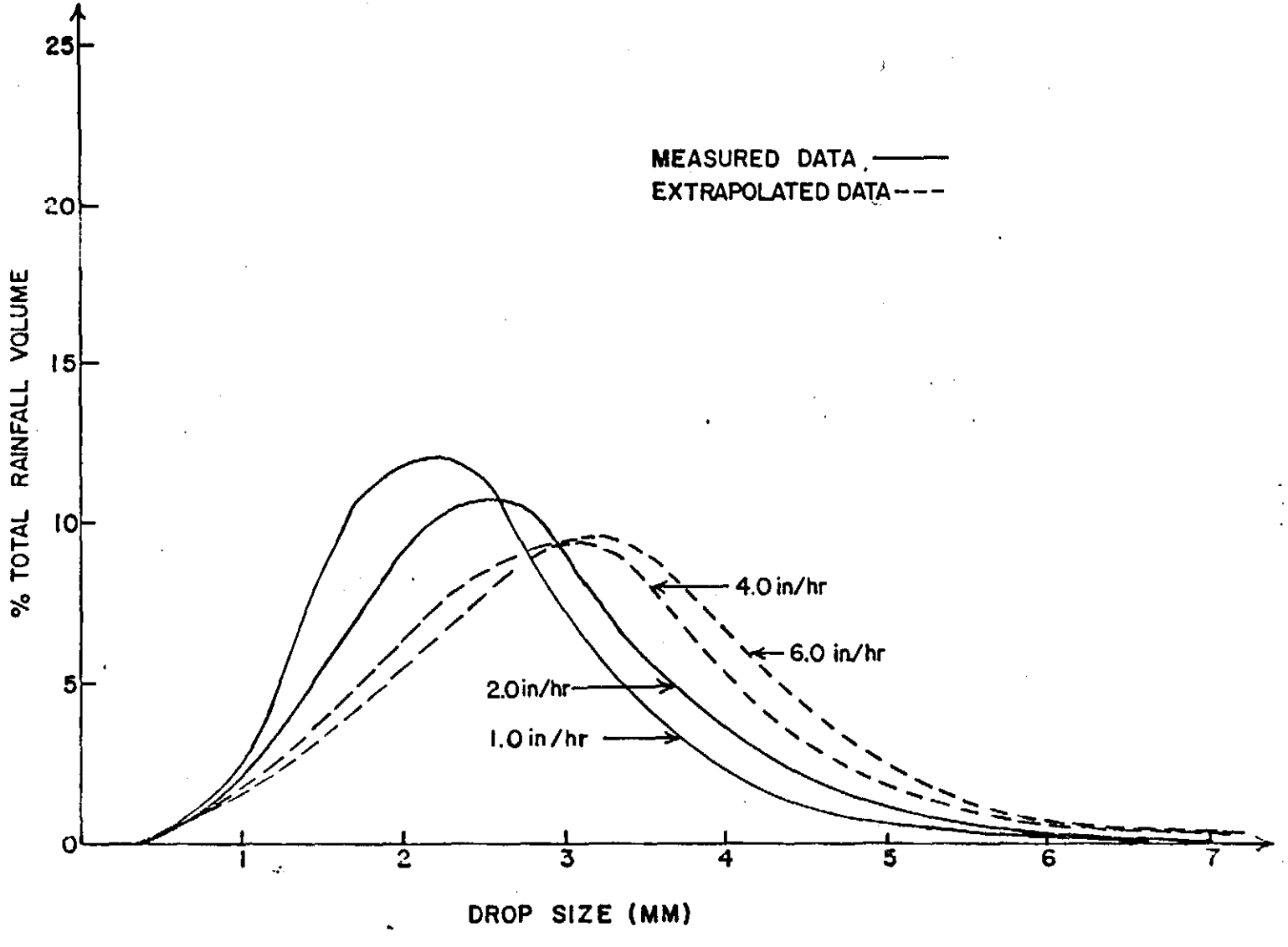

Figure 2.5 Raindrop distribution for Washington, D.C. from Laws and Parson (1943)

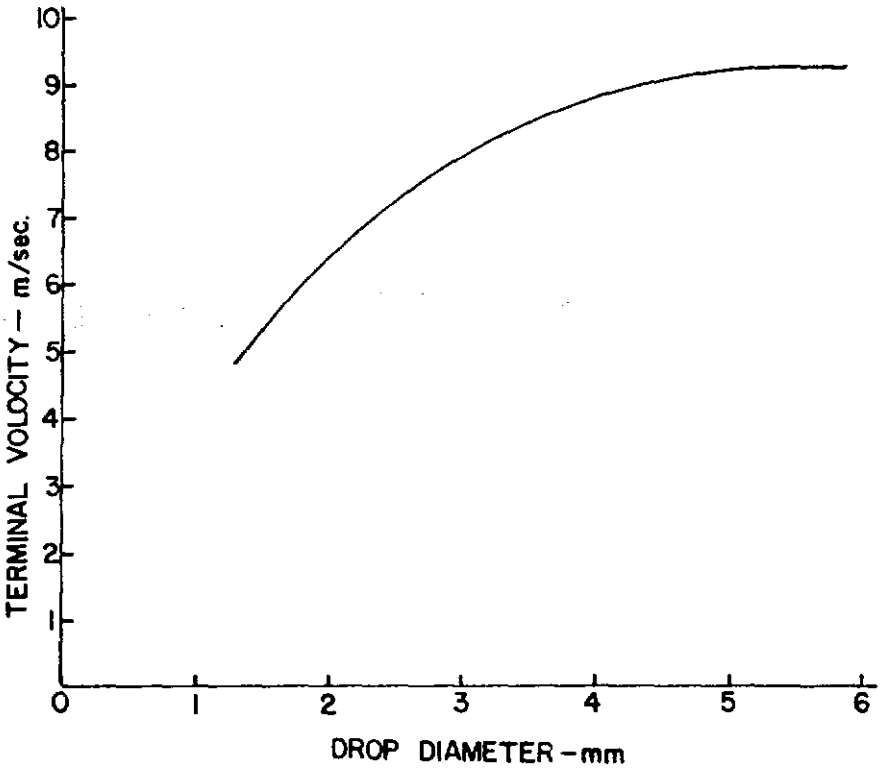

Figure 2.6 The terminal velocity of raindrops (data from Laws, 1941)

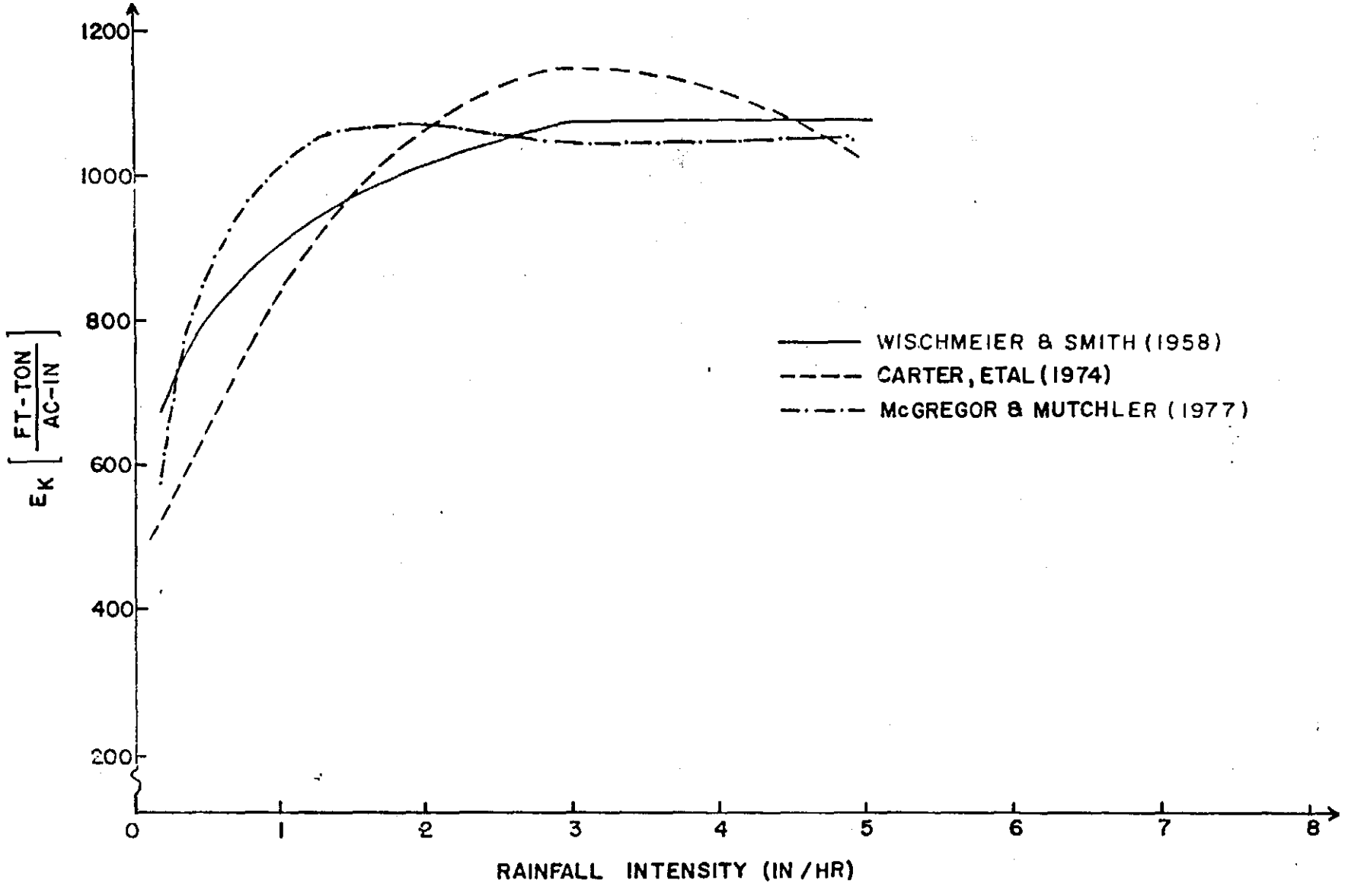

Figure 2.7 Kinetic energy of rainfall for various locations

Wischmeier and Smith (1958) developed an energy equation for the Washington, D.C., data of Laws and Parsons based on the drop size distribution data of Laws and Parsons (1943) and the drop terminal velocity data of Gunn and Kinzer (1949) and Laws (1941). Their equation is:

$$E_K = 916 + 331 \log_{10} i \qquad (2.4)$$

where E is the rainfall kinetic energy in foot-tons per acre-in and i is the rainfall intensity in inches per hour. According to Wischmeier and Smith, E_K should be held constant at the 3 in/hr value at intensities above 3 in/hr. Carter et al. (1974) proposed a best fit equation to data collected at Baton Rogue, Louisiana, and Holly Springs, Mississippi, as:

$$E_K = 429.2 + 534.0\ i - 122.5\ i^2 + 7.8\ i^3 \qquad (2.5)$$

where E_K is the rainfall kinetic energy in foot-tons per acre-in of rain and i is the rainfall intensity in inches per hour. McGregor and Mutchler (1977) developed the following relationship to "best fit" their data:

$$E_K = 1035 + 822\ e^{-1.22i} - 1564\ e^{-1.83i} \qquad (2.6)$$

The curves shown in Figure 2.7 can lead to the misleading conclusion that rainfall kinetic energy is uniquely related to the average storm intensity. While this may be true when averaged over many storms, it is certainly not true for a single storm. From the data base for the McGregor and Mutchler (1977) equation shown in Figure 2.8, one can obviously conclude that factors other than rainfall intensity affect kinetic energy. If an accurate model is to be developed on a single storm basis, it should have kinetic energy as an input, and not rainfall intensity.

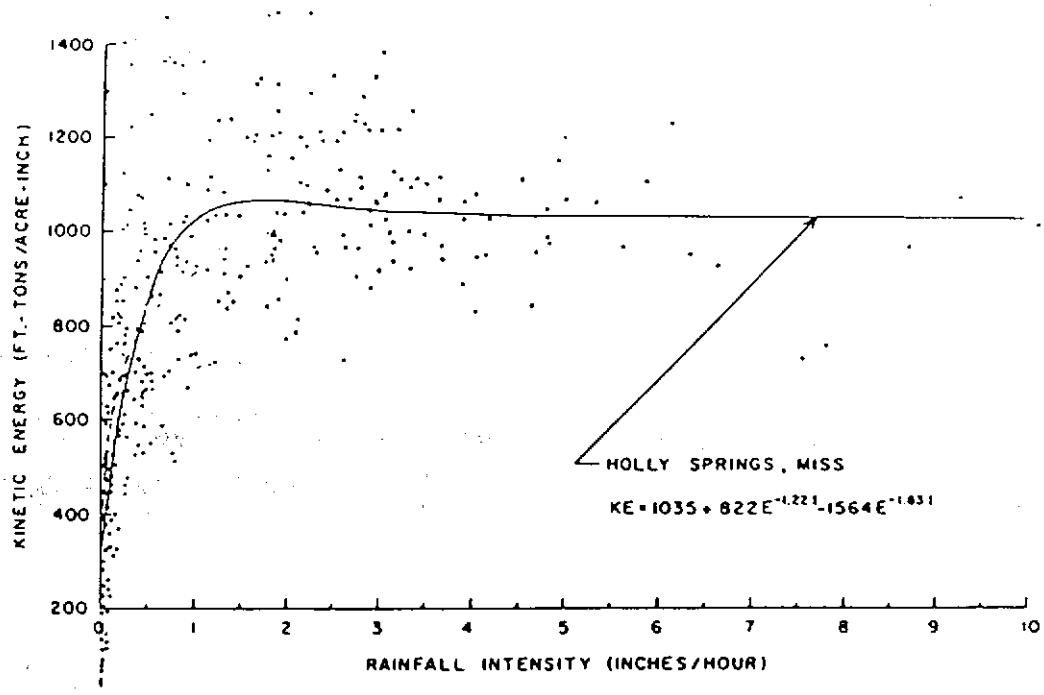

Figure 2.8 Relationship of kinetic energy and rainfall intensity computed from 315 raindrop samples collected at Holly Springs, Mississippi (after McGregor and Mutchler, 1977)

CHAPTER 3 RAINFALL ABSTRACTIONS

Introduction

Abstractions from rainfall include all losses between impact and runoff or

$$Q = P - A \tag{3.1}$$

where Q is runoff volume, P is rainfall volume and A is the total abstractions. Abstractions typically include infiltration, surface storage, evaporation, and interception. For this treatment, only infiltration and surface storage are considered important.

Surface Storage

Surface storage is the volume of water required to fill depressions and other storages before surface runoff begins. Actual measurements of surface storage are extremely difficult to make and consequently are practically nonexistent. Wright-McLaughlin Engineers (1969) in a special study of urban hydrology in the Denver, Colorado area, recommended the values shown in Table 3.1 for surface storage. Some investigators (Linsley et al., 1949) recognized that a watershed surface is made up of depressions of various sizes and that as some of the smaller depressions were filled, surface runoff could begin even though the larger depressions were still filling.

Gayle and Skaggs (1978) described two types of surface storage: macro-storage and micro-storage. They defined macro-storage as the "storage in larger depressional basins caused by topographic undulation of the land surface." Definable relationships between the volume, surface area, depth and contributing area of depressions were determined by Haan and Johnson (1967) for macro-depressions found in the Upper Midwest region of the United States,

Table 3.1 Typical Values for Surface Storage (from Wright-McLaughlin, 1969)

Land Cover	Surface Storage (inches)	Recommended Value
Impervious		
Large paved areas	0.05 - 0.15	0.10
Roofs - flat	0.10 - 0.30	0.10
Roofs - sloped	0.05 - 0.10	0.05
Pervious		
Lawn grass	0.10 - 0.50	0.30
Wooded area and open fields	0.20 - 0.60	0.40

which is an area characterized by depressional topography. Moore and Larson (1979), Campbell and Johnson (1975) and others have developed watershed models that consider the effects of macro-depressions on flood runoff, particularly in relation to drainage practices associated with these depressions. Micro-storage is the "storage in small pockets or depressions which may not be readily observed visually," or in other words, the depressional storage due to small scale variations in the surface relief, including those created by tillage. The depression properties identified by Linsley et al. (1949) apply just as well to micro-storage as they do to macro-storage.

Agricultural soils have varying degrees of potential micro-relief surface storage. This storage is highly dependent on the past history of the soil surface and is constantly being modified by the action of rain, wind, tillage and cultivation practices. Micro-relief storage is most important in soil conservation measures, particularly those associated with cultivation, tillage and irrigation practices. These measures aim at both increasing surface storage, which in turn makes more water available for infiltration and subsequent plant uptake, and controlling surface runoff so that minimal erosion occurs.

Seginer (1968a, 1968b, and 1971) developed a model to predict both the drainage pattern and the surface storage capacity of cultivated fields assuming that furrows and random roughness can be superimposed over the general topography of the field. He considered three topographical components which affect the drainage pattern on a local scale: (a) the slope of the fields, (b) the depth and direction of the furrows, and (c) the roughness of the field. Seginer's results show that surface storage capacity increases with the depth of furrows and roughness and decreases with increasing slope. Intuitively this is what one would expect.

Several researchers have developed equations for predicting surface storage. Monteith (1974) developed a regression equation for predicting surface storage from the roughness index. Davis (1961) proposed an equation for calculating the surface storage capacity in terms of the shape and slope of the furrows, and a "puddle factor," dependent somewhat on roughness and land-grading accuracy. Mitchell and Jones (1976) developed a depth-storage regression equation of the form:

$$S = a\, D^{b} \tag{3.2}$$

where S = storage depth (i.e., volume/unit area); D = depth above the lowest point on the soil surface; and a,b = equation parameters (fitted). This equation was used in a later study by Mitchell and Jones (1978) to describe the changes in micro-relief storage with empirical equations, using rainfall, surface hydrology, and soil parameters and their cross products as independent variables.

An exponential relationship has been proposed to predict the volume of surface storage as related to precipitation and infiltration (Tholin and

Keifer, 1960) or:

$$V_d = S_d(1 - e^{-K_d(P-F)}) \tag{3.3}$$

where V_d is the volume of water in surface storage, S_d is the available surface storage, P-F is the accumulated mass of surface storage supply (i.e., accumulated rainfall minus infiltration and other losses except surface storage), and K_d is a constant.

The value of the constant K_d can be estimated by noting that when P-F is near zero, all of the water goes to filling depressions so that $dV_d/d(P-F)$ is essentially one. Based on this reasoning, K_d is equal to $1/s_d$.

Neglecting interception losses, the rate at which water becomes available for surface runoff, σ, is $i-f-\phi$ where i is the precipitation rate, f is the infiltration rate and ϕ is equal to dV_d/dt. Based on these assumptions, the surface runoff supply rate becomes:

$$\sigma = (i - f)(1 - e^{-(P - F)/s_d}) \tag{3.4}$$

The ratio of surface runoff supply rate to the difference in the rainfall and infiltration rates can then be written as:

$$\sigma/(i - f) = 1 - e^{-(P - F)/s_d} \tag{3.5}$$

which ranges from 0, at the beginning of the precipitation event, (P - F = 0) to one when P>>F.

Equation 3.5 is plotted in Figure 3.1 for a turf area with an average overall s_d of 0.25 inches or a pavement with s_d equal to 0.0625 inches. The vertical dashed line in Figure 3.1 represents the surface runoff supply ratio if it is assumed that the overall average surface storage must be

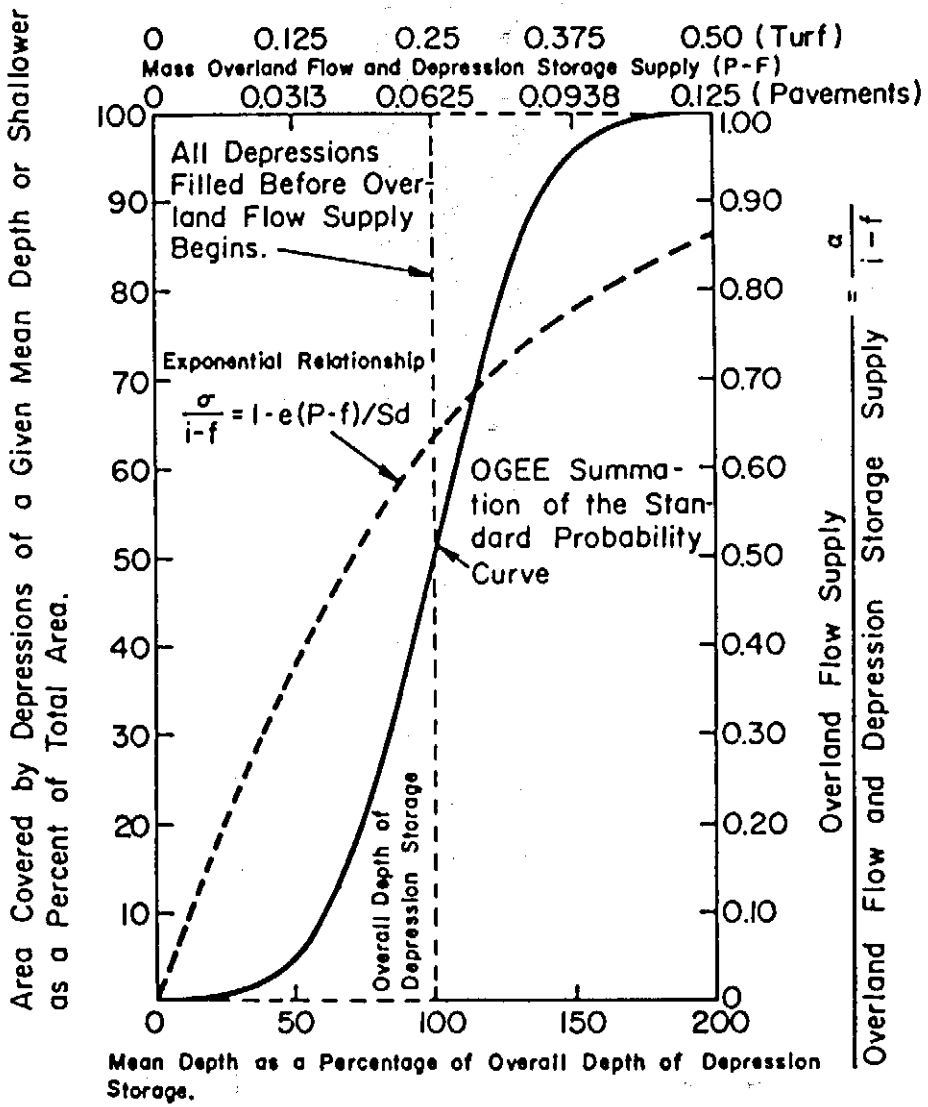

Figure 3.1 Exponential and normal functions relating runoff to surface storage (modified from Tholin and Keifer, 1959)

filled before any runoff can begin. This would be the case if the abstractions indicated in Table 3.1 were subtracted directly from the beginning of a storm before any water was allowed to become available for surface runoff.

Tholin and Keifer (1960) surmised that the actual situation might be between that given by Table 3.1 approach and that given by Equation 3.5. They found that the curve of the normal distribution, as shwow in Figure 3.1, fell within their desired range. This curve can be approximated using a normal distribution with a mean equal to s_d and a standard deviation of 1/3 s_d. The value of s_d might be estimated from the data in Table 3.1.

As might be expected, surface storage is of greater importance on flat surfaces than on steep surfaces. Viessman (1967) found the relationship shown in Figure 3.2 for 4 impervious drainage areas. The line in Figure 3.2 should be extrapolated with care. More likely the surface storage would decrease exponentially with slope reaching zero at very steep slopes.

If long duration rainfalls are being studied, the values of surface storage will not appreciably affect estimated runoff rates since the early part of the storm would fill this storage prior to the occurrence of the major runoff producing part of the rainfall. Note that the values in Table 3.1 do not include built-in storage in the form of detention basins.

The simulations shown in Figure 3.2 are for impervious areas that are typically relatively smooth. Agricultural lands are typically very non-uniform. A procedure is needed that can define surface storage as influenced by both slope and random roughness.

The effect of surface roughness and land slope on available surface storage is an important consideration for this study. Linden (1979) reported that available depression storage on an agricultural soil can be

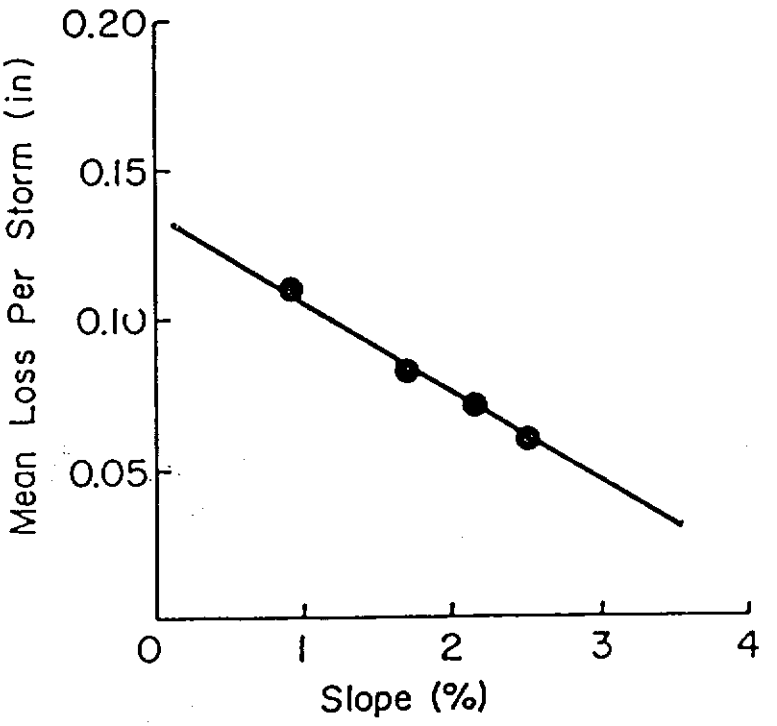

Figure 3.2 Depression-storage loss versus slope for four impervious drainage areas (after Warren Viessman, Jr., "A Linear Model for Synthesizing Hydrographs for Small Drainage Areas", paper presented at the Forty-eighth Annual Meeting of the American Geophysical Union, Washington, D.C., April 1967)

estimated from the land slope and a surface roughness index, termed random roughness (see Figure 3.3). Random roughness as defined by Allmaras et al. (1966) is calculated by measuring a grid of soil heights, performing a natural logrithmic transformation and then removing the row column and overall means. The upper and lower ten percent of these net values are eliminated and the standard error of the remaining corrected heights is defined as the random roughness. Random roughness values for various tillage practices (along with other roughness indices) were reported by Currance and Lovely (1970). They found that transforming the heights through a natural-logarithmic increased the variation of the soil heights over linear corrections although the final values of the indices for a given tillage treatment are very similar.

The discussions presented thus far have assumed that surface storage is a static phenomena. Moore et al. (1980) showed that rainfall energy caused a degradation of surface storage on base plots with much of the degradation occurring early in the storm. This degradation typically occurred over a short period of time after the start of rainfall. Moore et al. (1980) developed a complex algorithm that accurately predicted degradation under simulated rainfall conditions. Simple relationships have not been developed.

Infiltration

Introduction

Infiltration is the major rainfall abstraction for pervious areas. The process of infiltration and moisture distribution is highly complex, even for idealized soils. Moisture redistribution during a rainfall event, subsequent drying, and a following rainfall is shown in Figure 3.4a for an idealized soil in which vertical moisture movement is by diffusion process only. Even in this idealized state, prediction of moisture movement is difficult at best.

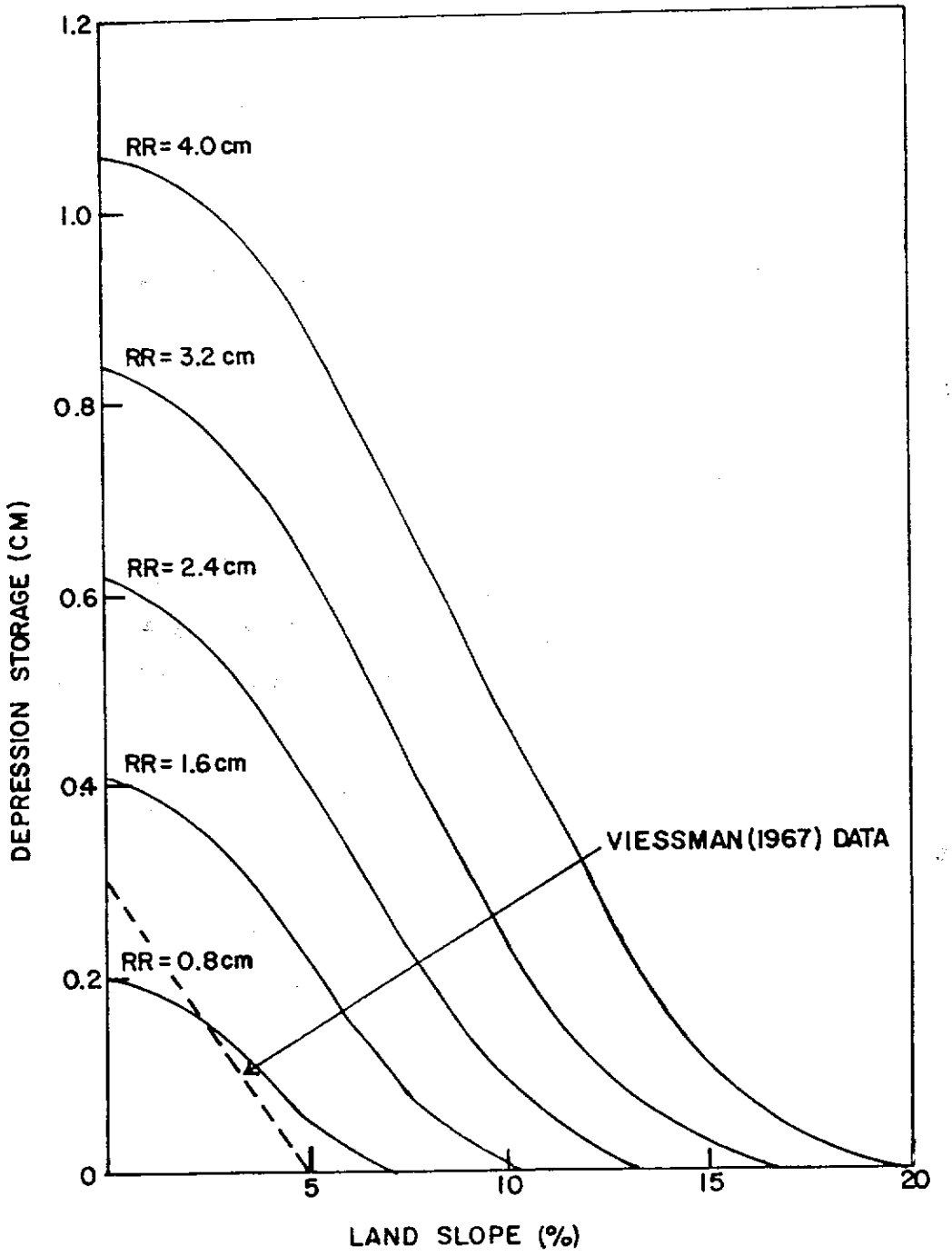

Figure 3.3 The upper limit to depression storage versus general land slope for five values of random roughness (RR) for agricultural soils (after Linden, 1979)

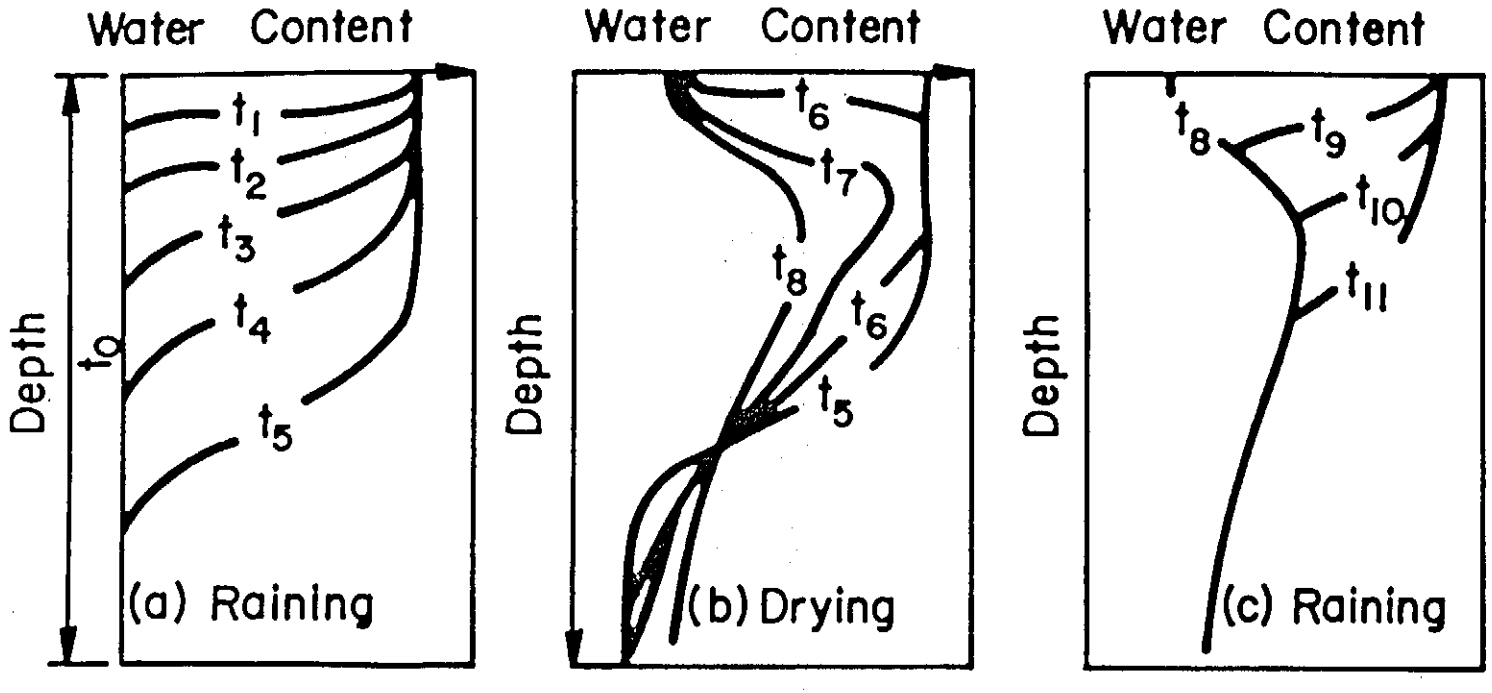

Figure 3.4 Moisture redistribution in a rainfall, drying, rainfall cycle

Infiltration is affected by soil physical parameters, vegetative cover, antecedent moisture conditions, rainfall intensity and the slope of the soil surface (Barfield et al., 1981). The effects of these factors have beeb summarized as (Barfield et al., 1981 and Biggerstaff and Moore, 1983):

(1) Rainfall Intensity Effects. High rainfall intensities typically have larger drop sizes which disperse aggregates on the surface resulting in a washing of clay particles into soil capillaries and formation of a surface seal. This surface seal decreases infiltration. In addition, the breakup of aggregates and clods results in a smoothing of the surface and decrease in surface storage. The net effect is an increase in infiltration.

(2) Antecedent Moisture Effects. An increase in antecedent moisture results in a decrease in infiltration as a result of lowered capillary suction in the pores.

(3) Vegetative Cover and Mulches. An increase in surface cover absorbs rainfall energy and reduces the breakup of aggregates and formation of surface seals. In addition, covers on the surface intercept moisture which is subsequently evaporated. Decaying roots of sour vegetation cover tend to increase the porosity of soil and form channels or macropores for water movement deep into the soil. The vegetative roughness decreases the runoff velocity and increases the opportunity time for infiltration. The net effect of surface cover is to increase infiltration rates.

(4) Soil Physical Parameter Techniques. Soil physical parameters which effect infiltration can be grouped into hydraulic properties, size distribution and shear strength. Hydraulic properties affect the rate at which water can flow through the soil for a given hydraulic gradient. The size distribution gives the fraction of fines and hence the potential for surface sealing. The shear strength determines the resistance to dispersion by the shearing forces of falling raindrops.

(5) Slope Effects. As slope increases, the overland flow velocity increases, surface storage decreases, and hence the opportunity time for infiltration decreases.

If one is to adequately model infiltration, equations should be developed which include these influences.

Mathematical models of the infiltration process have been categorized as (1) empirically derived equations and (2) theoretically derived equations. A summary of each of these approaches is given.

Empirically Derived Equations

Horton's Equation

Because of the difficulty of using theoretically based equations to describe the infiltration process, a great many empirical relationships have been proposed. Horton (1940) found that an equation of the form:

$$f(t) = f_c + (f_o - f_c)\, e^{-kt} \qquad (3.6)$$

fit experimentally decreasing infiltration rates as a function of time. In this equation f(t) is the infiltration rate for any time, t; f_c and f_o are the final and initial infiltration rates and k is a measure of the rate of decrease in the infiltration rate. Horton's equation requires knowledge of 3 soil parameters, f_o, f_c, and k. A plot of Equation 3.6 for a particular set

of these parameters is shown in Figure 3.5. There are no general tables or guidelines for selecting values for the three parameters of Horton's equation. Occasionally, locally derived data are used.

Spatially nonhomogeneous soils require spatial variability in the parameter values. Furthermore, if the soil is nonhomogeneous with depth, i.e. a restricting layer will often exist at some shallow depth, the infiltration rate will not smoothly decrease as in Figure 3.5, but will have a rather abrupt drop in infiltration rate as the wetting front reaches the restricting layer. Another difficulty with the Horton equation is that it makes infiltration rate a function of time and does not account for variations in rainfall intensity. The equation has no provision for a recovery of infiltration capacity during periods of low or no rainfall.

Holtan's Equation

Holtan (1961) proposed an empirical infiltration equation based on the concept that the infiltration rate is proportional to the unfilled capacity

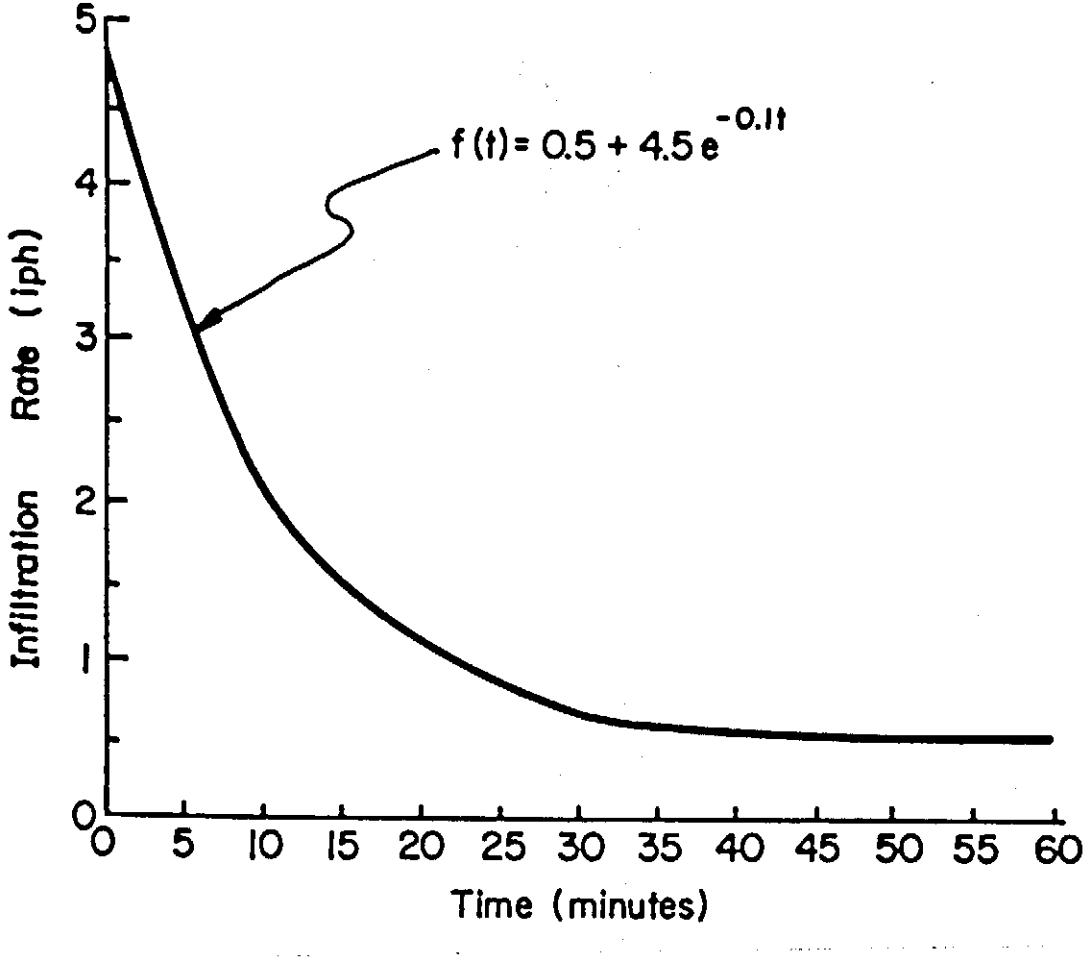

Figure 3.5 Example infiltration curve of Horton (1940)

of the soil to hold water. The Holtan model for infiltration is

$$f = a F_p^n + f_c \tag{3.7}$$

where f is the infiltration rate, f_c is the final infiltration rate, F_p is the unfilled capacity of the soil to store water and a and n are constants. The exponent n has been found to be about 1.4 for many soils. The value of F_p ranges from a maximum of the available water capacity (AWC) to zero. The AWC is a measure of the ability of a soil to store water. Values for AWC are given for many soils in an Agricultural Research Service publication (U.S. Department of Agriculture, 1968).

The Holtan model for infiltration has the advantage over the Horton model in that it has a somewhat physical basis and can describe infiltration and the recovery of infiltration capacity during periods of low or no rainfall. Huggins and Monke (1967) modified Holtan's model to give:

$$f = f_c + a (S - F)/T_p^b \tag{3.8}$$

where f is the infiltration rate, f_c is the final steady infiltration rate, F is the accumulated infiltration, S is the potential storage in the "control" zone and T_p is the void volume of a "control" zone. Rates are expressed in in/hr or cm/hr and volumes are expressed in inches or centimeters. The "control" depth is defined as the depth to the impeding layer. An evaluation of the 'a', 'b', and 'f_c' values for four soils reported in the study by Huggins and Monke indicated that 'a' was 5-6 times 'f_c' and 'b' could be approximated by 0.65. By substituting these results into equation 3.8 we obtain:

$$f = f_c + 5f_c [(S - F)/T_p]^{0.65} \tag{3.9}$$

where a in equation 3.8 is approximated as $5f_c$.

If the steady state infiltration rate is approximated by the field saturated hydraulic conductivity K_{fs}, and total saturation is assumed to occur at a field saturated moisture content, θ_{fs}, then equation 3.9 can be written as:

$$f = K_{fs} + 5K_{fs}\left[((\theta_{fs} - \theta_i)\, L - F)/L\theta_{fs}\right]^{0.65} \qquad (3.10)$$

where θ_i is the initial moisture content and L is the depth of the control zone. The modified model is thus written in terms of soil physical characteristics.

Φ Index

Over the years many other empirical models have been proposed. Because of the general lack of values for model parameters and the nonhomogeneity of soils, these models have not been widely applied in storm water management. Instead what typically has been done is to define a steady infiltration loss rate from the rainfall rate to get the effective rainfall rate. Sometimes a two-stage constant loss rate is used. For example, for the Denver region, Wright-McLaughlin Engineers (1969) proposed that the following constant infiltration loss rates be used in the absence of measured data.

Storm Frequency	First 1/2 Hour	Remainder
2 to 5-yr.	1 iph	1/2 iph
10 to 100 yr.	1/2 iph	1/2 iph

Wright-McLaughlin Engineers (1969) went on to urge that each area being considered be field tested for infiltration rates and that the measured values be used in preference to those shown in the above table. Often the constant infiltration rate is termed the Φ index.

SCS Curve Number Method

The Soil Conservation Service (SCS) (1973) combines infiltration losses with surface storage and estimates rainfall excess or equivalently the run-off volume by the relationship:

$$Q = \frac{(P - 0.2)^2}{P + 0.8S} \quad P > 0.2S \tag{3.11}$$

where Q is the accumulated runoff volume or rainfall excess in inches, P is the accumulated precipitation in inches and S is a parameter given by:

$$S = \frac{1000}{CN} - 10 \tag{3.12}$$

where CN is known as a curve number. It should be noted that equation 3.11 is a runoff equation and not an infiltration equation. Using it as an infiltration equation can lead to erroneous results. The SCS method is widely used to predict runoff on a watershed basis.

Theoretical Models

Theoretical models considered in this section are those based on Darcy's Law and the equation of continuity. These equations require the input of measured soil water characteristics that are related to the infiltration process via the capillary pressure headwater content relationship (soil water characteristic), unsaturated hydraulic conductivity - water content relationship, total porosity, and initial water content. Often the unsaturated hydraulic conductivity - water content relationship is derived from the saturated hydraulic conductivity and the soil water characteristic curves. An example of these relationships is the Campbell equation (Campbell, 1974).

Richard's Equation and Philip's Equation

Darcy's Law for vertical flow through a porous media can be written as

$$V_z = -K(\phi) \frac{\partial h}{\partial z} \tag{3.13}$$

where V_z is the vertical velocity, $K(\phi)$ is the hydraulic conductivity which is a function of capillary potential ϕ, and total energy head. Writing h as:

$$h = \phi + z \tag{3.14}$$

where ϕ is the capillary potential, we have:

$$V_z = -K(\theta) \frac{\partial \phi}{\partial z} - KL(\phi) \tag{3.15}$$

Using equation 3.15 in the continuity equation one obtains the well known Richard's equation. In its simplest one-dimensional form it is written as:

$$\frac{\partial \theta}{\partial t} = \frac{\partial[K(\theta)\frac{\partial h}{\partial z}]}{\partial z} - \frac{\partial (K(\theta))}{\partial z} \tag{3.16}$$

where θ is the water content (vol/vol), t is time, K is the unsaturated hydraulic conductivity ($K = K(\theta)$], h is the pressure head (capillary potential), and z is the distance below the soil surface (i.e., positive in the downward direction). A more convenient form of Equation 3.16 for numerical solution, written in terms of the specific water capacity C ($C = \frac{\partial \theta}{\partial h}$) is:

$$C \frac{\partial h}{\partial t} = \frac{\partial[K(h) \frac{\partial h}{\partial z}]}{\partial z} - \frac{\partial[K(\theta)]}{\partial z} \tag{3.17}$$

or in diffusivity form as:

$$\frac{\partial \theta}{\partial t} = \frac{\partial[D(\theta) \frac{\partial \theta}{\partial z}]}{\partial z} - \frac{\partial[K(\theta)]}{\partial z} \tag{3.18}$$

where

$$D(\theta) = K(\phi) \frac{\partial \theta}{\partial \phi} \tag{3.19}$$

Equations 3.17 and 3.18 are idealized formulations that neglect air movement, compression of air in the profile and non-Darcian flow in macropores.

Philip (1957, part 2) developed an analytic soultion to equation 3.18 assuming a homogeneous, semi-infinite medium with a uniform initial moisture content and ponded conditions at the surface, i.e., non-limiting rainfall. By using the first term of an infinite series solution, Philips proposed that:

$$f = \frac{St^{-1/2}}{2} + A \tag{3.20}$$

or

$$F = St^{1/2} + At \tag{3.21}$$

where f is infiltration rate, S is the sorptivity, F is cumulative infiltration and A is a parameter dependent on physical properties of the soil. The equation is not accurate at large t due to the assumption that gravity is small compared to capillarity (Morel-Seytoux, 1973). The constants A and S have been evaluated theoretically (Whisler and Bower, 1970) but the procedures are complex. Typically, values are obtained by optimizing the fit of equation 3.21 to experimental data.

Green-Ampt Model

Green and Ampt (1911) developed an infiltration equation for ponded surfaces based on Darcy's law and a capillary-tube analogy. This equation can be written as:

$$f = K_s[(L + S)/L] \tag{3.22}$$

where S is the capillary suction at the wetting front, L is the depth to the wetting front from the surface, K_s is the saturated hydraulic conductivity of the wetted zone, and f is the infiltration rate.

Mein and Larson (1971, 1973) modified the Green-Ampt model to account for infiltration prior to surface ponding. Their two-stage infiltration model, known as GAML, is described by two equations. Stage 1, up to the time of surface ponding, t_s, is described by:

$$F_s = \frac{S(\theta_{fs} - \theta_1)}{[1/K_{fs} - 1]} \tag{3.23}$$

where F_s is the volume of infiltration at the time of surface ponding. At the time of surface ponding, the infiltration rate is equal to the rainfall rate and $t_s = F_s/1$. The second stage of infiltration is described by:

$$K_{fs}(t - t_s + t_s') = F - S(\theta_{fa} - \theta_i)\ln[1 + F/S(\theta_{fs} - \theta_i)] \tag{3.24}$$

where t_s' is the time required to infiltrate a volume equivalent to F_s under ponded surface conditions.

Moore and Eigel (1981) developed a solution of the GAML model for a two-layer soil profile. A conceptual soil profile for the procedure is illustrated in Figure 3.6. If Darcy's law is applied to the system and the depth of ponding is negligible, f is determined as:

$$f = \frac{L + S_{w2}}{\frac{L_1}{K_1} + \frac{L_2}{K_2}} \quad \text{for } L \geq L_1 \tag{3.25}$$

where S_{w2} is the capillary drive at the wetting front in the subsurface soil. At time, t, the volume of water infiltrated is:

$$F = L_1\Delta\theta_1 + L_2\Delta\theta_2 \tag{3.26}$$

By substituting f = dF/dt into equation 3.25 and combining equations 3.25 and 3.26, the following expression for dF/dt is obtained:

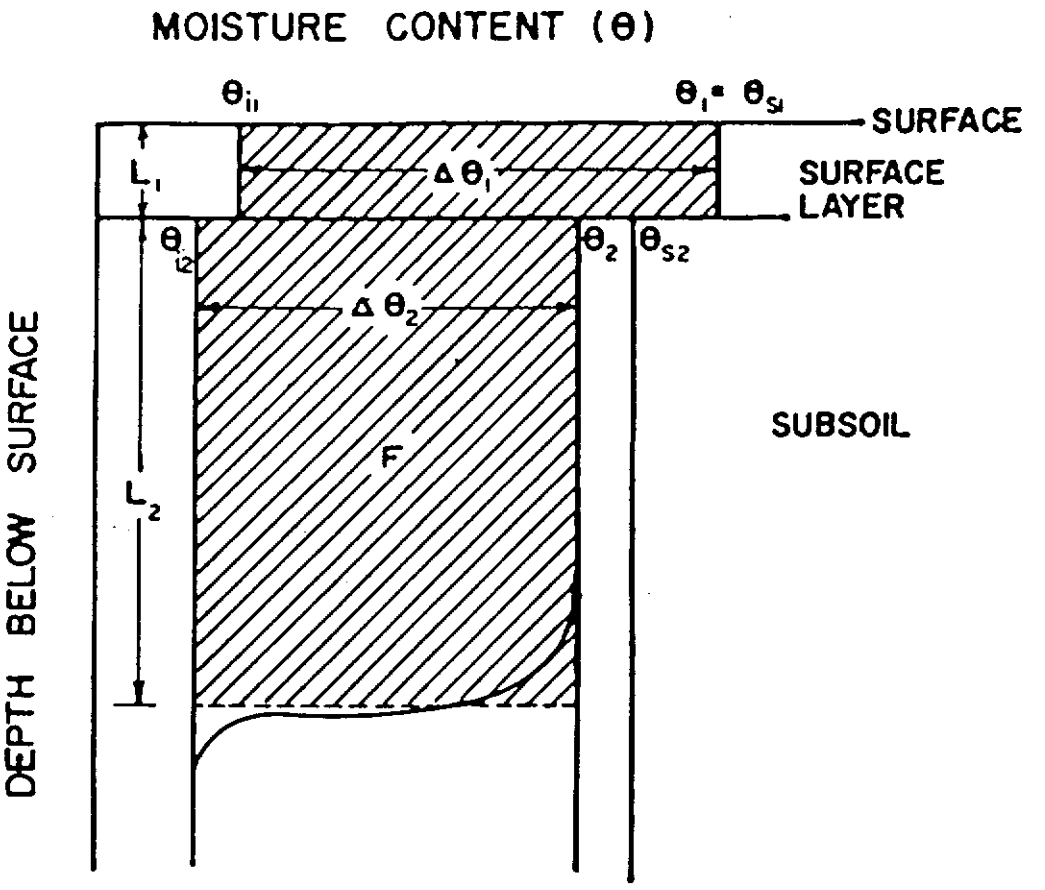

Figure 3.6 Conceptual diagram of two layer soil profile (from Moore and Eigel, 1981)

$$\frac{dF}{dt} = \frac{L_1 + \frac{F - L_1\Delta\theta_1}{\Delta\theta_2} + S_{w2}}{\frac{L_1}{K_1} + \frac{F - L_1\Delta\theta_1}{\Delta\theta_2 K_2}} \tag{3.27}$$

If equation 3.27 is integrated between the limits $t = t_1$ ($F = F_1$) and $t = t$, the following expression for the infiltration process is obtained:

$$F + (E - H)\ln\left(1 + \frac{F - F_1}{H}\right) = K_2(t - t_1) + F_1 \tag{3.28}$$

where $E = L_1\Delta\theta_2(K_2/K_1)$; $H = \Delta\theta_2\ (L + S_{w2})$; and $F_1 = L_1\Delta\theta_1$.

Equation 3.28 is the form of the Green Ampt equation for single stage infiltration through a two-layer system. For the GAML model for two-stage infiltration through a two-layer system, the equation can be written in the same form as equation 3.25 or:

$$F + (E - H)\ln\left(1 + \frac{F}{(H - F_1)}\right) = K_2(t - t_s + t_s') \tag{3.29}$$

where F_s is given by the equation:

$$F_s = \frac{H - E\,\frac{1}{K_2}}{\frac{1}{K_2} - 1} + F_1 \tag{3.30}$$

Equation (3.30) applies if F_s exceeds the storage volume in the surface layer. If $L_s > L_1$, equation 3.28 is used with parameter estimates for the surface layer. The procedure is well suited to solution by computer.

Gregory (1977) developed an infiltration equation to include an entrance function in which surface effects might be accounted for. This equation lacks simplicity and manageability. Gregory also presented a modified Green-Ampt equation to account for the effect of surface changes, but this equation is also cumbersome. The reader is referred to the original paper for more complete details.

Moore (1981) and Moore and Eigel (1981) modified the GAML model to account for surface sealing effects and infiltration into layered profiles. This approach was similar to Bouwer's (1976) in that a weighted harmonic mean hydraulic conductivity was also used. It should be noted that Bouwer (1976) required increasing saturated hydraulic conductivity for his equations to be valid, but Moore (1981) applied a similar technique to a two layer soil with both increasing and decreasing saturated hydraulic conductivities. Moore and Eigel (1981) compared this modified GAML model to observed data and a numerical solution of Richard's equation. Results ranged from excellent to fair.

Moore (1982) extended his previous two layer model to soil profiles with "n" layers. The average relative hydraulic conductivity term becomes:

$$J = \frac{\sum_{j=1}^{i} Z_j}{\sum_{j=1}^{i} \frac{Z_j}{K_j}} \tag{3.31}$$

where Z_j and K_j are the thickness and hydraulic conductivity of the j^{th} layer, respectively. The resulting Green-Ampt equation for a soil with n layers is:

$$f = \frac{\sum_{j=1}^{i} Z_j}{\sum_{j=1}^{i} \frac{Z_j}{K_j}} \qquad \frac{Z + S_{wi}}{Z} \tag{3.32}$$

where Z is the depth to the wetting front, which is in layer i, and S_w is the suction at the wetting front. Moore's equations are restricted by the same assumptions as were used to derive the GAML and Green-Ampt equations, but appears well adapted to simple layering configurations that may be encountered in the field. The difficulty with this method is some parameters

need to be known apriori. For more than two layers, their determination is quite difficult.

Summary

Surface storage accounts for rainfall abstractions required to fill surface depressions prior to initiation of runoff. Maximum values of surface storage have been tabulated for a limited number of surfaces. Models of surface storage effects on runoff range from simple step function approaches which assume that all surface storages are satisfied prior to runoff, to statistical or exponential approaches which assume a distribution of runoff as surface storage is filled. The exponential or statistical approaches conform closer to field observation than the step function approach. Empirical data indicate that surface storage varies with tillage technique and slope, with surface storage decreasing to near zero at slopes greater than 20 percent. For the erosion model a technique is needed to describe surface storage changes with slope and surface roughness and to define runoff changes as surface storage is filled. The data of Linden (1979) provide a base for describing slope and surface roughness effects on surface storage and the exponential relationship given by equation 3.3 provides a reasonable framework for predicting runoff as related to surface storage. Moore's data can be used to predict the effects of rainfall on surface storage.

Infiltration is the most significant rainfall abstraction for pervious soils. Models of the process range from simple parametric models of Horton (1940) and Holtan (1961) to the more complex theoretical treatments given by the Richard's equation and the Green and Ampt equation. A procedure is needed to calculate infiltration which accounts for soil physical and hydraulic properties and is based on physical principles. Since the model is being developed for disturbed lands, macropore flow will not be an

important phenomena. Surface sealing will be an important phenomena and will need to be modeled. The Green-Ampt relationship as modified by Moore and Eigel (1981) for two layers provides an acceptable theoretical framework for making these computations.

CHAPTER 4 SOIL EROSION: FUNDAMENTALS

The Erosion-Deposition Process

Soil erosion involves detachment, transport and subsequent deposition (Meyer, 1974). Soil is detached by raindrop impact and the shearing force of flowing water. Sediment is transported downslope primarily by flowing water, although there is a small downslope transport by raindrop splash. Runoff and resulting downslope transport do not occur until the rainfall intensity exceeds the infiltration rate. For this reason, soil erodibility decreases as the infiltration rate goes up. Once runoff starts, the quantity and size of material transported increases with the velocity of runoff water. At some point downslope, the slope may decrease, resulting in a decreased velocity and transport capacity. At this point, sediment will be deposited with the larger aggregates deposited first and the smaller aggregates carried further downslope. For this reason the size distribution of the eroded aggregates and particles has a large effect on soil erodibility.

Soil eroded from exposed areas comes from rill and interrill areas. Rills are small channels which form in the exposed soil due to concentrations of runoff[1]. Erosion in interrill areas tends to occur in uniform sheets. The primary force causing detachment in this sheet erosion is raindrop impact. Detachment in rill erosion is a result primarily of shear forces from the flowing water. Shear forces and resulting rill erosion increase with increasing slope and runoff rate. Interrill erosion, conversely, is affected much less by slope and runoff rate (Lattanzi et al., 1974). As shown in Figure 4.1, the relative contribution of rill erosion increases as slope length increases while the interrill contribution decreases (Meyer et al., 1976b).

---

1. A rill is a drainage channel that can be removed by ordinary tillage equipment. Anything larger is a gully.

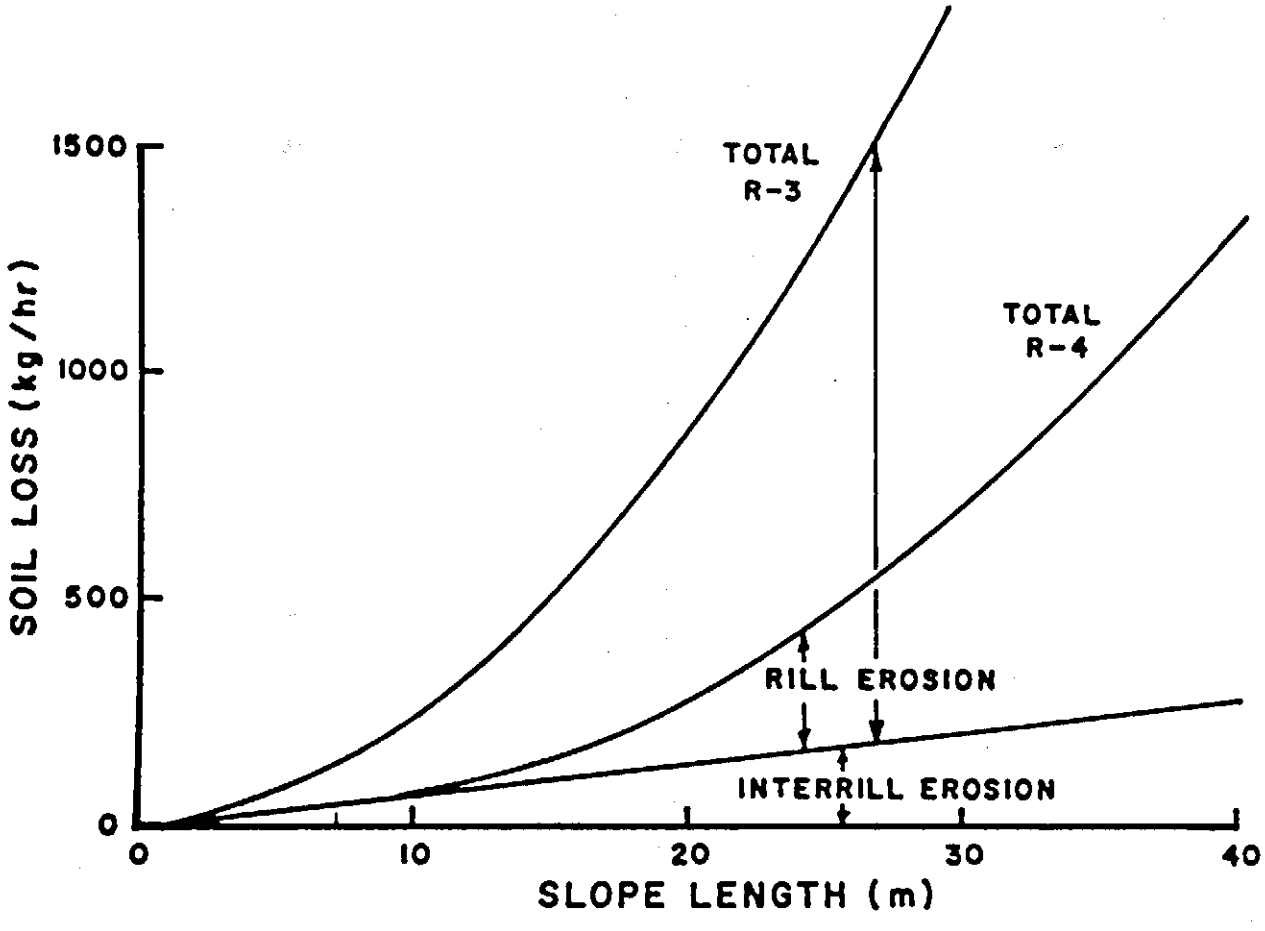

Figure 4.1 Relative rill and interrill erosion rates as affected by slope length for two soils with differing susceptabilities to rilling (after Meyer et al., 1977)

Also shown in Figure 4.1 is the importance of the rilling process or total erosion. Both plots R-3 and R-4 were equally susceptible to interrill erosion, but R-3 was more susceptible to rill erosion, thus the total erosion was much greater on R-3 than R-4. This example illustrates the importance of an understanding of the rilling process to modeling soil erosion.

Early models of soil erosion were based entirely upon empirical studies using parameters developed primarily by statistical techniques. The Universal Soil Loss Equation (USLE) is the most well known example (Wischmeier and Smith, 1978). In more recent years models have been developed based on physical concepts. In this chapter, the statistical models, called USLE type models, will be discussed first and then followed by a description of the concepts on which the physically based models are developed. Descriptions of the physically based models are given in Chapters 5, 6 and 7.

USLE Type Models

USLE Model

According to Meyer (1982), developments which led to the Universal Soil Loss Equation (USLE) started in 1917 with the establishment of the first erosion plot at the University of Missouri Agricultural Experiment Station. Other stations followed suit and by 1943 a large volume of data had been collected. The studies were discontinued at that point. In 1946 a basic relationship known as the Musgrave equation (Musgrave, 1947) was developed at a workshop in Cincinnati, Ohio based on the plot studies. The Musgrave equation related soil loss to slope, slope length, soil cover, conservation practices, rainfall intensity, rainfall energy and a measure of soil erodibility.

Wischmeier and Smith (1965) improved the Musgrave equation and proposed procedures and nomographs for its use. The resulting procedure became known as the Universal Soil Loss Equation since it did not contain geographic

constraints inherent in earlier equations. The procedure has been used in a useful manner far beyond the expectations of its developers. Since Meyer's development of the Purdue rainulator in 1958 (Meyer & McCune, 1958), the use of rainfall simulators on erosion plots has greatly enhanced erosion research, particularly in the area of sediment control from denuded areas.

The rate of erosion from an exposed area depends on the erosive power of rainfall, soil erodibility, slope and slope length, degree of soil cover and conservation practices. Based on data from 48 locations in 26 states, factors have been developed to represent these characteristics and have been combined into the Universal Soil Loss Equation (Wischmeier and Smith, 1965) as:

$$A = R\ K\ LS\ C\ P \qquad (4.1)$$

where A is computed soil loss per unit of area (tons/acre), R is a rainfall factor usually expressed as the product of rainfall energy times the maximum 30-minute intensity for a given rainstorm, K is soil erodibility (tons/acre per R unit), LS is a dimensionless length slope factor to account for variations in length and slope, C is a dimensionless cover factor relating the effectiveness of vegetal cover in reducing erosion and P is a dimensionless conservation practice factor.

Gross erosion as predicted by the USLE is the estimated sediment produced by rill plus interrill erosion from a field sized area. To obtain sediment yield at some point beyond the field area, additional erosion from gullies and stream banks must be added and deposition subtracted. Wischmeier (1976) cautioned against the use of the USLE in situations where deposition is likely. The model is basically a model for detachment, and does not predict deposition.

Erosion values can be predicted for erosion for average annual, average storm, return period annual, or return period storm using the USLE by simply

utilizing the appropriate R value. Wischmeier (1976) lists several potential problems when using the USLE for single storm erosion. First, use of the single storm EI_{30} index for R and the crop stage, C, value for C will estimate the soil loss averaged over numerous occurrences of that same event at that crop stage. The soil loss in any one event may vary widely. The primary reasons for this variation are variation in the energy content in a single storm from the value used in the EI_{30} index and variations in antecedent moisture. As shown in Chapter 2, the E value is calculated for an average storm at the given intensity whereas the actual energy in a storm for a given intensity varied widely about the average. Secondly, the K value used in equation 4.1 is for average moisture conditions. The actual moisture at the start of a storm may vary widely from average conditions.

The USLE predicts gross erosion from field sized plots in which deposition is not occurring. In order to measure sediment yield into a channel, the gross erosion must be modified by a delivery ratio. Methods for predicting delivery ratios are given in Barfield et al. (1981).

Williams (1976) proposed that the rainfall energy term, EI_{30} index, in the USLE could be replaced with a runoff energy term in the USLE to predict sediment yield directly, and called the procedure the Modified USLE or MUSLE. Procedures were developed for homogeneous watersheds using a lumped parameter approach and for nonhomogeneous watersheds using sediment routing procedures. A lumped parameter approach is one in which the entire watershed is represented by one characteristic parameter.

Williams (1975) developed the MUSLE using data from 778 storms on watersheds near Riesel, Texas, and Hastings, Nebraska. The drainage areas ranged from 2.7 to 4380 acres and the average slope and slope lengths ranged from 0.9 to 5.9 percent and 258 to 470 feet. He replaced the R factor in the USLE with various parameters and used the resulting equation to predict the sediment

yield from the watersheds. The parameter that gave the best estimate was Q x q_p, the product of runoff volume and peak discharge. Williams denoted this term runoff energy. The resulting equation is:

$$Y = 95(Q \times q_{pi})^{0.56} \overline{K}\ \overline{LS}\ \overline{CP} \qquad (4.2)$$

where Y is the single storm sediment yield in tons, Q is runoff volume in acre-ft, q_{pi} is peak discharge in cfs, and $\overline{K}$, $\overline{LS}$ and $\overline{CP}$ are standard USLE terms, each of which is an area weighted average over the watershed. Typical prediction accuracy of the MUSLE is shown in Figure 4.2. The spread of the data is typical of most prediction procedures for sedimentology.

Equation 4.2 is intended for use on a watershed basis. Foster et al. (1982) evaluated the use of a similar type equation for single storms on individual plots and found that the EI_{30} index was a better predictor of single storm erosion than the product (Q x q_p).

Combination Type Models of Soil Erosion

Soil erosion is predicted from the USLE by the rainfall energy term, EI_{30}, and sediment yield in the MUSLE by the runoff energy term $(Q \times q_p)^{.56}$. Onstad and Foster (1975) proposed that a combination of these two approaches would improve erosion predictions. They proposed that the USLE be modified to:

$$A = W\ K\ LS\ CP \qquad (4.3)$$

where

$$W = m\ R + (1 - m)\ [(30Q)\ (q_p)]^{1/3} \qquad (4.4)$$

where R is the EI_{30} index, m is a constant (typically 0.5), Q is runoff volume in inches and q_p is peak runoff rate in in/hr.

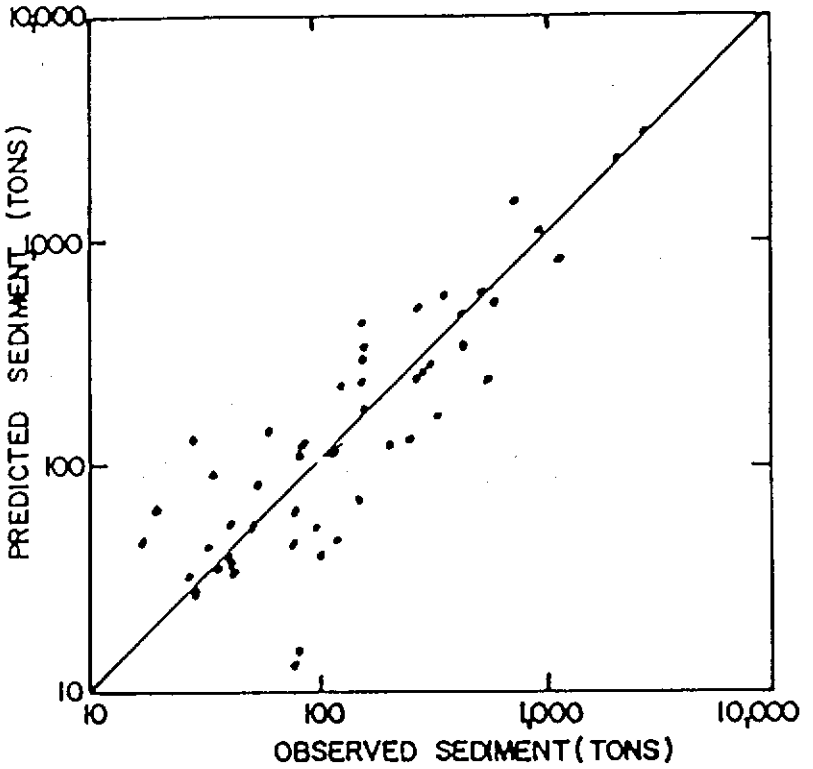

Figure 4.2 Comparison of observed and predicted sediment yields when using the MUSLE for watersheds W-3 and W-5 (from Williams, 1975)

Using the W factor improved the prediction of erosion based on studies reported by Onstad and Foster, however, the improvements were only slight (correlation coefficients of .98 versus .991). Further studies by Foster et al. (1982) also showed the same slight improvement over the EI_{30} index. The equation only predicts erosion and not sediment yield.

Foster, Meyer, Onstad Rill-Interrill Model

Foster, Meyer, and Onstad (1977) used basic principles and developed an erosion model which considers rill and interrill detachment separately. These model techniques will be discussed in Chapter 5.

Physically Based Models of Soil Erosion: Basic Concepts

The Meyer-Wischmeier Model

Meyer (1974) proposed that the components of the soil erosion-sedimentation process for a discrete slope segment are interrelated as shown in Figure 4.3. The soil available at any slope segment is the sum of that carried from upslope plus that detached in the slope increment. The soil carried downslope is the lesser of the transport capacity or the material available for transport. Preliminary methods proposed by Meyer for predicting each of the components are:

$$D_i = S_{Di} A_1 I^2 \tag{4.5}$$

$$D_R = S_{DR} A_1 S^{2/3} q^{2/3} \tag{4.6}$$

$$T_i = S_{TI} S I \tag{4.7}$$

$$T_R = S_{TR} S^{5/3} q^{5/3} \tag{4.8}$$

where A_1 is the area of slope segment, I is rainfall intensity, S is slope, q is flow rate and S_{Di}, S_{DR}, S_{Ti}, S_{TR} are empirical cooefficients. The

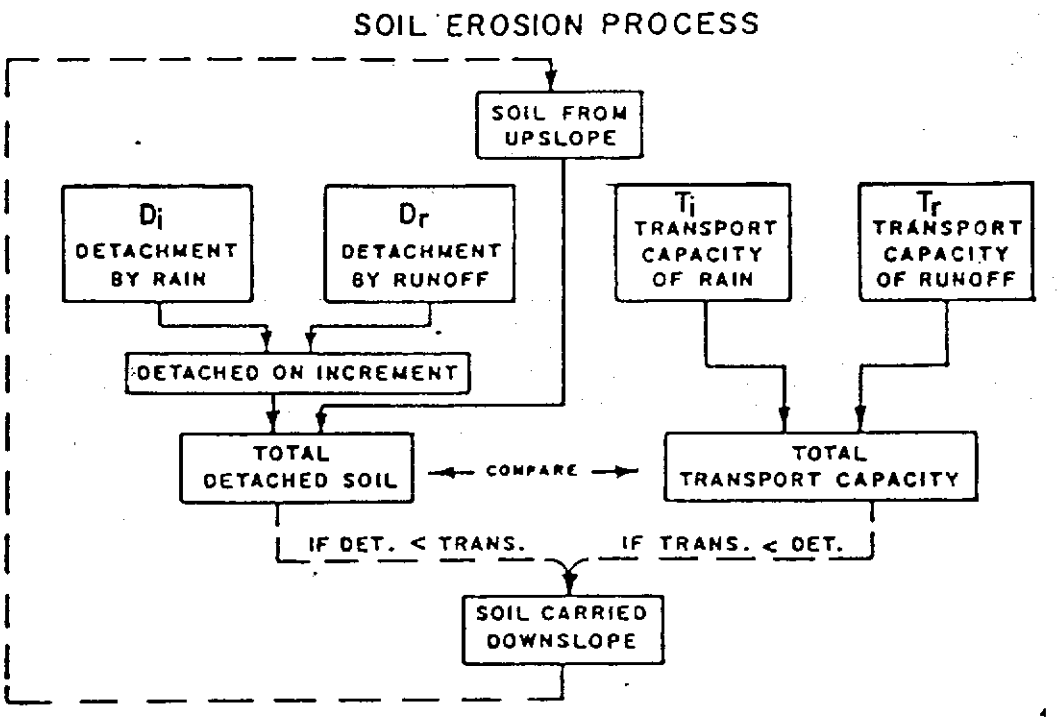

Figure 4.3 Conceptual model of erosion (Meyer and Wischmeier, 1969)

Meyer-Wischmeier model is a good conceptual base for making computations. Better equations have been developed for computing each component.

Curtis (1976) added a parameter to the Meyer-Wischmeier model to account for deposition in previous time steps. His computational methods are essentially the same as those of Meyer and Wischmeier.

Foster and Meyer Closed Form Equation

In the Meyer-Wischmeier model, it was assumed that erosion was its equilibrium rate at the end of a slope segment. This may not be true. An interaction exists between the sediment load and the rate of detachment, given by (Foster and Meyer, 1972):

$$D_R = C\ (T_C - G_F) \tag{4.9}$$

where D_R is the rate of detachment by flow at X, C is a constant of proportionality, T_C is the transport capacity of flow at X, and G_F is the sediment load at X. Simplifying Foster and Meyer obtained:

$$\frac{D_R}{CT_C} + \frac{G_F}{T_C} = 1.0 \tag{4.10}$$

By letting G_F equal zero in (4.10) Foster and Meyer obtained:

$$D_R = CT_C \tag{4.11}$$

which represented the maximum value for detachment. This maximum value was denoted as D_C, thus:

$$\frac{D_R}{D_C} + \frac{G_F}{T_C} = 1.0 \tag{4.12}$$

Equation (4.10) was presented as a statement of balance between transport capacity, sediment load, actual detachment rate, and potential detachment

rate. By assuming that:

$$D_C = C_c \tau^{3/2} \tag{4.13}$$

$$T_c = C_t \tau^{3/2} \tag{4.14}$$

and by using the Chezy equation

$$\tau = C_r q^{2/3} S^{2/3} \tag{4.15}$$

Foster and Meyer obtained:

$$D_c = C_D C_r S\ q \tag{4.16}$$

$$T_c = C_T\ C_r\ S\ q \tag{4.17}$$

By assuming steady runoff rates for short time durations, the discharge at any X was given by:

$$q = \frac{X}{L_o} q_o \tag{4.18}$$

where q_o is the discharge at X equal to L_o. Also, by combining C_T, C_r, L_o, and q_o into one constant Foster and Meyer obtained

$$D_C = C_D\ X_* S \tag{4.19}$$

$$T_c = C_T\ X_*\ S \tag{4.20}$$

where $X_* = \frac{X}{L_o}$ (4.21)

By defining D_{co} and T_{co} as the detachment and transport potentials at $x = L_o$, then

$$g_* = \frac{D_c}{D_{co}} = \frac{C_D\ X_*\ S}{C_{D(1)} S_D} = X_* S_* \tag{4.22}$$

was obtained. Likewise

$$g_* = \frac{T_c}{T_{co}} = X_* \, S_* \tag{4.23}$$

where

$$S_* = \frac{S}{S_o} \tag{4.24}$$

Rearranging equation (4.12) Foster and Meyer obtained

$$\frac{D_R}{D_{co} \, \frac{D_c}{D_{co}}} + \frac{G_F}{T_{co} \, \frac{T_c}{T_{co}}} = 1.0 \tag{4.25}$$

However, since

$$\frac{D_G}{D_{CO}} = \frac{T_C}{T_{CO}} = g_*; \tag{4.26}$$

equation (4.25) was modified to

$$\frac{D_R}{D_{CO}} + \frac{G_F}{T_{CO}} = g_* \tag{4.27}$$

The equation of sediment continuity for steady state was given by Bennett (1974) as

$$\frac{dG_F}{dx} = D_R + D_i \tag{4.28}$$

where G_F is the sum of rill and interrill erosion rates, or

$$G_F = (D_R + D_i) \, dx \tag{4.29}$$

Hence,

$$\frac{D_R}{D_{CO}} + \frac{(D_R + D_i) \, dx}{T_{co}} = g_* \tag{4.30}$$

Since $X_* = \frac{X}{L_o}$; $dx = L_o dX_*$, then

$$\frac{D_R}{D_{CO}} + L_o \int \frac{(D_R + D_i)\, dx_*}{T_{co}} = g_* \qquad (4.31)$$

Finally, Foster and Meyer differentiated equation 4.31 with respect to X_* to obtain

$$\frac{d}{dX_*} \left[\frac{D_R}{D_{co}} + \frac{D_i L_o}{T_{co}} + \frac{D_R L_o}{T_{co}} \right] = \frac{dg_*}{dx_*} \qquad (4.32)$$

By defining the terms

$$\theta = \frac{L_o D_i}{T_{co}} \qquad (4.33)$$

$$\alpha = \frac{L_o D_{co}}{T_{co}} \qquad (4.34)$$

they obtained the differential equation

$$\frac{d}{dx} \left[\frac{D_R}{D_{co}} \right] + \alpha \frac{D_R}{D_{co}} = \frac{dg_*}{dx_*} - \theta \qquad (4.35)$$

The general solution to 4.35 is

$$\frac{D_R}{D_{co}} = \frac{1}{e^{\alpha x_*}} \int \left(\frac{dg_*}{dx_*} - \theta \right) e^{\alpha x_*}\, dx_* + \text{constant} \qquad (4.36)$$

By assuming a uniform slope and constant rainfall, then $S = S_o$ for all X_* and equation (4.36) was reduced to

$$\frac{D_R}{D_{co}} = \frac{(1 - \theta)}{\alpha} \left(1 - e^{-\alpha x_*} \right) \qquad (4.37)$$

Equations (4.36) and (4.37) are general relationships which should always hold

true, regardless of the formulation of D_{co}, T_{co}, D_i. In order to use the relationships, it is necessary to have auxillary equations for D_{co}, T_{co}, and D_i. These relationships are discussed in the next two chapters.

CHAPTER 5: SOIL EROSION: DETACHMENT

Introduction

Soil is detached by raindrop impact and the shear forces caused by runoff. Detachment in the rill (channelized flow) areas is primarily due to shearing forces of runoff while detachment in the interrill areas is primarily due to raindrop impact, although a small component of interrill detachment is due to shear from overland flow.

For a given rainfall the actual rate of detachment depends on the presence of materials to shield the surface from raindrop impact (i.e. crop canopy, mulch, ponded water), the presence of material to absorb the shear as a result of runoff (i.e., mulch, vegetation), the inherent resistance of soil to detachment, and the infiltration capacity of the soil. In this chapter, the mechanisms causing detachment will be discussed along with the resistance of soil to detachment. Since the model being developed is for bare soil, the effects of surface cover will not be covered. Infiltration effects are covered in Chapter 2.

Detachment by Raindrops or Interrill Erosion

Rainfall Factor

Interrill detachment models have typically utilized rainfall rate, momentum, kinetic energy, intensity, or a combination of these parameters as predictors of erosion. Numerous investigations have failed to yield a definitive physical model. In the discussion that follows, a distinction must be made between splash detachment and interrill erosion. The two terms cannot be used interchangeably. For the purposes of this discussion, the following definition will be used;

> Splash detachment - detachment of soil by raindrop impact including all particles which are dislodged from the soil matrix and made available for transport.

Interrill erosion - The quantity of soil which is moved from the interrill areas into flow channels known as rills.

Interrrill erosion will typically be equal to or less than splash detachment since it is the minimum of that material detached or the transport capacity of overland flow to the rills.

Young and Wiersma (1973) utilized a rainfall simulator with bare plots protected by a screen to show that raindrop impact was the primary factor causing interrill erosion. In their studies, raindrop energy was reduced by 89% between the screen covered and bare plots without a change in rainfall intensity. The interrill erosion rates were reduced by more than 90 percent in all cases. Hudson (1971) found similar results with natural rainfall.

Although the Young and Wiersma (1973) and Hudson (1971) studies showed that raindrop impact is the primary factor causing erosion, the studies do not elucidate the prediction parameter which should be used to predict interrill erosion. In the following discussion of studies which were oriented toward defining that prediction parameter, a distinction is made between those studies developing predictors of interrill erosion and those developing predictors of splash detachment.

Splash Detachment

Investigators of splash detachment have utilized splash cups and cloth strips to measure detachment rate. Splash cups are typically small circular cylinders (approximately 3 inches in diameter) which are tilted at the desired slope and exposed to a given rainfall. Splash detachment is measured as the total material splashed out of the cup and splash transport measured as the difference between upslope and downslope splash. Where cups are used, a correction must be made for the effect of the cup rim on splash as the surface of the soil is displaced below the rim of the cup due to soil loss during the

test. Cup rim corrections were developed by Bisal (1950) to compensate for this problem.

Rose (1960) studied splash detachment from 5 soils ranging from sands to clays under simulated rainfall. Based on his analysis, the most consistent predictor of splash detachment depended more heavily on momentum than kinetic energy or rainfall volume.

Bubenzer and Jones (1971) used a rainfall simulator and splash cup to study erosion splash detachment for 5 different soils. No discussion was given of cup rim corrections. The results of their study given in Table 5.1, indicate that kinetic energy is highly correlated to splash detachment (correlation coefficient ranging from .90 to .91 for individual soils) but that a slight improvement in prediction is obtained by using both kinetic energy and rainfall intensity (correlation coefficient ranging from .91 to .96). Other researchers have also shown that splash detachment is a function of rainfall energy (Free, 1960; Mihara, 1951; and Quansah, 1981).

Park et al. (1982) conducted a dimensional analysis of the parameters involved in splash detachment and concluded that detachment should be a linear function of impact velocity; however, the data they present from Ellison (1944) indicate that detachment is more a linear function of kinetic energy than velocity.

Smith and Wischmeier (1957) used data from Ellison (1947) to indicate that splash erosion is proportional to rainfall intensity expressed as $I^{1.1}$. Since kinetic energy was shown in Chapter 2 to be highly related to intensity, this correlation is not surprising.

Interrill Erosion

Equations which predict the total sediment flowing into a rill must combine the processes of raindrop detachment, detachment by thin sheet flow,

Table 5.1 Results of the Bubenzer and Jones (1971) Study

Soil	Regression Equation	Correlation Coefficient
Regression Equations Relating Soil Splash to the Kinetic Energy of the Simulated Rainfall		
All soils	$ss = 14.49\ (kc)^{1.56}$	0.84
Darwin silty clay	$ss = 13.17\ (kc)^{1.77}$	0.91
Cisne silt loam	$ss = 9.12\ (kc)^{1.25}$	0.90
Flanagan silt loam	$ss = 19.72\ (kc)^{1.03}$	0.90
Hagener loamy sand	$ss = 18.87\ (kc)^{1.40}$	0.91
Multiple-Regression Equation Relating Soil Splash to the Rainfall Intensity and Kinetic Energy of the Simulated Rainfall		
All soils	$ss = 1.55(i)^{0.42}(kc)^{1.20}$	0.87
Darwin silty clay	$ss = 3.10(i)^{0.27}(kc)^{1.49}$	0.92
Cisne silt loam	$ss = 0.63(i)^{0.40}(kc)^{0.83}$	0.96
Flanagan silt loam	$ss = 1.04(i)^{0.55}(kc)^{1.08}$	0.96
Hagener loamy sand	$ss = 2.89(i)^{0.37}(kc)^{1.13}$	0.94

transport by splash and transport by thin sheet flow. Detachment by sheet flow is typically minor and transport by raindrop splash is minor on mild slopes but can be substantial on steep slopes. Studies of plot erosion have related plot erosion to intensity, I, to the following powers:

Researcher	Intensity function
Ekern (1950, 1953)	$I^{1.5}$
Neal (1938)	$I^{2.2}$
Wischmeier and Smith (1978)	EI_{30}

where E is rainfall energy and I_{30} is the maximum thirty minute intensity.

Foster et al. (1977b) proposed that interrill erosion (which they called interrill detachment) could be calculated as

$$D_i = K_i\ I\ (bS + C) \qquad (5.1)$$

where D_i is the interrill detachment rate, K_i is the interrill erodibility factor, I is a measure of interrill erosivity, S is slope and b and c are constants. Initially Foster and Meyer proposed the use of the EI_{30} index for I.

Subsequently, due to the success of other modelers in defining interrill erosion as a function of intensity alone (Meyer and Wischmeier, 1969; Moldenhauer and Long, 1964; and David and Beer, 1975). Foster (1982) proposed that interrill erosion be modeled as

$$D_i = .0138\ K_i\ i^2\ [2.96 \sin \theta^{0.79} + .56]\ C_i \qquad (5.2)$$

where i is rainfall intensity, θ is the slope angle and C_i is the interrill cover factor.

Meyer (1982b) evaluated erosion from the side slopes of furrows using a rainfall simulator and found that the erosion rate could be predicted by

$$D_i = a\ i^b \qquad (5.3)$$

where a and b are exponents dependent upon the individual soil. He found that the exponent of 2.0 was a good value for b for silt, loam, silt-loam, and sandy loam soils, but was too large for clay soils. A good estimate was found using

$$b = 2.1 - (\text{clay function}). \qquad (5.4)$$

The coefficient a was found to be dependent on the individual soil.

Resistance to Erosion in Interrill Areas, Resistance to Splash Detachment

For bare soils the resistance tofunction primarily of the soil properties and slope. Quansah (1981) found that splash detachment varied with kinetic energy and slope to a variable power depending on the type soil as shown in Table 5.2.

Cruse and Larson (1977) showed that splash detachment for a 4.8 mm drop falling from a height of 177 cm was closely related to shear strength of a soil as measured with a triaxial test. Durrah and Bradford (1981) evaluated splash detachment with drops of 3.0, 4.6 and 5.6 mm diameter as related to

Table 5.2 Power Equations Relating Splash Detachment (Q_{det}) and Transport (Q_{trans}) to Slope (S) and Kinetic Energy (KE) (Quansah, 1981)

Soil	Equation	KE r^2	S r^2	R^2
Standard sand	$Q_{det} = 0.0002\ KE^{1.06}$	0.84		
	$Q_{det} = 0.0002\ KE^{1.06}S^{0.13}$	0.84	0.06	0.90
Sand	$Q_{det} = 0.0007\ KE^{0.84}$	0.72		
	$Q_{det} = 0.0003\ KE^{0.84}S^{0.13}$	0.72	0.08	0.81
Clay loam	$Q_{det} = 0.00004\ KE^{1.16}$	0.66		
	$Q_{det} = 0.00003\ KE^{1.16}S^{0.25}$	0.66	0.14	0.79
Clay	$Q_{det} = 0.00002\ KE^{1.35}$	0.74		
	$Q_{det} = 0.00001\ KE^{1.35}S^{0.27}$	0.74	0.14	0.88

shear strength of an Ida Silt Loam measured by a Swedish Fall Cone Device. Their results showed that detachment could be predicted on a single drop basis by

$$D_S = 0.36 + 0.007\ KE/\tau \qquad (5.5)$$

where D_S is splash detachment and KE is kinetic energy of a drop, and τ is shear strength. The correlation coefficient for equation 5.5 was .97.

Bubenzer and Jones (1971) evaluated splash detachment from 5 soils and found that detachment could be predicted by

$$D_S = 7.50\ (i)^{.41}\ (KE)^{1.14}\ (PC)^{-0.52} \qquad (5.6)$$

where PC is percent clay. The correlation coefficient for equation 5.6 was .93 as compared to .87 for KE and i alone. Massie (1980) utilized equation 4.6 to model splash detachment, but proposed that PC should not be used

below values of 6.6%, which is below the Bubenzer et al. data base.

A water film on the surface can absorb the energy of falling drops if the film is thick enough. Palmer (1965) evaluated the effects of a water film on the soil surface and found that the filter increased detachment up to a thickness of one drop diameter and decreased detachment at greater depths up to about 3 drop diameters. The increase at small film thickness was attributed to an increase in mass entrained by the drop as it fell from the surface to the soil.

Resistance to Interrill Erosion

When one lumps the detachment and transport processes together to form a lumped interrill erosion, the resistance factor must be considered separately from that for detachment by splash. Typically, for bare soils, resistance to erosion in this dumped case is given by an erodibility factor, or using the Foster (1981) model cited earlier as equation (5.2). In this case K_i, the interrill erosivity, accounts for the inherrent soil factors affecting erosion and C_i accounts for tillage surface roughness, mulching and cropping effects.

Sheet Flow Detachment

The detaching capacity of sheet flow is very small. Most of the soil detached from the areas where sheet flow occurs is by raindrop impact. As discussed earlier, Young and Wiersma (1973) found that an 89% reduction in raindrop energy reduced the soil loss on sheet flow areas by 91, 94, and 90% for a Barnes loam, a Crofton silt loam, and a Central sandy loam, respectively. Alberts et al. (1980) reported similar results for a Miami silt loam. These studies indicate that the major portion, if not all, of the soil detachment on sheet flow areas is due to raindrop impact, not the sheet flow itself.

If sheet flow detachment is to be considered, relationships similar to

those for rill flow will probably emerge. Those relationships will be discussed in the rill flow section. They essentially are empirical equations based on the concept of excess shear. The excess of surface shear stress above the critical shear stress is used as a predictor of detachment. Sheet flow detachment is normally considered to be insignificant, however, when compared to raindrop detachment and concentrated flow detachment.

Rill Detachment

Once rills are formed, the channelized runoff which they contain provides energy for both detachment and transport of soil particles in the erosion process. Detachment relationships are few, and usually contain empirical constants that need to be fitted to actual data. The detachment and transport relationships are key components of the processes contributing to erosion and so the available relationships must be considered and adapted if possible.

Existing relationships for rill flow detachment are basically similar in approach. The most commonly used relationships are based on USLE parameters. Other equations are available, but few are based on measurable soil properties.

Ellison and Ellison (1947) describe the general flow/soil characteristics that influence surface flow (and hence, rill flow) detachment. They defined the soil detachment hazard, D_1 as a function of the soil detachability, D_2, and the detaching capacity of the flow, D_3. The soil factors involved in D_2 would be the same as those for rainfall detachment, given by Ellison (1947) including particle size and aggregate stability. In general, soil, cohesiveness and plant residues are also involved. Ellison stated that the detaching capacity of the flow, d_3, is a function of the flow energy gradient, the quantity of abrasive particles in the flow, and the abrasiveness of those particles.

USLE Based Equations

The criterion for labelling an equation as USLE-based is its reliance upon USLE parameters, especially the USLE soil erodibility parameter, K. Although the use of a "soil constant" does not mean that an equation is simply an offshoot of the USLE, many equations specify use of the USLE-K values.

The problem with the utilization of USLE parameters is that the USLE was designed as a long-term management tool, not a storm-based research tool. The parameters, therefore, are very approximate averages that yield reasonable long-term estimates and reflect relative effectiveness of practice combinations. To be used for a given site, the soil parameters must be fully investigated, as the published values are only averages over varying soil conditions and not applicable for a particular site. These problems were discussed in Chapter 4.

CREAMS Rill Detachment Equation

Foster et al. (1980) proposed separate detachment equations for rill and interrill erosion for the USDA-ARS model for Chemicals, Runoff and Erosion from Agricultural Management Systems (**CREAMS**). Their equations are based on those developed by Foster, Meyer and Onstad (1977 a & b). The **CREAMS** rill detachment equation is

$$D_{Fr} = 37983\ mV_u\ \sigma^{1/3}\ (x/72.6)^{m-1}\ S^2\ KCP\ (\sigma p/vu) \qquad (5.7)$$

where D_{Fr} is the rill detachment rate (lb/ft^2-s), x is the distance downslope (ft), S is the sine of the slope angle, m is the slope length exponent, given by $m = 1.0 + 5.011/\ln x$, K is the USLE soil erodibility factor (hr/100 ft-in), C is the soil loss ratio of the USLE cover-management factor, P is the USLE contouring factor, V_u is the runoff volume per unit area (ft), and σ_p is the peak runoff rate per unit area (ft/s).

Because the **CREAMS** equation is derived from the Foster, Meyer and Onstad (1977b) relationship, the usefulness of the latter should indicate the value of the **CREAMS** equation. Foster, Meyer, and Onstad (1977b) presented a comparison of observed soil loss from 12 events versus estimated soil loss by three equations, the USLE, the USLE with modified R factor, and the rill-interrill equation from which the **CREAMS** equations were derived. The correlation between observed and predicted erosion for these equations were 0.98, 0.991 and 0.995, respectively. Therefore, the rill-interrill equation is a slight improvement over the USLE, and the **CREAMS** equations should reasonably predict soil loss.

Foster's Rill Detachment Equation

Equation 5.7 is for erosion over an entire storm. A detachment function is needed for instantaneous erosion rates.

Foster (1982) coalesced much of the work done in the area of rill detachment. He assumed that rill erosion could be described by:

$$D_{rc} = a\ (\tau - \tau_{cr})^{b} \qquad (5.8)$$

where D_{rc} is the rill erosion detachment capacity rate, τ is the flow's shear stress, τ_{cr} is the critical shear stress, and a and b are constants. Foster then described many additional prediction parameters, most of which are linked to the USLE and gave a simpler alternative to equation 5.8 and its subfactors:

$$D_{rc} = C_{B}\ q\ s\ K\ C_{SLR} \qquad (5.9)$$

where D_{rc} is the rill erosion detachment capacity rate, C_{B} is a constant to be calibrated, q is the runoff rate, s is the sine of the slope angle, K is the USLE soil erodibility factor, and C_{SLR} is the soil loss ratio from the USLE. The need to evaluate constants by fitting is a major drawback to Foster's equations.

Hughes Scour Probability Study

Hughes (1980) studied ephemeral streams to check the concept of maximum non-eroding velocity for unvegetated channels. Data was utilized from 300 sites in Colorado, New Mexico and Oklahoma. His study does not provide a flow detachment equation, but it gives relationships to predict when detachment (scour) occurs. Scatter diagrams of probability of channel erosion versus channel velocity and flow depth were presented for three soil classes; sandy-silt, silty-clay and clay. Straight lines were fitted to the data for each probability level. The equation of the lines is

$$V = K' Y^m \tag{5.9}$$

where V is flow velocity in ft/sec, Y is flow depth in ft, m is the log-log regression slope and K is the log intercept of the probability lines. The lines give probability of scour given the peak velocity and corresponding depth of the event in question.

The soils to be dealt with in agricultural and surface mine situations typically would mainly fall in the sandy-silt and silt-clay categories. These soils typically have an n value of 0.2. The K values for given probabilities are close, indicating that an average value might be appropriate. A critical flow depth for scour can be obtained from these relationships by relating V and Y using Manning's equation and as assumed channel geometry. For this analysis, assume a triangular channel with 2:1 sideslopes and a Manning's roughness value of 0.040. Then the hydraulic radius is:

$$R_n = \frac{2y^2}{2y\sqrt{1 + 2^{26}}} = 0.45\ y \tag{5.10a}$$

and equation 5.10a becomes

Table 5.3 Critical Depths for Scour Probability Using Assumed Geometry and Soil (after Hughes, 1980).

P_{scour}	K'_{crit}	(N = .040) Y(in)	(N = .040) Q(gpm)	(N = .050) Y(in)	(N = .050) Q(gpm)
.01	2.06	0.21	0.12	1.62	22.4
.05	2.25	0.22	0.14	1.95	36.0
.50	2.83	0.28	0.26	3.19	136.4
.95	3.41	0.34	0.44	4.76	396.5
.99	3.66	0.37	0.55	5.54	594.2

$$\frac{1.49}{0.04} (.45\ y)^{2/3} (\sin \theta)^{1/2} = K'\ y^{2/10} \qquad (5.10b)$$

Rearranging terms,

$$y = \left[\frac{K' (.04)}{1.49 (.45)^{2/3} (\sin \theta)^{1/2}} \right]^{15/7} \qquad (5.11)$$

or

$$y = \frac{1}{743.5} \left[\frac{K'}{\sin \theta} \right]^{15/7} \qquad (5.12)$$

Assuming a 9% slope ($\theta = 5.1°$),

$$y = \frac{(K')^{15/7}}{56.1} \qquad (5.13)$$

Table 5.3 gives the critical K' and corresponding depths for the assumed conditions for various probabilities of scour, using average K' values. The relationship is extremely sensitive to Manning's n. Therefore if this analysis is to be used, care must be taken in selecting an 'n' value or the results will be meaningless.

Park and Mitchell Model

Park and Mitchell (1981) expressed flow erosion as a time-series function of runoff rates:

$$E_f = \text{fctn} (Q_t, Q_{t-1}, Q_{t-2}, \ldots, Q_{t-n}) \qquad (5.14)$$

They then stated that for steady-state conditions,

$$E_{fn} = b\, Q_{*} \tag{5.15}$$

where the $_{*}$ indicates the steady state conditions. A Taylor-series expansion of equation (5.15) together with finite difference approximations of the derivatives gives flow erosion as a function of the runoff rates at previous times:

$$E_f = \sum_{i=0}^{n} b_i\, Q(t - i) \tag{5.16}$$

where (t - i) refers to a specific time period. Equation 5.16 was then coupled with a similar equation for raindrop detachment and calibrated as an erosion model, with n equal to 2. The simulator results showed good fit for the runs presented, but that is to be expected because the model was calibrated using data from these runs.

Critical Tractive Force Equations

The parameter most frequently used to define the resistance of a soil to rill erosion is critical tractive force. Procedures have been developed by different researchers to relate critical tractive force to measurable soil parameters. Kelly and Gularte (1981) showed that the critical shear stress for surface erosion of cohesive soils is dependent upon the interparticle bond density in a similar fashion to soil shear strength at high stress levels. They concluded, therefore that erosion resistance and soil shear strength are similar phenomena.

Kelly and Gularte presented data relating critical shear stress as a function of soil salinity (ppt - NaCl) and moisture content (% by volume). Multiple linear regression on this data gave the following best-fit equation:

$$\tau_c = 2.19\ (S_{NaCl}) - 0.2565\ \theta_{pv} + 15.75 \tag{5.17}$$

Equation (5.17) explains 83.9% of the variation in the data. The data was also

analyzed linearly after a log-transformation. The resulting equation, equation 5.17, explained 84.7% of the variance.

$$\tau_c = 2465\ (S_{NaCl})^{0.966}\ (\theta_{pv})^{-1.711} \qquad (5.18)$$

These relationships could be used to predict movement of clay particles and to predict break-away of aggregates from the soil matrix during rill erosion.

In a similar manner, Smerdon and Beasley (1961) gave critical tractive force as a function of plastisity index, dispersion ratio, mean particle size, and percent clay. Correlation coefficients ranged in magnitude from 0.795 to 0.980. Later, Lyle and Smerdon (1965) related critical tractive force to void ratio and eight other properties to obtain eight different equations. The soil properties were plasticity index, dispersion ratio, percent organic matter, vane shear strengths, cation-exchange-capacity, mean particle size, calcium-sodium ratio, and percent clay. These relationships have potential for characterizing the detachment rate during rill flow.

Erosion by Failure of Rill Banks

So far only shear detachment by rill flow has been considered. This writer has observed that in the field a major source of detached sediment in the rills is the undercutting and ultimate failure by sloughing of the rill walls. Large blocks of transportable material are input to the rills in this manner. A void exists in the rill literature on this topic, necessitating exploratory research into rill sloughing and the utilization of gully erosion studies for guidance. The problem with the use of gulley erosion studies to predict rill erosion quantities is the extreme magnitude and time frame difference between gully erosion and rill erosion. More work needs to be done on rill wall stability and failure. This phenonmenon will be more fully discussed in the rill development chapter.

Recommendations

The detachment of soil in rills is poorly understood. For the present time it can be qualitatively viewed as an excess shear stress phenomenon with additional soil detachment due to seepage forces and rill wall failure. Quantitatively, any of the equations presented above must be fitted at some stage to the soil in question. An equation based on soil physical parameters is needed if detachment is to be included in erosion modeling. The most physically sound procedure for estimating potential detachment rate appears to be Foster's shear excess formula given by equation 5.8.

Detachment by splash in the interrill areas was described alternately by a function of rainfall intensity, momentum, and kinetic energy. The power relationship given by Bubenzer and Jones (1971) includes both intensity and kinetic energy. Additionally, predictions of detachment are given as a function of percent clay. Of the relationships given, the Bubenzer-Jones equation appears to be the most adaptable in terms of predictive parameters.

CHAPTER 6 SOIL EROSION: TRANSPORT EQUATIONS

Introduction

Most erosion models that use transport relationships utilize river sediment transport equations. It is important to discuss the assumptions and empiricism inherent to each of these equations to ascertain the applicability of their use for rill and interrill flow. The major equations considered for use for rill and interrill flow transport are described in the following sections.

Rill Transport Equation

Yalin Equation

The Yalin (1963) sediment transport equation was recommended for overland flow by Neibling and Foster (1980). Their conclusion was that the Yalin equation could be used "as is" for computing overland flow sediment transport rates. They based the conclusion on compared performance of six different sediment transport equations using 176 tests and six different materials. Their results showed that only the Yalin equation performed adequately.

The assumptions inherent in the Yalin equation are extensive; vis,

1) steady, uniform flow,
2) turbulent flow, with a laminar sublayer of thickness less than the size of bed roughness elements,
3) cohesionless, moveable bed,
4) equal sized grains,
5) grain motion by saltation, and
6) Shields' shear-velocity curve is accurate.

Most of these assumptions are not very restrictive. However, the assumption that grain movement is only by saltation makes the Yalin equation a bedload equation that, although suitable for shallow flow, may not consider enough of the sediment transport processes to handle

rapid rill flow, with its high suspended solids content. Alonso (1980) tested eight sediment transport equations using seven sets of data and 265 total runs. Field data and flume data were utilized, the depths ranging from 1.13 inches to 22.7 inches, velocities ranging from 0.5 fps to 4.2 fps, slopes from 0.03 percent to 2.2 percent and sediment concentrations from 10 ppm to 61,000 ppm.

The Yalin equation only did an average job while the Yang (1973) total-load equation yielded the most accurate prediction. The Yang equation will be discussed in a later section. The Yalin equation's 95% confidence limits of the mean for predicted load/measured load ratio deviated significantly from 1.0, and the low limit was in fact about 1.5.

The Yalin equation was presented by Yalin (1972) as:

$$\frac{q_s \rho^{\frac{1}{2}}}{(\gamma_s D)^{3/2}} = 0.635 \frac{s}{\sqrt{\phi}} \left[1 - \frac{1}{as} \ln (1 + as)\right] \qquad (6.1)$$

where q_s is the sediment load in lb/ft-s, ρ is the fluid density in slugs/ft^3, γ_s is the sediment specific weight in water in lb/ft^3, D is a typical grain size in ft, ϕ is a reciprocal mobility number given by:

$$\phi = \frac{\gamma_s D}{\rho V_*^2} \qquad (6.2)$$

where V_* is the shear velocity in fps. The other two parameters, a and s, are given by

$$a = 2.45 \frac{\sqrt{Y_{cr}}}{W^{0.4}} \qquad (6.3)$$

and

$$s = \frac{1}{\phi Y_{cr}} - 1 \qquad (6.4)$$

(6.5)where Y_{cr} is from the Shields curve and is a function of either

$$\frac{V_{*cr}D}{\nu} \quad \text{or} \quad \frac{\overline{\gamma_s D^3}}{\rho \nu^2}$$

depending on the version of the Shields curve available, and W is the solid/fluid density ratio (ρ_s/ρ). The modified Shields curve from Yalin (1972) is shown in Figure 6.1. For computerization, the Shields curve will need to be tabulated, or have functions fitted to various sections of it.

Modified Yalin (CREAMS) Equation

Foster et al. (1980, 1981) developed a model for estimating erosion and sediment yield from field-sized areas. They utilized a modified Yalin equation from Foster and Meyer (1972) for overland flow and rill flow sediment transport. The modification was necessary to take varying sediment sizes and densities into account. The sediment transport is calculated using the following steps:

1) Calculate the excess tractive force for each size of particle, assuming only that size is present (denoted δ_i).
2) Calculate the non-dimensional transport for each sediment size, assuming only that size is present (denoted P_i).
3) Calculate the total excess tractive force for the mixture, by summing the individual excesses, e.g.

$$T = \sum_{i=1}^{n_s} \delta_i \qquad (6.5)$$

where n_s is the number of difficult sediments.

4) Calculate the individual non-dimensional transport of each size in the mixture by multiplying P_i by δ_i/T (denoted $(P_e)_i$).
5) Calculate the individual transport capacity for each size in the mixture,

$$W_{si} = (P_e)_i \, (S_g)_i \rho_w g d_i V_* \qquad (6.6)$$

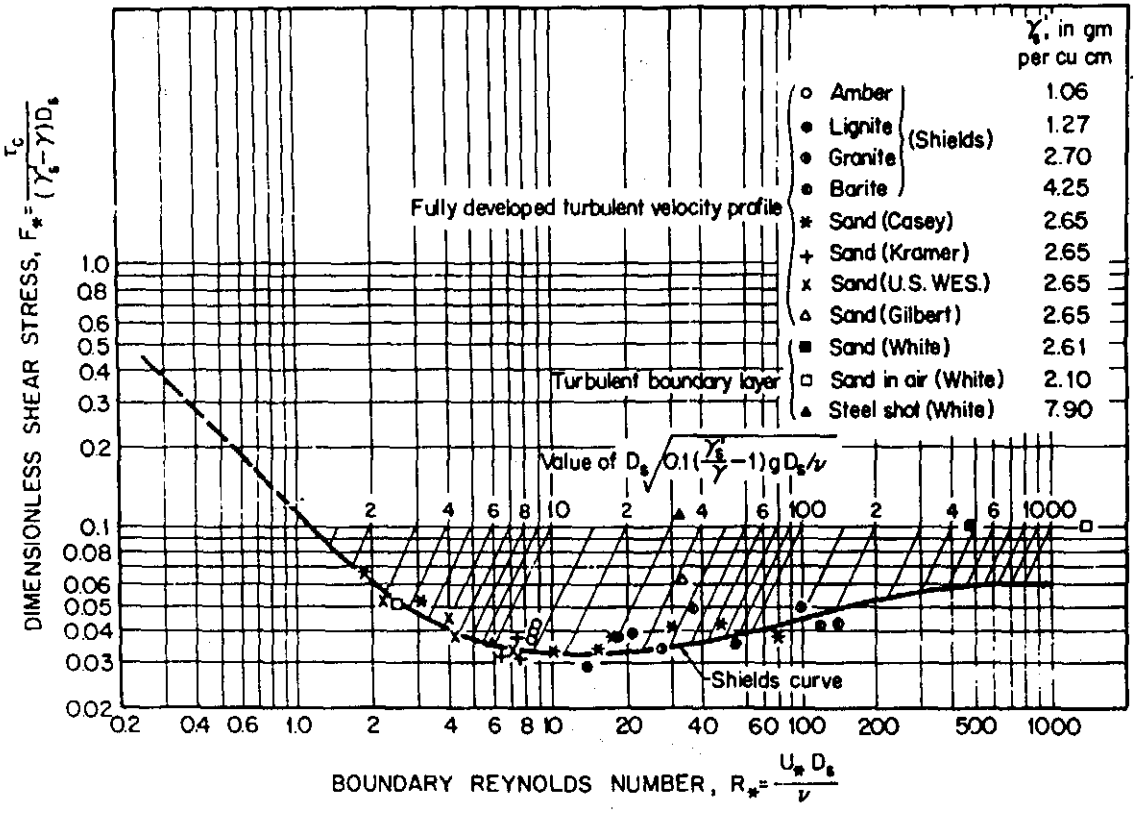

Figure 6.1 Shield's diagram

where W_{si} is the transport capacity.

6) Redistribute the transport capacity according to the sediment load for each size, and calculate the required non-dimensional transport by,

$$P_{i,\,req} = \frac{q_{si}}{(S_g)_i\, g \rho_w d_i V_*} \tag{6.7}$$

7) Calculate the fraction of transport capacity used by those particles with $W_{si} > q_{si}$ by,

$$SPT = \sum_{i=1}^{n_s} (P_{ireq}/P_i)K_i \tag{6.8}$$

where $K_i = 1$ for $W_{si} \geq q_{si}$, and $K_i = 0$ for $W_{si} < q_{si}$.

8) The excess transport to be distributed is then

$$E_{xc} = 1 - SPT \tag{6.9}$$

9) Determine the total excess tractive force for those particles for which W_{si} q_{si}

$$SDLT = \sum_{i=1}^{n_s} \delta_i \ell_i \tag{6.10}$$

10) Distribute the excess according to δ_i fractions and q_{si}

$$T_{ci} = (\delta_i/SDLT)\,(E_{xc})\,(P_i)\,(S_g)_i g \rho_w d_i V_* \ell_i \tag{6.11}$$

and

$$T_{ci} = q_{si} K_i \tag{6.12}$$

where ℓ_i and K_i are as above.

11) Repeat steps 6-10 until either all $T_{ci} \leq q_{si}$ or all $T_{ci} \leq q_{si}$. If all $T_{ci} \leq q_{si}$ then proper T_{ci}s have been found. If all $T_{ci} \geq q_{si}$ then all of the excess will be given to the particle size, so redistribute by

$$SMUS = \sum_{i=1}^{n_s} (P_{i,req}/P_i) \tag{6.13}$$

and

$$T_{ci} = q_{si}/SMUS \tag{6.14}$$

Data presented by Foster and Meyer (1972) shows that this method does a fair job for 7 and 10% slopes and 70 and 100 foot refined plots the prediction for shorter plots and shallower slopes was poor at best.

The Yalin equation in its original form and in its modified form utilize the Shields' diagram to relate the critical shear Reynolds' number to the critical dimensionless lift force. A problem arises because Shields' curve was developed for coarse, cohesionless granular solids. Mantz (1977) extended the Shields' diagram to include fine grains and flakes. The grains tested ranged in diameter from 15 μ to 66 μ. Mantz plotted his own data together with data from the literature as a Shields-type diagram. The regression line of the low Reynolds' number data is greatly different in slope from the Shields' curve, crossing at a Reynolds' number of about 1.2. The extended Shields' diagram presented by Mantz has a confidence limit that would allow a multitude of curve shapes including two straight lines intersecting at a boundary Reynolds' number of about 8. Mantz's extended curve is shown in Figure 6.1. Foster et al. (1980) used the Mantz (1977) relationship for the Shields curve for their modified Yalin equations.

Yang Equation

Yang (1973) proposed a sediment transport equation based on unit-stream- power concepts. In a previous study, Yang (1972) found through

regression that the most dominant flow characteristic for sediment transport is unit-stream-power, defined as the product of the average flow velocity and the energy slope of the flow. Unit-stream-power as defined by Yang (1973, pg. 1680) is:

> "...the time rate of change of potential energy expenditure per unit weight of water in an alluvial channel,..." (Yang, 1973, pg. 1680).

He expressed the sediment transport concentration as

$$\ln C_t = \alpha + \beta \ln (VS - V_{cr}S) \tag{6.15}$$

where C_t is the sediment concentration, VS is the unit-stream-power, $V_{cr}S$ is the critical unit stream power required at incipient motion, α and β are parameters. The difference, $(VS - V_{cr}S)$, is denoted the effective unit stream power. Yang states that the equation was verified by 1,225 sets of laboratory data and 50 sets of field data and that most of the data exhibits a correlation coefficient of 0.98 or higher. Yang (1973) improves on this equation by making the unit-stream-power parameters dimensional.

The Yang equation was developed for noncohesive sand with a median sieve diameter greater than 62 μm and a specific gravity of 2.65. The energy slope is approximated by the water surface slope. Yang's final proposed equation is

$$\ln C_t = 5.435 - 0.286 \ln \left[\frac{wd}{\nu}\right] - 0.457 \ln \left(\frac{V_r}{w}\right) + \left[(1.799 - 0.49 \ln\left(\frac{wd}{\nu}\right) - 0.314 \ln \left(\frac{V_*}{w}\right)\right] \ln\left(\frac{VS}{w} - \frac{V_{cr}S}{w}\right) \tag{6.16}$$

where w is the particle fall velocity, d is the particle diameter, ν is the kinematic viscosity, and V_* is the shear velocity. The dimensionless quantities, $\frac{wd}{\nu}$ and $\frac{V_*}{w}$ might be denoted the fall Reynolds' number and the dimensionless shear velocity, respectively.

Alonso (1980) and Alonso et al. (1981) found that the Yang equation yielded the most accurate prediction of eight transport equations tested, especially for sand transport. In Alonso (1980) the mean ratio of predicted and measured load for the Yang equation fell close to 1.0 for both field and flume data with the 95% confidence interval including unit for all three groups of data. Yang's equation yielded predictions for field data (ratio mean = 1.01) and the flume data with depths greater than 70 particle diameters (ratio mean = 0.99).

The Yang equation uses a single particle size for its determination. An algorithm must be developed to utilize this equation for multi-particle size transport. A Foster et al. (1980, 1981) style approach might be utilized, but more research is necessary to validate the procedure. Once that algorithm can be developed, the Yang equation shows promise for accurately estimating sediment transport in channelized flows.

Ackers and White Equation

Ackers and White (1973) developed a sediment transport equation based upon sediment mobility considerations and dimensional analysis. In the development, noncohesive sediments and steady-uniform flow are assumed. The data used for verification excludes supercritical and transition flows. The maximum Froude number is 0.8. The calculation procedure is spelled out in Appendix II of Ackers and White (1973).

The Ackers and White equation procedure is as follows:

1) Calculate the dimensionless particle size, D_{gr}, for the representative particle diameter by:

$$D_{gr} = D(g(S_s - 1)/\nu^2)^{1/3} \qquad (6.17)$$

2) Determine the transition exponent, n; the initial motion Froude number, A; the sediment transport function exponent, m; and the sediment transport function coefficient, C; by:

$$n = 1.00 - 0.56 \log_{10} D_{gr} \quad (\text{if } D_{gr} > 60 \; n = 0.0) \tag{6.18}$$

$$A = \frac{0.23}{\sqrt{D_{gr}}} + 0.14 \quad (\text{if } D_{gr} > 60, \; A = 0.17) \tag{6.19}$$

$$m = \frac{9.66}{D_{gr}} + 1.34 \quad (\text{if } D_{gr} > 60, \; m = 1.50) \tag{6.20}$$

$$\log_{10} C = 2.86 \log_{10} D_{gr} - (\log_{10} D_{gr})^2 - 3.53$$
$$(\text{if } D_{gr} > 60, \; C = 0.025) \tag{6.21}$$

3) Compute the particle mobility, F_{gr}, by:

$$F_{gr} = \frac{V^n}{\sqrt{g \, D(S_s - 1)}} \left[\frac{V}{32 \log_{10} \left(\frac{\alpha d}{D} \right)} \right] \tag{6.22}$$

where V is shear velocity, d is flow depth, α is rough-turbulent equation coefficient equal to $12.3D/k_s$, where k_s is a linear measure of grain roughness, and V is the new velocity of the flow.

4) Calculate dimensionless sediment transport rate, G_{gr}, by:

$$G_{gr} = C\left(\frac{F_{gr}}{A} - 1 \right)^m \tag{6.23}$$

5) Convert G_{gr} to sediment flux $\overline{X}$, by

$$\overline{X} = \frac{(G_{gr}) \, S_s \, D}{\partial} \left(\frac{\nu}{\nu_*} \right)^n \tag{6.24}$$

Equations (6.18) through (6.21) are based on measured data from almost 1,000 flume experiments. Uniform sediments were used, with flow depths up to 0.4 m (15.75 inches). One problem with the method is that no guidance is given for choosing k_s. No term for slope is utilized, although it is intrinsic to the velocity and shear velocity. The relationship is only good for sand size and larger particles, as D_{gr} must be > 1 by Ackers and White's recommendations (D ≃ 0.04 mm at 15°C).

Laursen Equation

Laursen (1958) developed a total sediment load equation for streams. His procedure is a combination of a multiple particle size average concentration equation and a graphical representative of total load/bed load relationship for dimensionless critical velocity. His equation.

$$\overline{c} = \sum p \left(\frac{d}{y_o}\right)^{7/6} \left(\frac{\tau_o'}{\tau_c} - 1\right) f \frac{\tau_o/\rho}{w} \qquad (6.25)$$

where p is the percentage of particles in fraction with representative diameter, d in feet, y_o is the depth of flow in feet, τ_o is the particle boundary shear, τ_c is the critical tractive force, and f ($\tau_o/\rho/w$) is given graphically as a function of ($\tau_o/\rho/w$), where τ_o is the average boundary shear, ρ is the fluid density and w is the sediment fall velocity in fps. The particle boundary shear is given by

$$\tau_o' = \frac{V^2 \, d^{1/3}}{30 \, y_o^{1/3}} \qquad (6.26)$$

and the critical tractive force is given by

$$\tau_c = C \, d \qquad (6.27)$$

where C is a coefficient dependent on the sediment characteristics and the flow near the boundary. A C value of 4 was used for most of the development analysis.

The data used for the development of this relationship included particle diameter from 0.011 mm to 4.08 mm, with $\overline{c}$ values from 0.001 to 11.1 in percent by weight (parts per 100) or 10 ppm to 111,000 ppm.

Ranga, Raju, Garde and Bhardwaj Equation

Ranjga Raju et al. (1981) presented sediment transport relationships for the total load in alluvial channels. They defined total load as bedload

plus suspended load originating from the bed. Wash load was assumed to be negligible. The data for the analysis were taken from the literature and ranged from 0.017 m (0.7 inches) to 10.0 m (33 ft) in depth, velocities of 0.126 m/s (0.413 fps) to 2.5 m/s (8.2 fps), and slopes of 0.0001 to 0.0229. Their final equation,

$$\varphi_T = 60\ (\tau_*')^3 \left(\frac{\tau_o'}{\tau_o}\right)^{-3m} \qquad (6.28$$

is claimed to be applicable for the range

$$0.05 \leq \tau_*' \left(\frac{\tau_o'}{\tau_o}\right)^{-m} \geq 1.0 \qquad (6.29)$$

where τ_o' is the average bed shear stress corresponding to grain roughness, τ_o is the average bed shear stress, τ_*' is the dimensionless grain shear stress, m is a constant based on dimensionless shear velocity, v_*/w, and φ_T is the dimensionless total load transport.

The dimensionless grain shear stress is given by

$$\tau_*' = \frac{\gamma_f R_b' S}{(\gamma_s - \gamma_f)\ d} = \frac{\tau_o'}{(\gamma_s - \gamma_f)d} \qquad (6.30)$$

where R_b' is from

$$U = \frac{24}{d^{1/6}} R_b'^{2/3} S^{1/2}, \qquad (6.31)$$

and γ_f is the fluid unit weight. γ_s is the sediment unit weight. S is the slope, d is the sediment diameter, and U is the average velocity. The average shear stress is

$$\tau_o = \gamma_f R_b S$$

where R_b is the flow hydraulic radius. Therefore, equation 6.31 becomes

$$\Phi_T = 60 \left[\frac{\gamma_f R_b' S}{(\gamma_s - \gamma_f) d} \right]^3 \left[\frac{\gamma_f R_b' S}{\gamma_f R_b S} \right]^{-3m} \tag{6.32}$$

The exponent, m, is fitted from channel data. For a dimensionless shear velocity less than 0.5, m is equal to zero. For large values, the equation is:

$$m = 0.2 \frac{V_*}{w} - 0.10 \tag{6.33}$$

The fall velocity equation of Ruby is used,

$$w = \frac{36\nu^2}{d^2} + \frac{2 (S_s - S_f) d}{3} - \frac{6\nu}{d} \tag{6.34}$$

and V_* is taken as $g R_b S$. No units were given for any parameters. Calculations by this writer indicate that overland flow and fine particles are outside of the range of applicability given by equation 6.34.

Other Equations and Conclusions

Other equations could be cited for use in an erosion model, i.e. Li et al. (1977), Einstein (1950), and numerous others. Most, if not all, exhibit the same general trends and have common constraints, such as non-cohesive sediment and shallow slopes. Their basis is theoretical, but all are empirical in their final form, making applications outside of their range of verification questionable at best.

Based on the above analysis, it can be recommended that a physically-based erosion model should utilize the Yalin equation as modified by Foster and Meyer (1972). This should only be done until such a time as data collection for steep slopes (< 3%) and shallow flows be used to develop a Yang (1973) style equation for multiple particle sizes. The stream-power concept seems to have the most promise for sediment transport prediction.

CHAPTER 7 RILL FORMATION

The formation of rills is indicative of a severe erosion hazard. The rills provide channels for concentrated runoff, with high detailing and transporting capability as compared to non-rill overland flow. Accordingly, a major portion of this study is devoted to developing relationships to predict rill formation.

Rill Equilibrium Properties

It is important to know the rill properties after the rills have developed to equilibrium. This knowledge guides examination of the processes producing such a shape.

Mosley (1972, 1974) used a layer bin of a sand-silt mixture under artificial rainfall to examine areal rill network properties at equilibrium. He related sediment discharge from each rill network to river-morphology-style parameters calculated from the rill network geometry and found that the rill network pattern is dendritic in nature, with a strong resemblence to a watershed drainage network of rivers and streams (see Figure 7.1). The equilibrium sediment discharge was most strongly related to the total length of the rill network, while the equilibrium sediment concentration and the equilibrium sediment contribution were most strongly related to the original soil surface shape. He concluded that rill drainage density, or the length of rill per unit area, is a crucial consideration in both analysis and control of soil erosion. His reasoning for this conclusion is based on the analysis-of-variance for sediment yield in his study and the realization that a higher rill drainage density indicates that a greater proportion of the eroding surface is under direct influence of channelized flow.

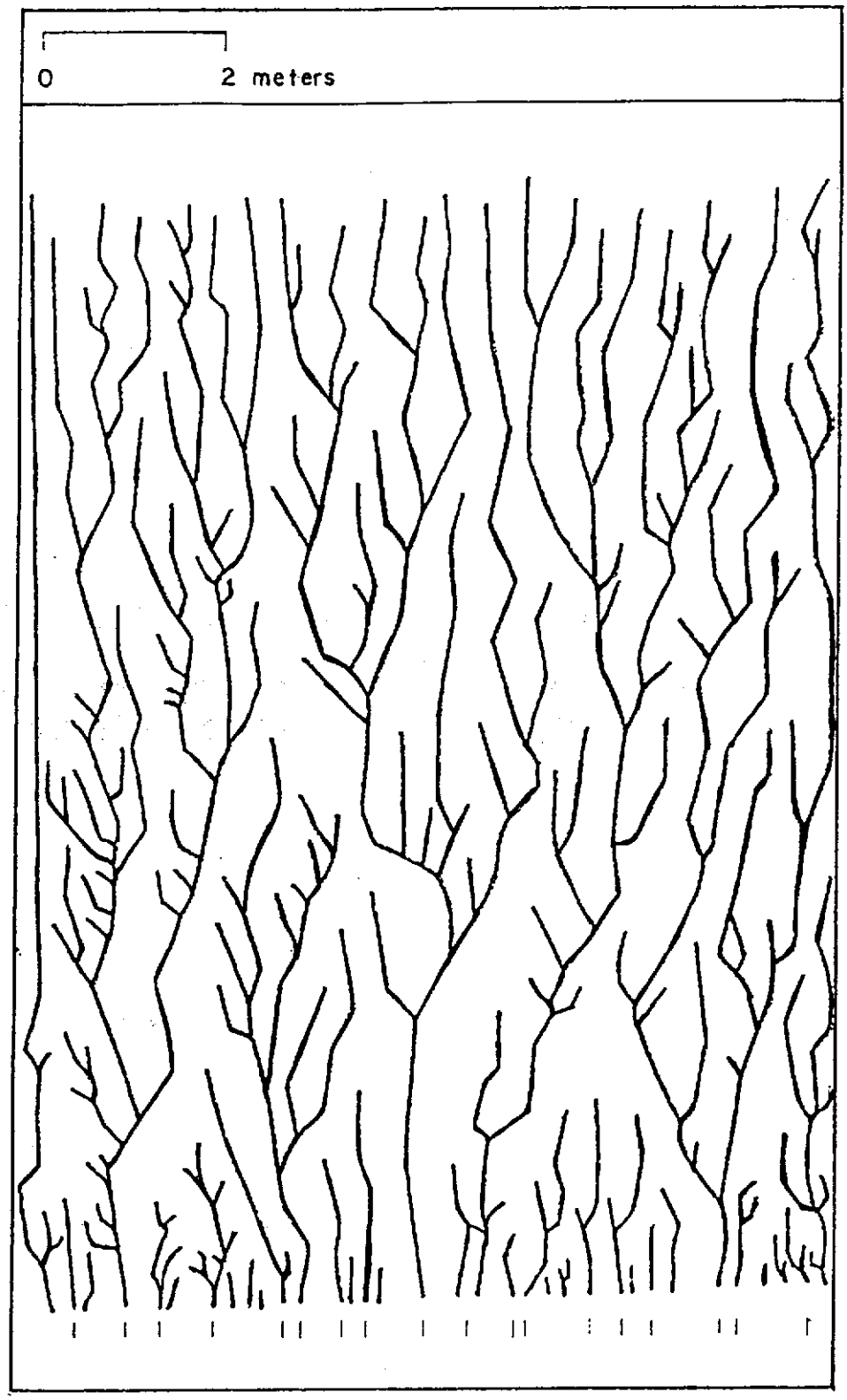

Figure 7.1 6.9% surface from Mosley (1972) showing a sample rill distribution

Li, Ponce, and Simons (1980) proposed a model to estimate the rill density, defined as the percentage of plot width that is within rill walls. They developed equations for rill density under both laminar and turbulent flow assumptions. Unfortunately, the equations contain numerous empirical constants, requiring fitting. In addition, the development of the equations utilizes the concept of armoring of the surface due to large, untransportable particles. Foster and Lane (1981) commented that agricultural soils do not armor in this fashion, and that the D_{84} criteria used in the Shields' diagram (as proposed by Li et al.) is also not appropriate for agricultural soils. It must be noted that agricultural soils do armor through development of a surface seal or crust, but the D_{84} criteria of Li et al. would not account for that armoring.

It can be concluded from Mosley's work that the areal equilibrium shape is dendritic and that thin shape affects the sediment delivery characteristics of the network. The work of Li et al. indicates that the equilibrium density of this pattern at any cross section on an eroding plane can be estimated if the appropriate parameter values can be determined.

The cross sectional pattern of the rills at equilibrium must also be considered. It is this shape that dictates the shear stress distribution and the flow conditions that prevail at equilibrium. Lane and Foster (1980) stated that the rill shape can be taken as rectangular with the width related to the flow by:

$$W = aQ^b \qquad (7.1)$$

where W is channel width, Q is flow rate, and a and b are constants. For the CREAMS model, however, Foster et al. (1980) stated that:

> "A triangular cross section, a reasonable approximation to most field channels, was used to develop the friction slope curves because the equations are simpler." (Page 52).

Rohlf (1981) utilized a channel cross section composed of straight-line segments. If the number of segments is allowed to be large, a very general shape will be formed. Rohlf examined Foster's rectangular section as defined in equation 7.1 along with the segmented section. He found that the segmented section formed a semi-circular shape at equilibrium unless an erosion resistant layer is encountered, in which case the shape goes to rectangular. Comparing his predictions to experimental results from other researchers, Rohlf indicated that the equation developed for sediment discharge utilizing a rectangular cross section yielded a better prediction than his segment-cross section model. It must be noted that there are many differences between the two algorithms, other than cross section shape, so shape conclusions must be drawn with caution.

Schwab et al. (1966) state that the equilibrium shape of a natural stream is parabolic rather than a rectangle. It seems appropriate, then, to utilize a line- segment shape more similar to parabolic for rill analysis, such as a trapezoidal shape or some higher order polygon. On that basis and on the basis of Rohlf's work, a segmented cross section is used in the study under consideration.

Rill Development

The development of a rill network is one of the least understood processes in hydrology. Very little work has been attempted in this area and it is the major emphasis of the study at hand. Both the initiation and the propagation of rills will be considered.

Initiation of Rills

An excellent qualitative discussion of the initiation of rills is given by Leopold et al. (1964), in which they describe the concept of micropiracy. This concept was explained by Horton (1945) as a consequence of the overtopping of ridges between adjacent microrills, to unify their watersheds, and to form a layer channel.

As indicated through Horton's ideas, the topography of the soil surface greatly affects the overland flow, and hence, the soil erosion. The watershed divides on the surface dictate the volume of water available for concentration in that watershed. Therefore, if a surface is very smooth, much water can concentrate because the entire area runs to one channel. At the other extreme, if the surface is very rough, little water can initially concentrate, so erosion is initially low, and rilling is slight.

For a given type of surface roughness, a change in slope will affect the erosion through a reduction in the sediment transporting power of the concentrated flows. Foster and Wischmeier (1974) recognized the importance of such a slope change and developed an algorithm to calculate an LS factor for the USLE for irregular slopes. Their factor gives much higher erosion for a convex shape slope than for a concave shape. This trend has also been observed in the field.

Seepage faces are important whenever moisture and a steep soil face are found together. In the case of soil erosion, as mini watersheds on the soil surface fill, the soil "walls" containing the flow saturate (or nearly saturate), reducing their stability. "Failure" of these soil walls allows more rapid concentration of flow than through micropiracy alone. Seepage is also important when considering rill

wall stability. The sloughing of rill walls into the flow adds a large, easily detached mass to the flow and changes the shape of the rill channel.

Propagation of Rills

After rills begin, they grow in areal influence and depth. The major mechanisms that cause this growth are flow shear and rill wall sloughing. Both mechanisms change the cross sectional shape of the rills and hence, affect the rill flow and sediment carrying characteristics.

The shear stress applied by flowing water has been a topic of research for many years. Average bed shear stress is given by Morris and Wiggert, 1972):

$$\tau_o = \gamma R_h S \qquad (7.2a)$$

for shallow slopes and

$$\tau_o = \gamma R_h \sin\theta \qquad (7.2b)$$

for general slopes, where τ_o is the average bed shear stress, γ is the specific weight of the fluid, R_h is the hydraulic radius of the flow. S is the bed slope and θ is the bed angle. Both equations assume uniform flow and are obtained by setting the gravitational component in the flow direction equal to the bed frictional resistance and solving for τ_o. Equations 7.2a and 7.2b give no indication of the distribution of this shear. The velocity distribution largely dictates the shear stress distribution, at least on the average. Raudkivi (1976) states:

> "It is generally assumed that the orthogonals to the isovels are surfaces of zero shear. This is true only on the average. At any instant, however, there is a turbulent shear stress on these orthogonals caused by the turbulent momentum transfer." (pp. 247-248).

Raudkivi goes on to state that, assuming that the isovels are surfaces of zero shear, the bed shear stress between isovels is given by,

$$\tau_o = \frac{\gamma \Delta A \sin\theta}{L} \qquad (7.3)$$

where τ_o is the average bed shear stress between the chosen orthogonals, L is the bed length between those orthogonals, ΔA is the area of water contained between those orthogonals and θ is the bed angle.

Many researchers have examined the shear distribution using this concept and each has used a slightly different manner to calculate ΔA. For example, Leighly (1932) developed a graphical method to obtain this area by drawing a cross section of the channel, superimposing a net formed by the isovels and their orthogonals, and measuring the area contained by the channel bottom, the isovel orthogonals and the line (or point) of maximum velocity. Lane (1953, 1955) utilized a power equation to represent the velocity with respect to the distance from the bed. A membrane analogy and numerical solutions were utilized to calculate the shear distribution for triangular, rectangular and trapezoidal cross sections. Rohlf (1981) utilized Lane's power function concept along with the assumption that the orthogonals to the isovels are perpendicular to the channel boundary. Using straight line channel segments, Rohlf derived an equation for the incremental shear stress.

A simpler method for calculating incremental shear stress was put forth by Lundgren and Jonsson (1964). They found that, for shallow channels, a method using channel bottom normals proved sufficient. Essentially, lines normal to the channel bottom extending to the surface

are calculated for each channel segment in question and the area formed by the normals, the surface and the channel bed is easily calculated, especially for straight line segmented channels. Their numerical solution showed little difference in prediction between their area method and the velocity distribution method, with much simpler analysis. The authors state that the channel must be smooth, not polygonal. However, it would seem that a polygon with a large number of segments would approach their method. Figure 7.2 shows their results for 5 different methods of analyses. Figure 7.3 shows data from Replogle and Chow (1966) and the prediction of Foster's (1982) equation, Rohlf's (1981) equation and Lundgren and Jonsson's method using a segmented channel (two to ten segments) to represent the semi-circular channel of Replogle and Chow. The shear distribution found using the latter method is discussed in more detail in the sediment generation component verification section of this report.

Rill wall sloughing is the other major mechanism by which the rills propagate. Few erosion models have considered this phenomenon. but we have observed it to be very important during erosion events. Rohlf (1981) observed rill wall failures in motion pictures taken of rills and states that the rill wall stability could be added to his model. Wu et al. (1982) included rill wall stability by setting an upper limit on the rill wall gradient (their rills are triangular). Once that gradient is reached, it is assumed that the wall falls to a new, stable slope gradient and the soil material is deposited into the rill. Deposition must be considered in detail, so Wu et al. ignore the sloughed mass in their model. Wu et al. stated that the limiting and

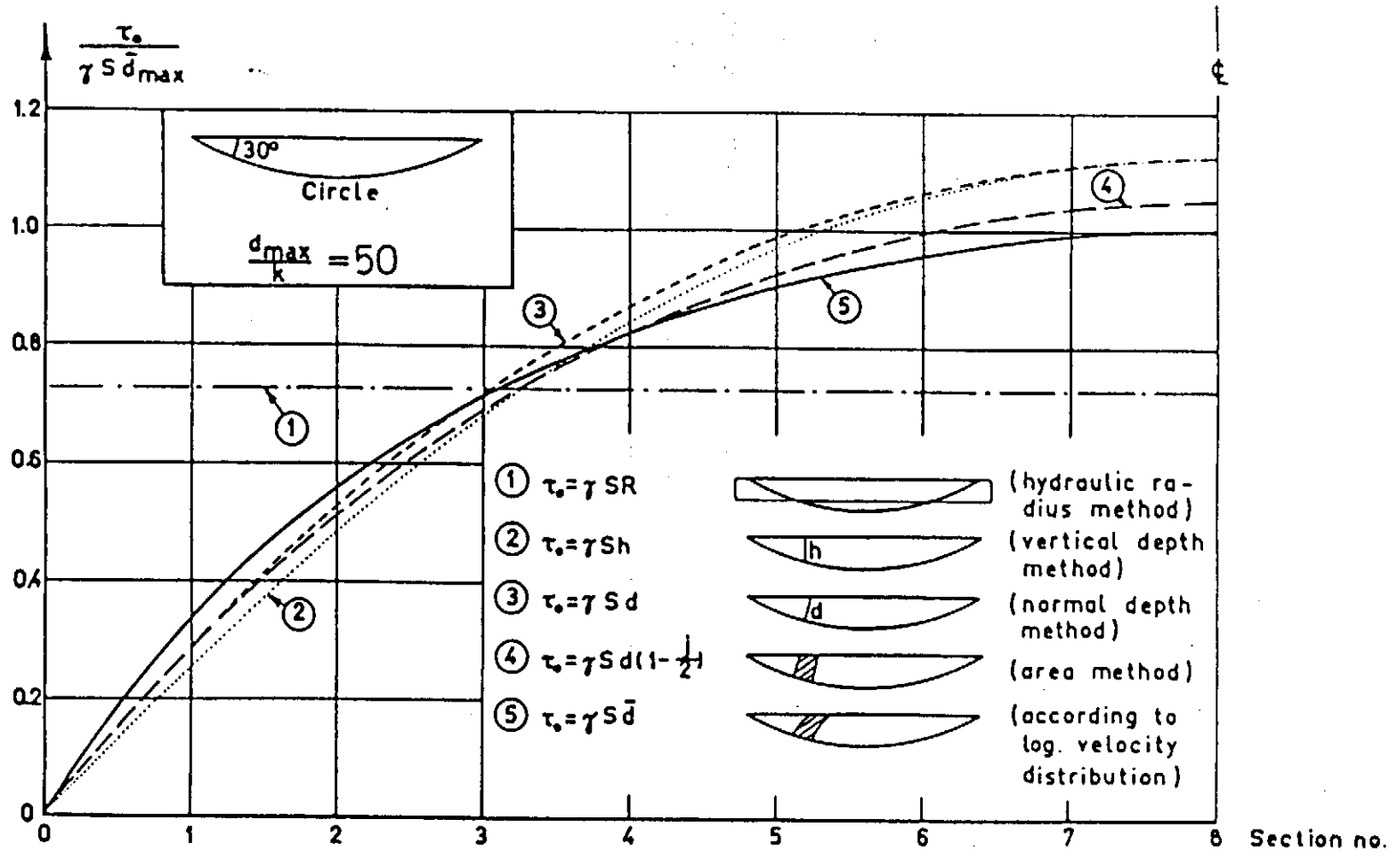

Figure 7.2 Comparison between five different methods of determining the shear stress distribution (from Lundgren and Jonsson (1964)

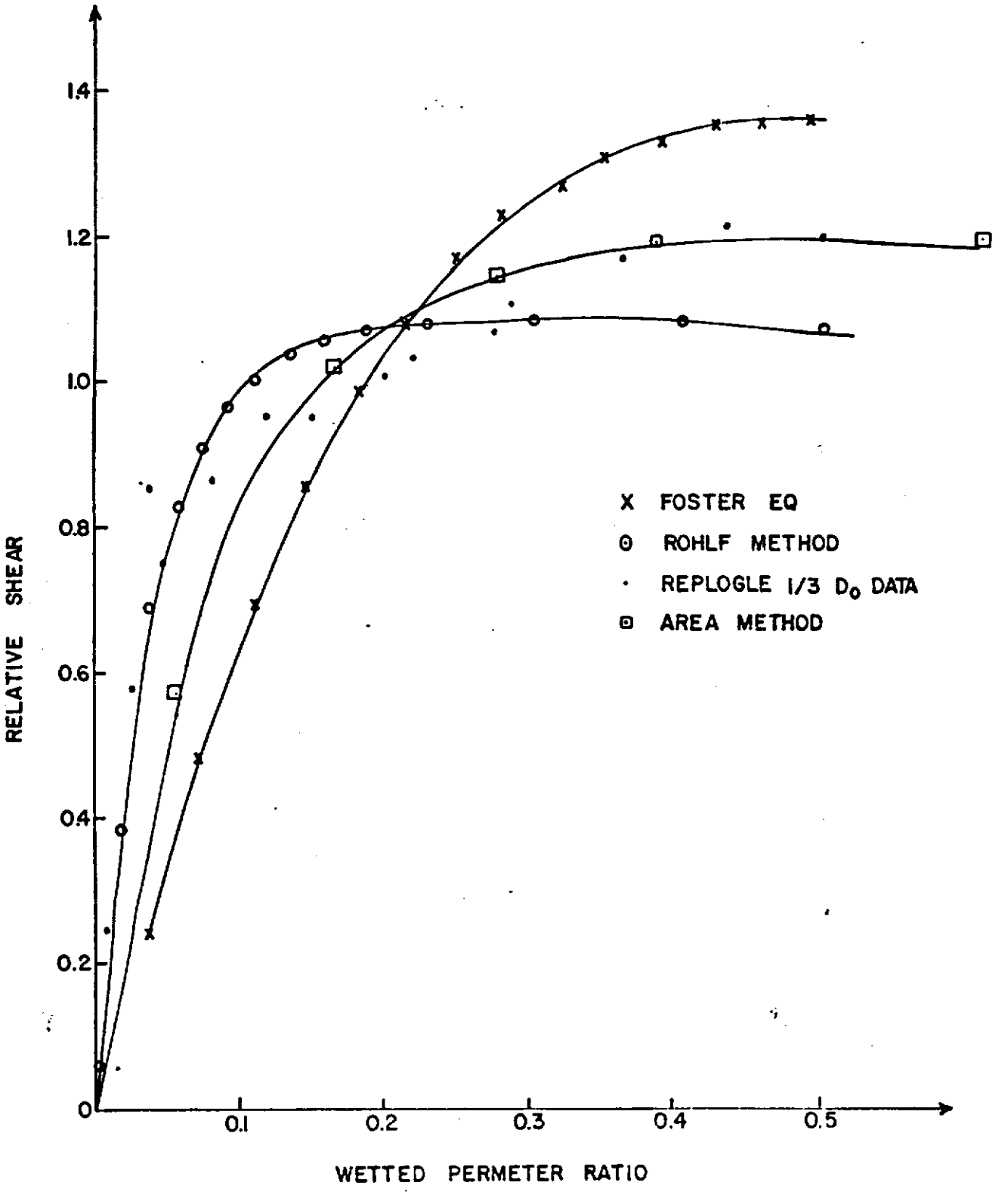

Figure 7.3 Comparison of methods to estimate relative shear with data of Replogle and Chow (1966)

equilibrium gradients could be set by experience. It would seem that a detailed slope stability analysis is needed to derive simple relationships for rill wall stability consistent with soil mechanics principles. At the present time, however, the Wu et al. approach is the best available.

Density Effects on Rill Formation

The effect of density changes in the soil profile on rill development have been observed by many researchers. The bottom of a tillage layer, for example, usually has a much lower erosion potential due to its higher density. Lane and Foster (1980) stated that a rill will erode downward until it reaches a nonerodible (or less erodible) layer and then widens. Rohlf (1981) used some unpublished data of Foster and observed the same phenomenon. A segmented cross section, as discussed in the shear stress section, would require keeping track of which sections have reached the less erodible layer and would change shape dramatically, eventually approaching the rectangular shape assumption used in the CREAMS model (Foster et al., 1980).

CONCLUSIONS

The following conclusions can be drawn about rill formation:

1) A detailed representation of the soil surface is necessary to determine the number of rill channels that will form.

2) A multi-segmented rill cross section can be used to calculate the shear distribution causing rill formation and propagation.

3) The layering effects of tillage must be taken into account to determine rill propagation, and

4) A "limiting gradient" approach to rill wall stability can describe the sloughing phenomenon, albeit greatly simplified.

CHAPTER 8 MODEL DEVELOPMENT

The Kentucky Erosion Model (KYERMO) was developed as a research tool to isolate the important aspects of the rainfall/runoff/erosion process. The development goals were to:

1) Include as many known aspects of the processes as possible, even if complete development will not be undertaken immediately.

2) Utilize measureable parameter relationships whenever possible.

3) Minimize limiting assumptions, such as shallow slopes for flow equations, to allow applicability to steep slopes.

The model consists of a main program and 27 subroutines. It is written in Microsoft FORTRAN for use on an IBM PC, requiring approximately 200K of random access memory to run, a disk drive for input and a printer for output. It must be noted that this model is in constant flux and is continually being improved as experience is gained in its use and as more research data becomes available.

Main Program and Support Programs

The MAIN program of KYERMO provides the framework for the model. The support programs (INITIA, PRINTO, RAINFA, MOVE, PRINT1, PRINT2, PRINT3) provide initialization, bookkeeping and output capabilities. The support programs are called from MAIN (except for PRINT , which is called from INITIA). Each will be discussed in detail in subsequent paragraphs. A software listinf for all programs is given in Appendix I.

The structure of the MAIN program can be represented by the flow chart in Figure 8.1. The generation and routing calls are to sub-main programs rather than to the actual subroutines to facilitate changes in program structure as the program is improved through experience and further research. A list of all variables is given in Appendix VI.

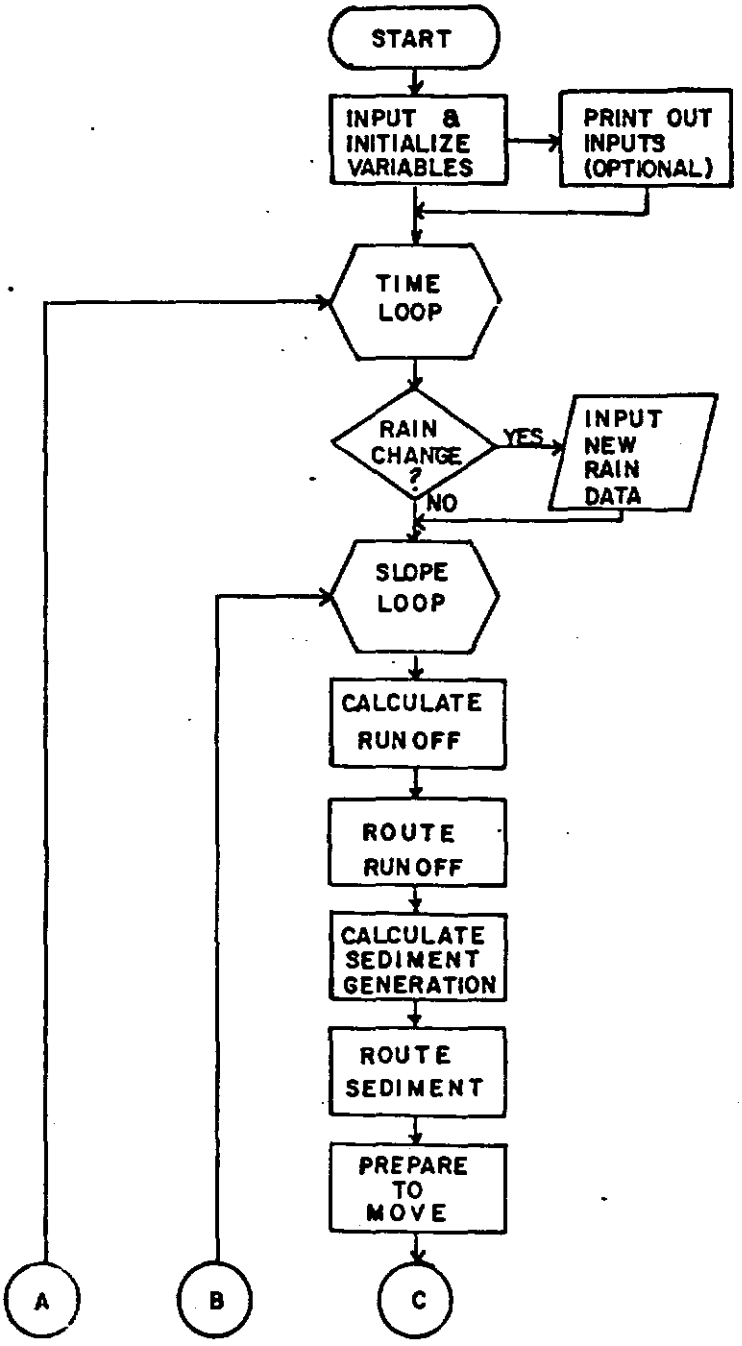

Figure 8.1 Flow chart of main program (see continuation on following page)

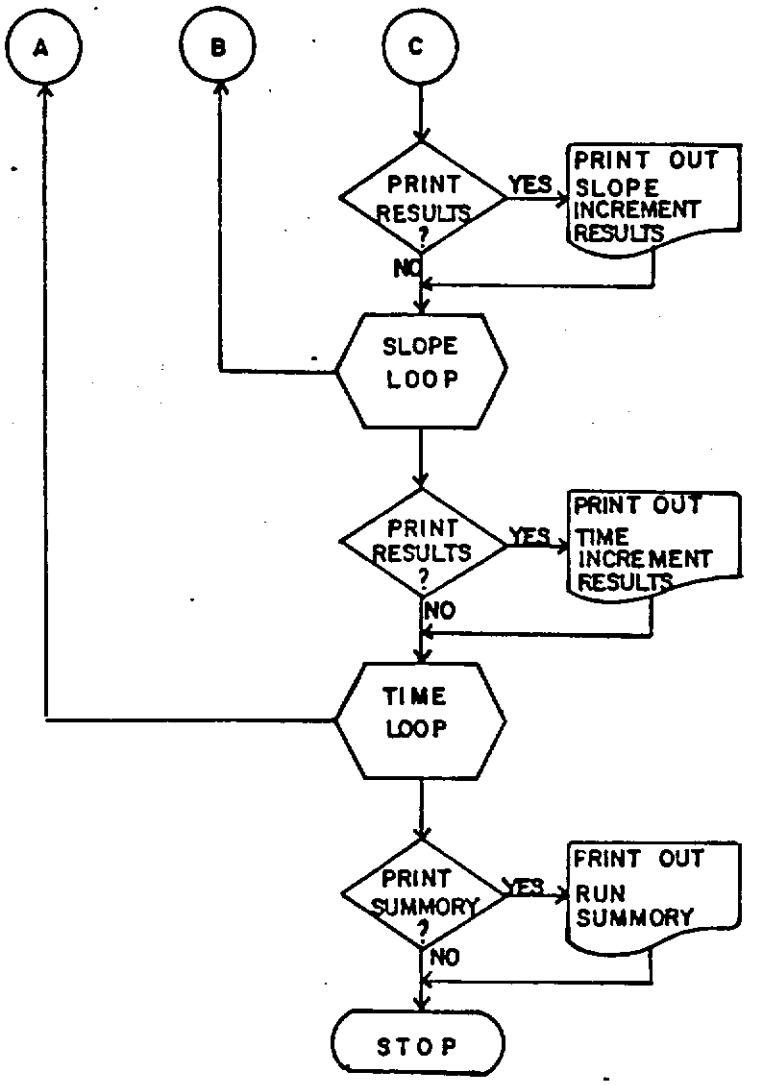

Figure 8.1 Continued

The INITIA subroutine is the parameter input and initialization routine for KYERMO. In this subroutine parameter values are read from disk and set up as variables for use by the rest of the model. In addition, the subroutine PRINTO is also accessed by INITIA. PRINTO can be used to print all of the input parameters if desired. A list of INITIA inputs is shown in Table 8.1.

The RAINFA subroutine is a second input subroutine. It reads rainfall intensity drop size distribution and energy data as the program runs. It is accessed at times that are input during the previously read operation. A future modification will be to have options for 1) natural rainfall energy and drop-size distribution for the given intensity, or 2) Kentucky Rainfall Simulation energy and drop-size distribution, 3) Rainulator energy and drop-size distribution. or 4) the option to specify all rainfall characteristics. At the present time the only option is (4). RAINFA accesses its own print routine to output the input parameters. A list of the inputs for RIANFA is given in Table 8.2.

The MOVE subroutine is utilized before each space or time increment to reset those variables that are to be utilized again. It also calculates statistics for the PRINT1, PRINT2, and PRINT3 subroutines.

The output subroutines (PRINT1, PRINT2 and PRINT3) are used to print the statistics and run information for KYERMO. All have on/off options specified in INITIA. The PRINT1 routine outputs after every slope increment. The PRINT2 routine outputs after each time increment. The PRINT3 routine is used to generate output after the run is completed. The output parameters are given for PRINT1, PRINT2, and PRINT3 in Table 8.3. A listing of PRINT1 is given in Appendix I.

Table 8.1 INITIA Inputs

Variable Name	Dimension	Variable Description/Units
HPL	2	Horizontal Plot Length (m)
PN	1	Plow Width (m)
NJ	1	Number of Plot Increments (-)
NR(J)	10	Number of Rills in Each Increment (-)
NSEG(J,M)	10,10	Number of Initial Sediments in Each Rill (-)
NSS(J,M,MJ)	10,10,10	Number of Sub-Segments for Each Segment (-)
SO(J)	10	Plot Increment Slope (m/m)
HLINC(J)	10	Horizontal Plot Increment Length (m)
TS	1	Simulation Time (min)
DTM	1	Time Step (min)
ITRS	1	Time of Initial Rain Start (min)
TCELS	1	Ambient Temperature (°C)
KS(L)	2	Lab Saturated Hydraulic Condition (cm/hr)
SMC(L)	2	Lab Saturated Moisture Content (cc/cc)
B(L)	2	Log-Log Slope or Moisture Rel. Curve (-)
XI(L)	2	Log-Log Intercept of Moisture Rel. Curve (cmH_2O)
DMM(I)	10	Sediment Type Diameter (mm)
SS(I)	10	Sediment-Type Specific Gravity (-)
FDMM(I)	10	Matrix Fraction of Sediment Type (-)
RDFDMM(I)	10	Rain Detached Fraction of Sediment Type (-)
DS(L)	2	Final Degree of Saturation (-)
MC(L)	2	Initial Moisture Content (cc/cc)
PCL(L)	2	Percent Clay (%)
EF	1	Infiltration Rate Criterion (cm/hr)
EV	1	Infiltration Volume Criterion (cm)
N(J,M)	10,10	Rill Manning 'n' (-)
NS(J,M)	10,10	Sheet Manning 'n' (-)
RWSW(J,M)	10,10	Rill Watershed Width (-)
ISSD	1	Sheet Trans Ed Choice (-)
IRSD	1	Rill Trans Ed Choice (-)
RR(J)	10	Plot Increment Random Roughness (cm)
CC	1	Bubenzer-Jones Coefficient (g/min)
E1	1	Bubenzer-Jones Intensity Exponent (-)
E2	1	Bubenzer-Jones Energy Exponent (-)
E3	1	Bubenzer-Jones Percent Clay Exponent (-)
PSM	1	Maximum Potential Soil Splash (-)
PS3	1	Potential Soil Splash at 3 Drop Diameters (-)
ARDET(L)	2	Foster Detach Ed Coefficient (g/min)
BRDET(L)	2	Foster Detach Ed Exponent (-)
POφ	1	Print Option φ (-)
PO1	1	Print Option 1 (-)
PO2	1	Print Option 2 (-)
PO3	1	Print Option 3 (-)
R1(J,M)	10,10	Flow ICTN Indicator (-)
K2(J,M)	10,10	Flow ICTN Indicator (-)
K3(J,M)	10,10	Flow ICTN Indicator (-)
RX(J,M,MJ)	10,10,10	Initial Rill Cross-Section (K Value) (cm)
RY(J,M,MJ)	10,10,10	Initial Rill Cross Section (K Value) (cm)

Table 8.2 RAINFA Inputs

Variable	Units	Fortran Format	Data Line	Item #
Rainfall Rate	cm/hr	F	1	1
Rainfall Energy	Joules/cm^2	F	1	2
Rainfall Duration	Min	I	1	3
Next Rainfall Start Time	Min	I	1	4
Rainfall Drop Size Distribution:				
Drop Class 1-12	Decimal Fraction	12F	2	1→12
Drop Class 13-24	Decimal Fraction	12F	3	1→12
Drop Class 25-28	Decimal Fraction	4F	4	1→4

In addition to the initialization and print routines, the framework formed by the MAIN program and its support routines includes the following four components:

1) Runoff generation component.

2) Runoff routing component,

3) Sediment generation component, and

4) Sediment routing component.

Each of these components will be discussed in subsequent sections.

Runoff Generation Component

The runoff generation component consists of its sub-main program, RUNGEN, and three subroutines: SURSTO, INFILT, and RUNOFF. These three subroutines calculate surface storage, infiltration rate, volume, runoff rate, and RUNGEN, respectively. All of the subroutines are listed in Appendix II.

In order to predict surface storage, the subroutine SURSTO utilizes the plot slope and an index of surface roughness termed "random roughness" (Allmaras et al., 1966) to estimate total available surface

Table 8.3 PRINT2 Outputs

Variable	Variable Description (Units)
J	Current Slope Increment (-)
T	Current Time (min)
HDDSL	Horizontal Distance Downslope (m)
F(J)	Infiltration Rate (cm/hr)
V(J)	Infiltrated Volume (cm)
QO	Interflow Out of Increment (cm/hr)
QI	Interflow into Increment (cm/hr)
RO(J)	Runoff Rate (cm/hr)
SSTO(J)	Potential Surface Storage (cm)
SSO(J)	Surface Storage Filled (cm)
M	Rill Watershed under consideration (-)
QSHEET(J,M)	Sheet Flow Rate (cc/sec)
QRILL(J,M)	Rill Flow Rate (cc/sec)
I	Sediment Particle Type (-)
RDET(I,J)	Raindrop Detachment Rate (g/min)
DETOTM(I,J,M)	Rill Flow Matrix Detachment Rate (g/min)
DETOTD(I,J,M)	Rill Flow Deposited Detachment Rate (g/min)
ST(I,M)	Sheet Flow Transport Rate (g/min)
RT(I,M)	Rill Flow Transport Rate (g/min)
DEP(I.J.M)	Deposition Rate (g/min)
QSRILL(I.2.M)	Sediment Delivery Downslope (g/min)
T	Current Time (min)
RORTOT	Total Runoff Rate (ℓ/min)
SEDRTO	Total Sediment Delivery Rate (kg/min)
TSPWFR	Total Sediment Plus Water Flow Rate (l/min)
QRILL(NJ,M)	Rill Flow Rate (cc/sec)
QSRILL(I,2,M)	Sediment Delivery Rate (kg/min)
ROTL	Cumulative Runoff (ℓ)
ROTCM	Cumulative Runoff (cm)
SDKG	Cumulative Sediment Delivery (kg)
SDMTHA	Cumulative Sediment Deliver (mt/ha)
SDTAC	Cumulative Sediment Delivery (t/ac)
WSDL	Cumulative Water and Sediment Delivery (L)
WSDKG	Cumulative Water and Sediment Delivery (kg)
RTOT	Cumulative Rainfall (cm)
RTOTL	Cumulative Rainfall (L)
NUM(I)	Sorted Sedimetn Type (-)
PFW(I)	Percent Finer by Weight (%)
HPL	Horizontal Plot Length (m)
PN	Plot Width (m)
NJ	Number of Plot Increments (-)
HLINC(J)	Horizontal Increment Lengths (m)
SO(J)	Increment Slopes (m/m)
TS	Total Simulation Time (min)
DTM	Time Step (min)
IMD1	Initial Moisture Deficit Layer 1 (cc/cc)
IMD2	Initial Moisture Deficit Layer 2 (cc/cc)
RIOT	Total Rainfall (cm)
RTOTL	Total Rainfal (L)
ROTL	Total Runoff (L)
ROTCM	Total Runoff (cm)
CN	Equivalent Curve Number (-)
SDKG	Sediment Delivery (kg)
SDMTHA	Sediment Delivery (mt/ha)
SDTAC	Sediment Delivery (t/ac)

storage using curves developed by Linden (1979). These curves were presented earlier in Figure 3.3. The representation of these curves for use in KYERMO was developed by fitting a four-point Lagrangian function through the inflection points on Linden's curves. Linden found that no appreciable storage exists on slopes above 20% (in the range of random roughness examined), so 20% is used as an upper limit.

The subroutine INFILT is the most involved subroutine in the run-off generation component. It is based upon the Moore (1981a) and Moore and Eigel (1981) extension of the Green-Ampt-Mein-Larson (GAML) model which was developed by Mein and Larson (1971) as an extension of the Green and Ampt (1911) equation. A modification of the Moore (1981a) work for use in this model is the use of the "field saturation" concept as outlined by Hirschi, Larson and Slack (1980) and Hirschi (1980).

The GAML model is an approximation to the infiltration process developed by combining Darcy's equation,

$$V = K \frac{dh}{dz} \tag{8.1}$$

and moisture continuity. The derivation is taken as the hydraulic head over the distance it acts, or

$$\frac{dh}{dz} = \frac{d_{pond} + L + S_{av}}{L} \tag{8.2}$$

where d_{pond} is the depth of the surface ponding (usually taken as zero and is assumed to be zero in KYERMO), L is the depth to the wetted front (moisture is assumed to move as piston flow) and S_{av} is the average capillary suction across the wetted front. Therefore, Darcy's equation can be represented by

$$V = K \frac{L + S_{av}}{L} \tag{8.3}$$

The piston flow assumption leads to a simple representation for continuity. The infiltrated volume must equal the product of the total fillable porosity minus the initial moisture content and the depth to the wetted front, or

$$F = (\theta_s - \theta_i)L \tag{8.4}$$

where F is the infiltrated volume expressed as water depth, θ_s is the total fillable porosity, and θ_i is the initial volumetric moisture content, assumed to be uniform. The difference between θ_s and θ_i is termed the initial moisture deficit (IMD). Solving for L,

$$L = \frac{F}{IMD} \tag{8.5}$$

Therefore, substituting for L and letting V be the infiltration rate, f,

$$f = K \frac{F/IMD + S_{av}}{\frac{F}{IMD}} \tag{8.6a}$$

or

$$f = K \frac{F + S_{av}(IMD)}{F} \tag{8.6b}$$

Simplification leads to the familiar GAML rate equation

$$f = K \left(1 + \frac{IMD\ (S_{av})}{F}\right) \tag{8.7}$$

At all times, if the rainfall rate is less than the infiltration rate, the value of f is limited to the rainfall rate.

The "field saturation" concepts put forth by Hirschi, Larson, and Slack (1980) use an unsaturated upper limit for soil moisture content. This condition is probably caused by air entrapment in the soil due to surface sealing (Moore, 1981b). The level of saturation in

the field is specified by the user, with a 90% moisture level being a good estimate if the actual value is unknown, as recommended by Slack (1978). The relationship between K and θ is given through the use of Campbell's (1974) method, which utilizes the moisture retention curve, the saturated hydraulic conductivity, and the saturated moisture content of a soil to estimate the K - θ relationship. Through the use of Campbell's equation,

$$K = K_s (\theta/\theta_s)^{2b+3} \tag{8.8}$$

where b is the absolute value of the log-log slope of the moisture retention curve, K_{fs} (conductivity at "field saturation") and S_{av} can be estimated. Moore (1979), using Campbell's concepts, developed a general equation for S_{av} which can be stated as,

$$S_{av} = \frac{S_e (k_{rfs}^a - k_{ri}^a)}{a(k_{rfs} - k_{ri})} \tag{8.9}$$

where S_e is the air entry suction, k_{rfs} and k_{ri} are respectively the relative conductivities (k/k_s) at "field saturation" and intitally, and a is a constant given by,

$$a = \frac{b + 3}{2b + 3} \tag{8.10}$$

A reasonable estimation of S_e can be obtained using the log-log intercept of the moisture retention curve. Therefore, from Hirschi (1980),

$$S_{av} = \frac{10^x \theta_s^{-b} (k_{rfs}^a - k_{ri}^a)}{a (k_{rfs} - k_{ri})} \tag{8.11}$$

where x is the log-log intercept of the moisture retention curve.

Moore and Eigel (1981) modified the GAML model to account for a two-layered system. Their final rate equation was used in KYERMO, after "field saturation" substitutions, or

$$f = K_{fs1} \quad 1 = \frac{S_{av1}\, IMD_1}{F} \qquad \text{for } L < L_1$$

$$f = K_{fs2} \frac{H + F - F_1}{E + F - F_1} \qquad \text{for } L > L_1 \tag{8.12}$$

where K_{fs1} and K_{fs2} are "field saturation conductivities for layers 1 and 2, respectively, F and f are as previously defined, L is the depth to the wetted front, L_1 is the depth of the upper layer (the lower layer is assumed infinite), F_1 is the infiltrated volume stored in the upper layer, and H and E are as follows:

$$H = IMD_2(L_1 + S_{av2}) \tag{8.13a}$$

$$E = L_1\, IMD_2 \quad K_{fs2}/K_{fs1}. \tag{8.13b}$$

Note that the subscripts 1 and 2 denote layers 1 and 2, respectively.

The final equations are solved at each time interval by iteration until the values of f and F change by less than small, user-selected amounts. A small amount of numerical instability was found at the layer interface, but this is remedied by recalculating the values using the upper layer equation if the rate immediately after crossing the interface is larger than the previous value. An example output is shown in Figure 8.2 .

The RUNOFF subroutine utilizes an exponential relationship presented by Barfield, Warner and Haan (1981), which can be stated as,

$$RO = (R - f)\,(1 - e^{-(P-F)/ss}) \tag{8.14}$$

where RO is the runoff rate, f and F are as defined above, R is the rainfall rate, P is the accumulated rainfall volume and ss is the total

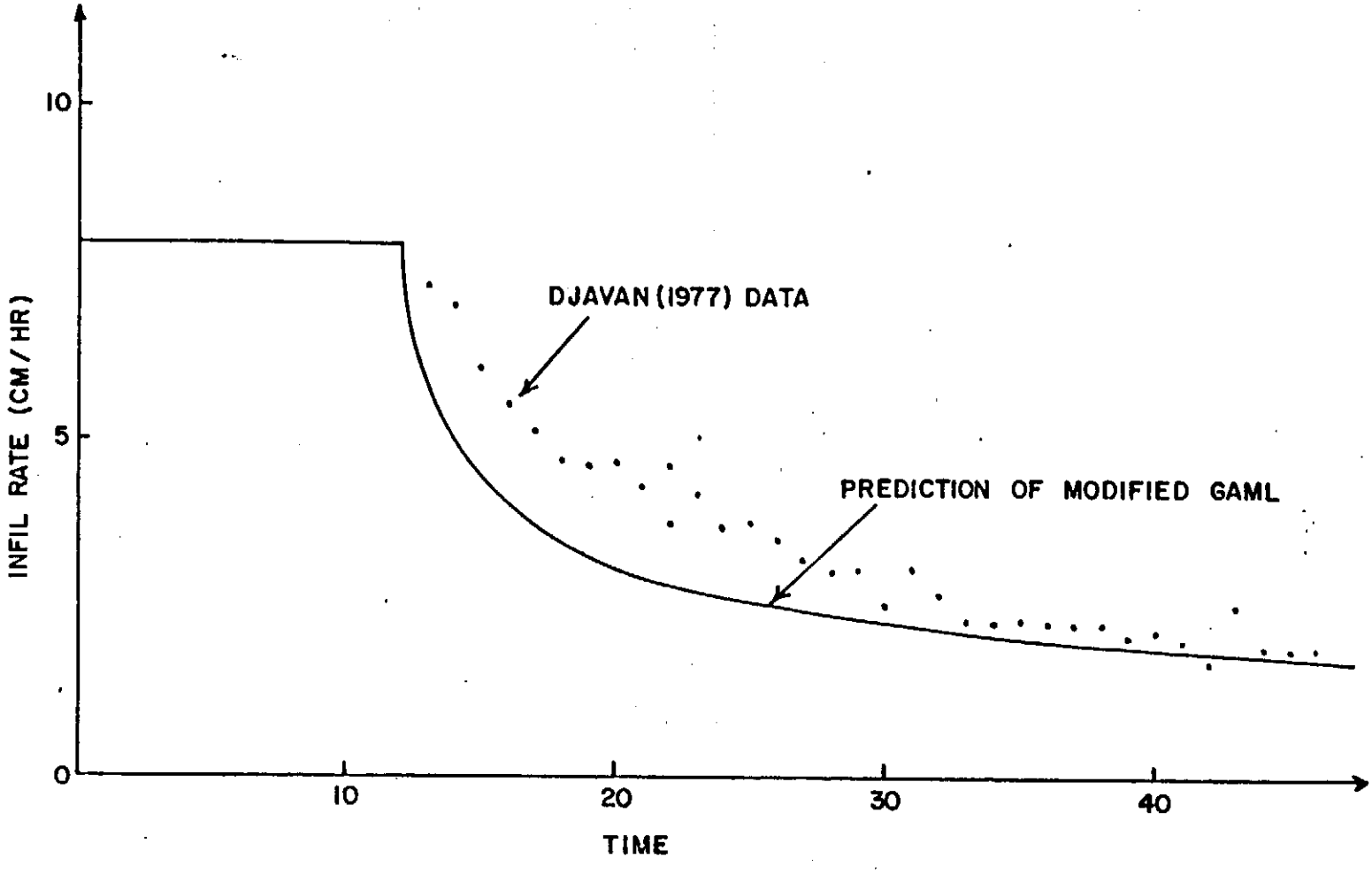

Figure 8.2 Example output of the infiltration routine in KYERMO compared with the Djavan (1977) data

available surface storage. If there is no surface storage (i.e. ss = 0), RO is assumed equal to (R - f).

The runoff rate on each slope increment during each time step is assumed to be inflow to the rill system. Runoff in the rill system is computed in the runoff routing component, along with other runoff variables and statistics.

Runoff Routing Component

The runoff routing component consists of a sub-main program, RUNROT. and three subroutines, RILLFL, RLFLOW, and RLCSSH. All are listed in Appendix III. The runoff is routed through a rill network initially set up in INITIA. The rill channel cross section is assumed as a series of segments, with the segment endpoints initially specified in INITIA. The cross sections are changed in the sediment generation component, reflecting detachment of sediment.

The subroutine RILLFL calculates the flow in each rill on a slope increment using Manning's equation. The flow routing breaks the model time step into smaller parts to gain accuracy and stability. RILLFL averages flow characteristics from the previous time step to set the routing time step at or below the critical time step required for routing method stability. RILLFL then calls the subroutine RLFLOW, which calculates the routing.

The subroutine RLFLOW uses a four-point kinematic routing procedure as outlined by Brakensiek (1966). The procedure uses a finite differencing method with Manning's equation as the rate equation and utilizes the known flow rate and area at previous time and space steps to calculate the flow rate and area at the current location and time. This concept is shown in Figure 8.3. The procedure is essentially an

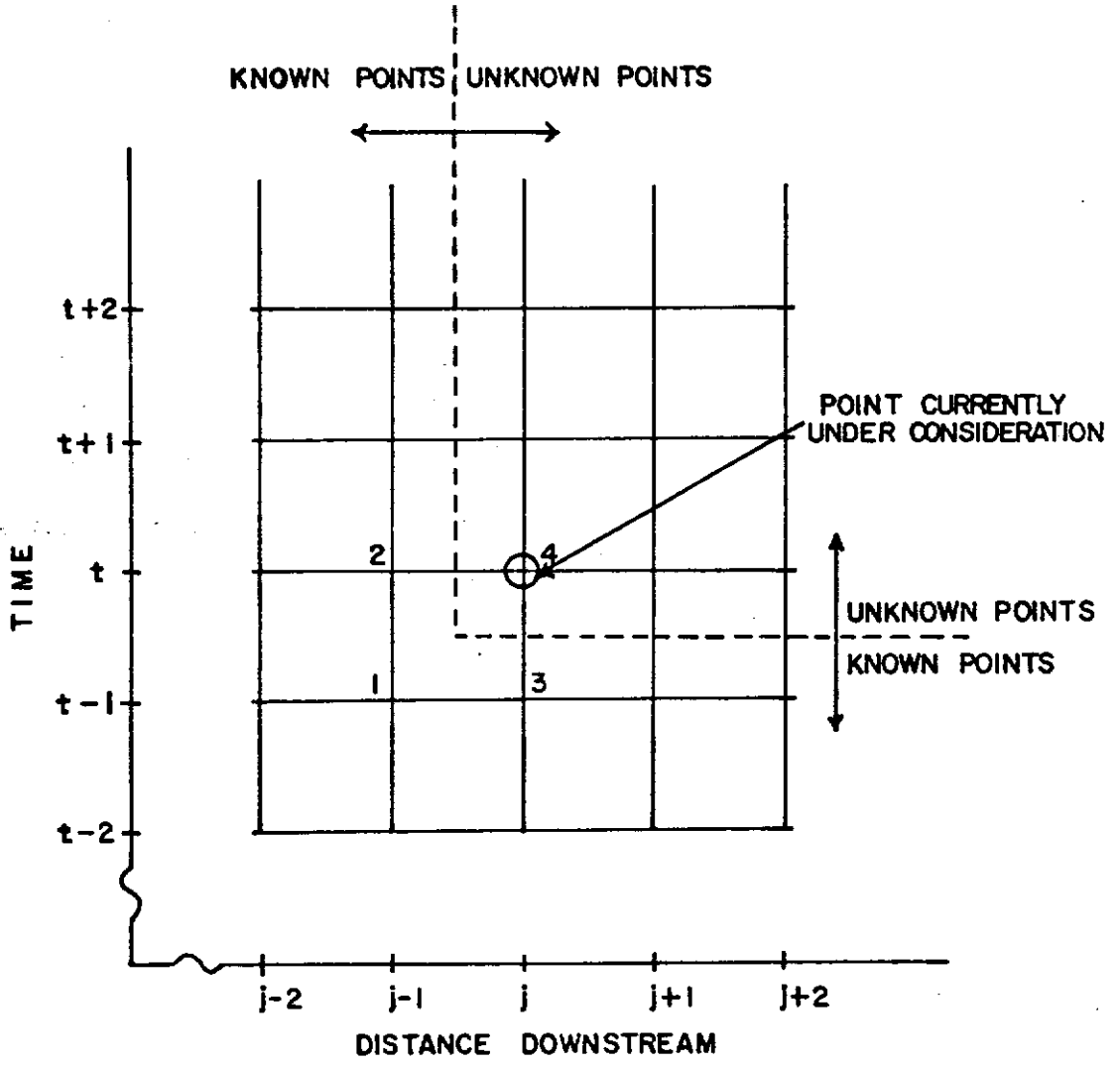

Figure 8.3 Grid for 4-point kinematic routing used in KYERMO (after Brakensiek, 1966)

initial value problem in two dimensions. Briefly the development is as follows:

Continuity Equation: $$\frac{\partial Q}{\partial x} + \frac{\partial A}{\partial t} = q \qquad (8.15a)$$

Rate Equation: $$Q = \frac{1}{n} R_n^{2/3} (\sin \gamma)^{\frac{1}{2}} A \qquad (8.15b)$$

where Q is flow rate, A is flow area, q is lateral inflow, n is Manning's coefficient, R_n is the flow hydraulic radius, and γ is the slope angle. The continuity equation (8.15a) is discretized by using finite difference approximations for all the terms. Brakensiek found that a central difference equation was best for $\frac{\partial A}{\partial t}$, but a forward difference equation was best for $\frac{\partial Q}{\partial x}$. The representations are

$$\frac{\partial A}{\partial t} = \frac{A_4 - A_3 + A_2 - A_1}{2\Delta t} \qquad (8.16a)$$

$$\frac{\partial Q}{\partial x} = \frac{Q_4 - Q_2}{\Delta x} \qquad (8.16b)$$

The continuity equation then becomes,

$$\frac{Q_4 - Q_2}{\Delta x} + \frac{A_4 - A_3 + A_2 - A_1}{2\Delta t} = q \qquad (8.17)$$

or

$$\lambda Q_4 + \frac{A_4}{2} = \alpha + \beta \qquad (8.18)$$

where:

$$\lambda = \Delta t/\Delta x \qquad (8.19a)$$

$$\alpha = (A_1 + A_3)/2 \qquad (8.19b)$$

$$\beta = \lambda Q_2 + \Delta t q - \frac{A_2}{2} \qquad (8.19c)$$

In RLFLOW the known quantities are calculated and the subroutine RLCSSH called to calculate the depth of flow, area of flow, wetted perimeter, and hydraulic radius for the multi-segmented channel cross section. The new flow rate is then calculated and the routing is continued.

The RLCSSH subroutine is a complex subroutine used to calculate the depth of flow in a channel cross section represented by straight segments. A Newton-Raphson technique is used to iterate to the new depth. Model points of the channel are redefined so that they begin and end at the new water's edge. In the algorithm small areas are essentially summed in an attempt to match the unknown left-hand-side to the known right- hand-side of the continuity equation. The depth estimate is then revised and the iteration is repeated until a 0.01% or smaller change is found between iteratives. The wetted perimenter, hydraulic radius, and area in RLCSSH are then calculated and the values returned to RLFLOW through COMMON blocks.

After the flow rates are obtained through the RUNROT routines, the sediment generation routines are called by the main program.

Sediment Generation Component

The sediment generation component consists of its submain program, SEDGEN, and five subroutines: RADET, RLDET, SHDIST, RLSHAP, and SLUFF. Raindrop detachment, rill flow detachment, rill wall sloughing, and the change of the rill channel cross section due to detachment and deposition are all computed in this routine.

In the RADET subroutine sediment detachment due to rainfall impact is evaluated. A base soil detachment rate is calculated using the final equation of Bubenzer and Jones (1971) which can be stated as,

$$ss = CR^{e_1} E^{e_2} P_{cl}^{e_3} \qquad (8.20)$$

where ss is the soil splash rate in g/min, C is a coefficient, e_1, e_2, and e_3 are exponents, R is rainfall rate in cm/hr, E is the rainfall energy in joules/cm^2, and P_{cl} is the percent clay of the surface layer. Coefficient and exponent values are input by the user, with Bubenzer and Jones' values being good estimates if actual values are not known. The base soil detachment rate is used for areas not covered by surface ponding, but the value must be adjusted to consider those areas covered by water. A potential soil splash coefficient is calculated for each drop size class to assess the drop detachment on ponded areas. Palmer (1965) examined the effect of surface water on soil detachment due to various sizes of raindrops and found that detachment rose to a maximum at a depth of about one drop diameter and was almost zero at a depth of three drop diameters. This phenomenon is provided for in RADET by allowing the user to specify a maximum coefficient (such as 1.5) and the coefficient at three drop diameters (such as 0.1) and then by fitting a function to the shape of Palmer's data through those points. The 28 raindrop size classes specified in RAINFA are considered separately, with their individual potential splash coefficient weighted by their fraction of the rainfall. The weighted individual coefficients are then summed and the resultant "average" coefficient is used to adjust for the surface ponding. A final raindrop detachment rate is thus obtained. The particles on the soil surface are assumed to be detached according to the fraction specified in INITIA.

The RLDET subroutine and the other subroutines called from RADET were the longest subroutines in development. Foster's (1982) empirical

equation utilizing excess shear is used as the basic equation, with user specified coefficient and exponent for each soil layer. Foster's equation can be stated as

$$D = \alpha (\tau - \tau_{cr})^{\beta} \qquad (8.21)$$

where τ is the channel boundary shear stress in N/m^2 and τ_{cr} is the critical shear stress for detachment in N/m^2. The critical shear stress was found to be a strong function of percent clay by Smerdon and Beasley (1961). Their relationship is used in RLDET for τ_{cr}. Matrix and deposited material were treated separately with a critical shear stress of 0.5 N/m^2 used for deposited material. The fraction of the surface covered by deposition and the particle size distribution exposed on the bed were considered in calculating the detachment rate for each sediment type.

The RLDET subroutine values for the bed shear are required for each segment of the rill cross section. These values are provided in the subroutine SHDIST through the use of the "area method" of Lundgren and Jonsson (1964). Essentially, each segment of the rill cross section was divided into a user-specified number of sub-segments and the area of water exerting stress on it was calculated. The lines of "zero stress" were assumed to be the bisection of the angles between the cross section segments. The water area over each sub-segment was summed to obtain the total area above a segment. The shear was then calculated based on the weight of the water, the length of the segment and the bed slope at that point. The nodal points in the RLSHAP subroutine were reset by defining the channel boundary according to the matrix detachment between the points. Continuity was obtained by matching the volume of soil removed

through detachment with the volume change in bed location. The new coordinates were then transferred to the subroutine SLUFF to consider rill wall sloughing.

In the SLUFF subroutine an algorithm similar to Wu et al. (1982) was used to calculate rill wall sloughing. In this subroutine the exposed slopes above the new water surface were evaluated for stability. If their slope exceeded a user-specified value, the area above an equilibrium slope line (also specified by the user) was calculated and added to the detachment of that flow situation. New channel nodal points were then calculated.

The SEDGEN sub-main and its subroutines were used to calculate the sediment detached and available for transport downslope. The sediment routing component was then used to evaluate sediment transportation and deposition.

Sediment Routing Component

The sediment routing component consists of its sub main, SEDROT and four subroutines: SHEET, RILLTR, SEDTRA, and YANGSE. In this component transport and deposition of sediment in the sheet and rill flow were evaluated. Two sediment transport equations were provided as options for each. After this component was considered, KYERMO prepares to move to the next slope segment or time step, and outputs statistics when instructed by the user.

In the SHEET subroutine the sheet flow transport of material detached by rainfall were evaluated. The sheet flow rate, wetted perimeter, and depth were calculated based on the runoff rate and a sediment transport routine called to calculate the transport. All sediment not transported was considered to be deposited and had to be re-detached. The sheet flow was assumed to flow at an angle to the rill, giving a

wider wetted perimeter than if it were parallel or perpendicular to the rill. It was further assumed that the rill was in the center of its watershed so that the runoff was input equally to each side of the rill.

The RILLTR subroutine was used for essentially the same calculations for rill flow as SHEET was for sheet flow, except that there were more sources for detachment. In RILLTR boundary shear detachment, sediment delivery from upslope, sediment delivery by sheet flow, and detachment due to sloughing of rill walls was calculated. Sediment transport capacity was then calculated by one of the transport equations and deposition was calculated.

In the SEDTRA subroutine the sediment transport capacity of either sheet or rill flow was calculated using a modified Yalin (1963) equation. The modification is that of Foster and Meyer (1972) and involved distributing the transport capability among various particle sizes. A full development of the modification algorithm is given by Foster et al. (1980) as part of the CREAMS model documentation. The Shields curve was used in SEDTRA. Shield's curve was represented by four straight lines and included the extension by Mantz (1977). The curve and the segments are shown in Figure 8.4.

The YANGSE subroutine was used to calculate the sediment transport using a modification of the Yang (1973) equation. The modification to Yang's equation involved the distribution of the sediment transport among particle types by first calculating a transport for an "average" particle type and then distributing that transport among the types according to their fraction of the whole load. At the current time, the priority for transport was given to the small particles, allowing then to fill the transport capacity first. However, a probable improvement

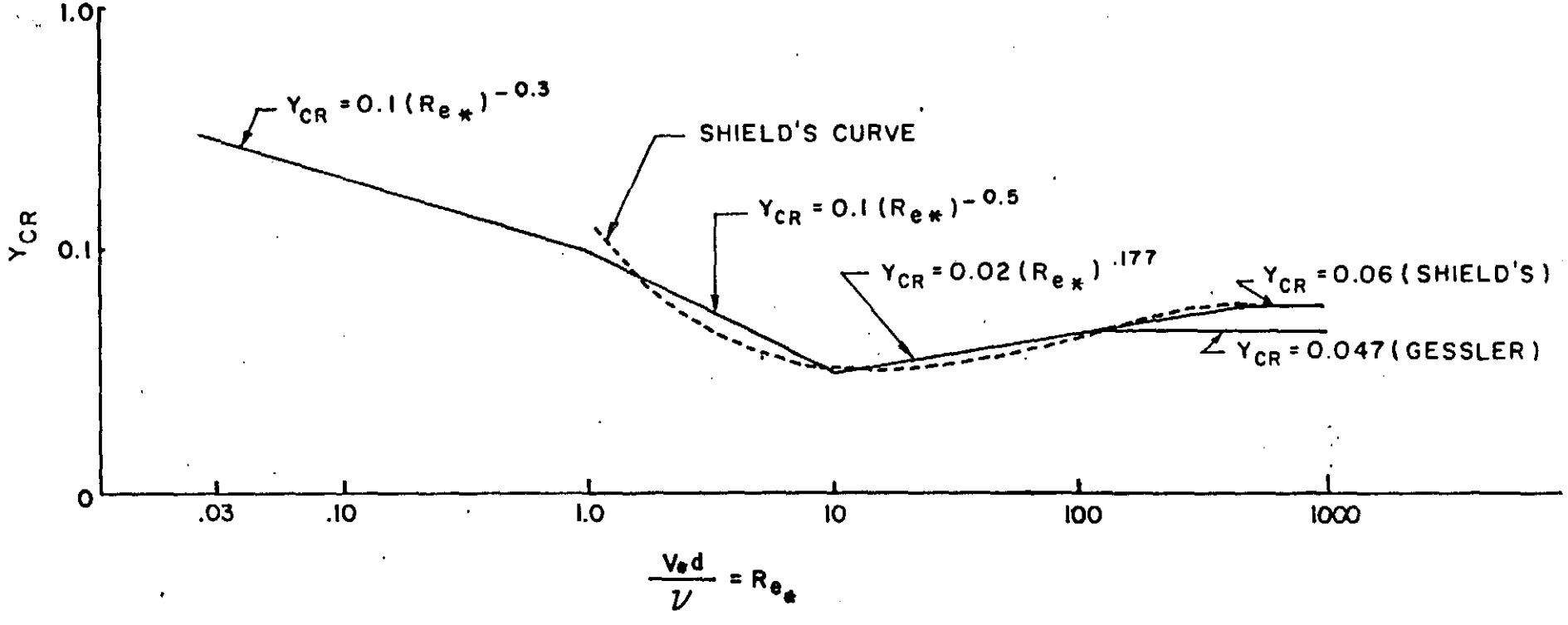

Figure 8.4 Modified Shield's curve as used in the KYERMO model

of the algorighm would be to use an iterative procedure similar to that of the SEDTRA algorithm. Each of the sediment transport equations in this model have been shown to be accurate in shallow flow applications. The user should evaluate the situation and choose which equation is more appropriate. Alonzo (1980) and Neibling and Foster (1980) presented data supporting the use of either of these equations in small-scale sediment transport situations.

The Kentucky Erosion Model has been and will be in constant flux throughout its development, verification, and use. It must be noted that the listings given in the appendices may be out-of-date at the time of final publication, due to improvements and corrections made in conjunction with its use.

KYERMO Uniqueness

It seems appropriate to outline some of the unique algorithms and interrelationships used in this model. Most of the components have relationships that have not been used in an erosion model or at least have not been used in the manner used in KYERMO.

The runoff generation routines that are unique to KYERMO are the surface storage calculations based on random roughness and slope, and the two-layer modified GAML model used to calculate infiltration. Both of these relationships allow great flexibility in the estimation of runoff from varying surfaces and soils. Because the surface storage and infiltration were calculated for each slope increment, some changes in the surface or soil could be handled directly.

The runoff routing routine that is unique in the model is the rill-cross sectional-shape routine that was used to calculate the flow depth through a Newton-Raphson numerical technique, which allowed complex geometries to be used for the rill channels.

The sediment generation component contains many unique routines. The raindrop detachment routine was used to calculate detachment under ponded conditions due to each drop size class utilizing input sizes and fractions. By using the Bubenzer and Jones style detachment equation intensity. energy and the were taken soil into account. The shear distribution relationship was used to calculate the shear on each face so that bed material removal and rill shape changes could be considered. The rill wall sloughing routine, coupled with the rill geometry change routine provided a tool for rill development research not seen previously.

CHAPTER 9 KYERMO COMPONENT VERIFICATION

Each component of KYERMO has been run with its own main program to check the output for consistency before all the components were linked together in the unit. A limited sensitivity analysis was performed on each to give insight about the problems and assumptions within each algorithm.

Runoff Generation Component

The runoff generation component was tested using the basic data inputs shown in Table 9.1. Each parameter was varied to give a range of outputs to demonstrate the "appropriateness" of the component calculations. Each set of runs is presented in chart form in Figures 9.1 through 9.5. In each case, the trends were consistent with observed natural behavior.

The first variable examined was the plot slope. The surface storage algorithm indicates that, for a given random roughness, available surface storage and plot slope are inversely related. Therefore, as the slope increases, the surface storage should decrease and the runoff rate should approach the rainfall excess rate more quickly. This relationship is shown in Figure 9.1.

The next variable checked was random roughness. The surface storage algorithm indicates that, for a given slope, as random roughness increases, surface storage decreases and the rate of change of runoff rate slows. Thhis relationship is shown in Figure 9.2.

Another variable examined was the rainfall rate. Because the infiltration rate was limited at the upper end by the rainfall rate, the speed at which the soil profile was wetted up, and hence the infiltration rate change, would be slowed. This phenomenon is indicated in Figure 9.3

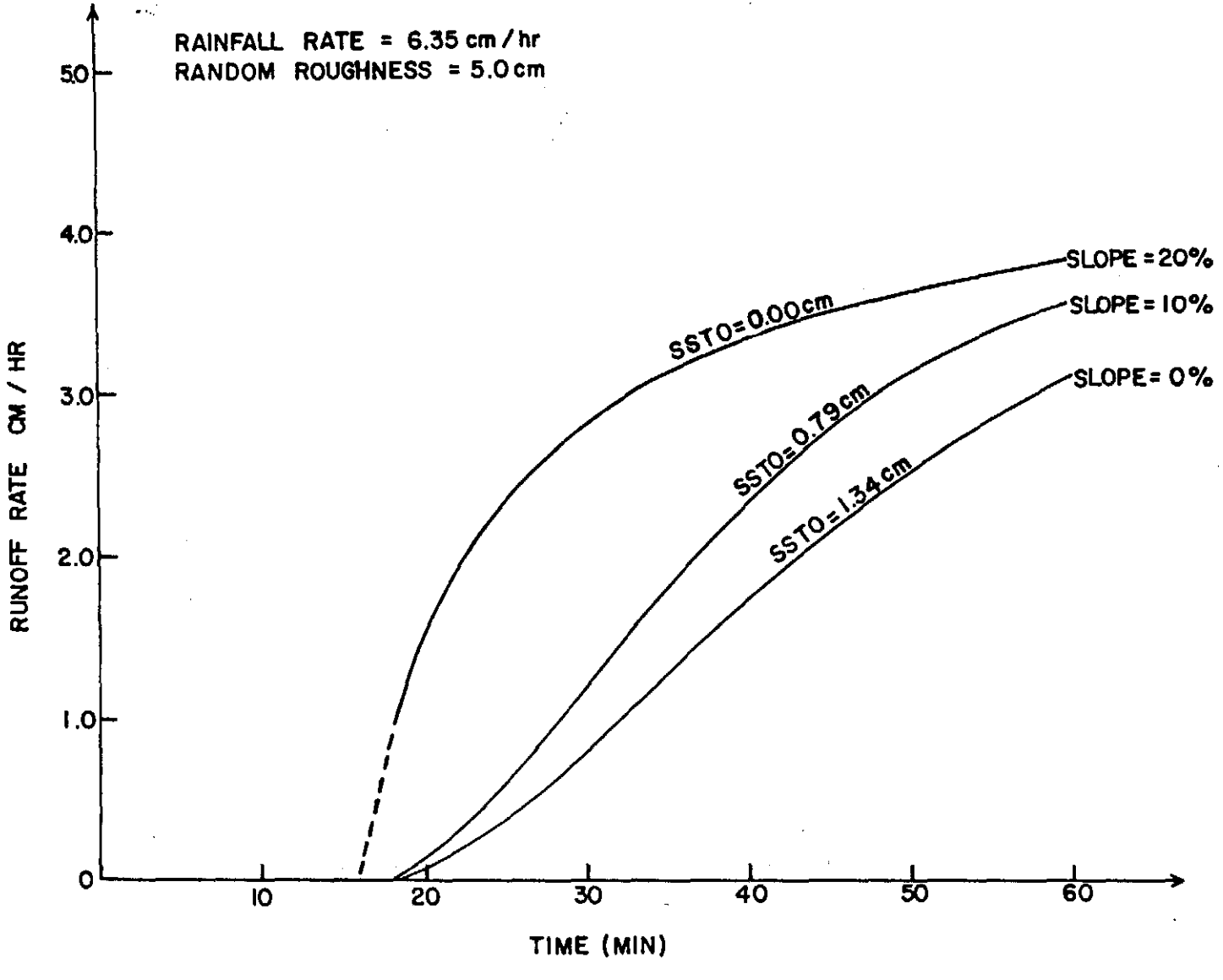

Figure 9.1 Effect of pilot slope on surface storage volume and runoff rate

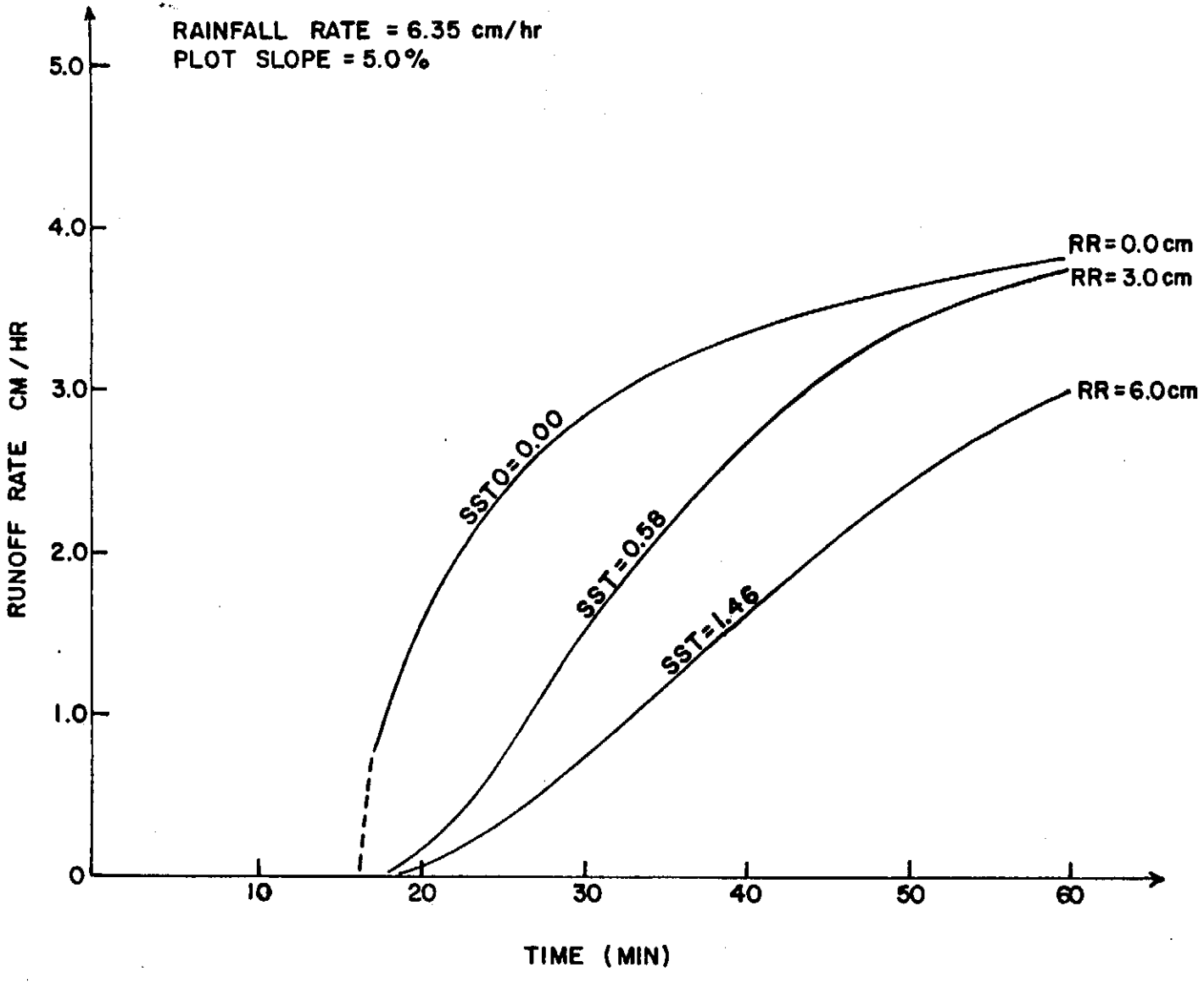

Figure 9.2 Effect of random roughness on runoff rate and surface storage

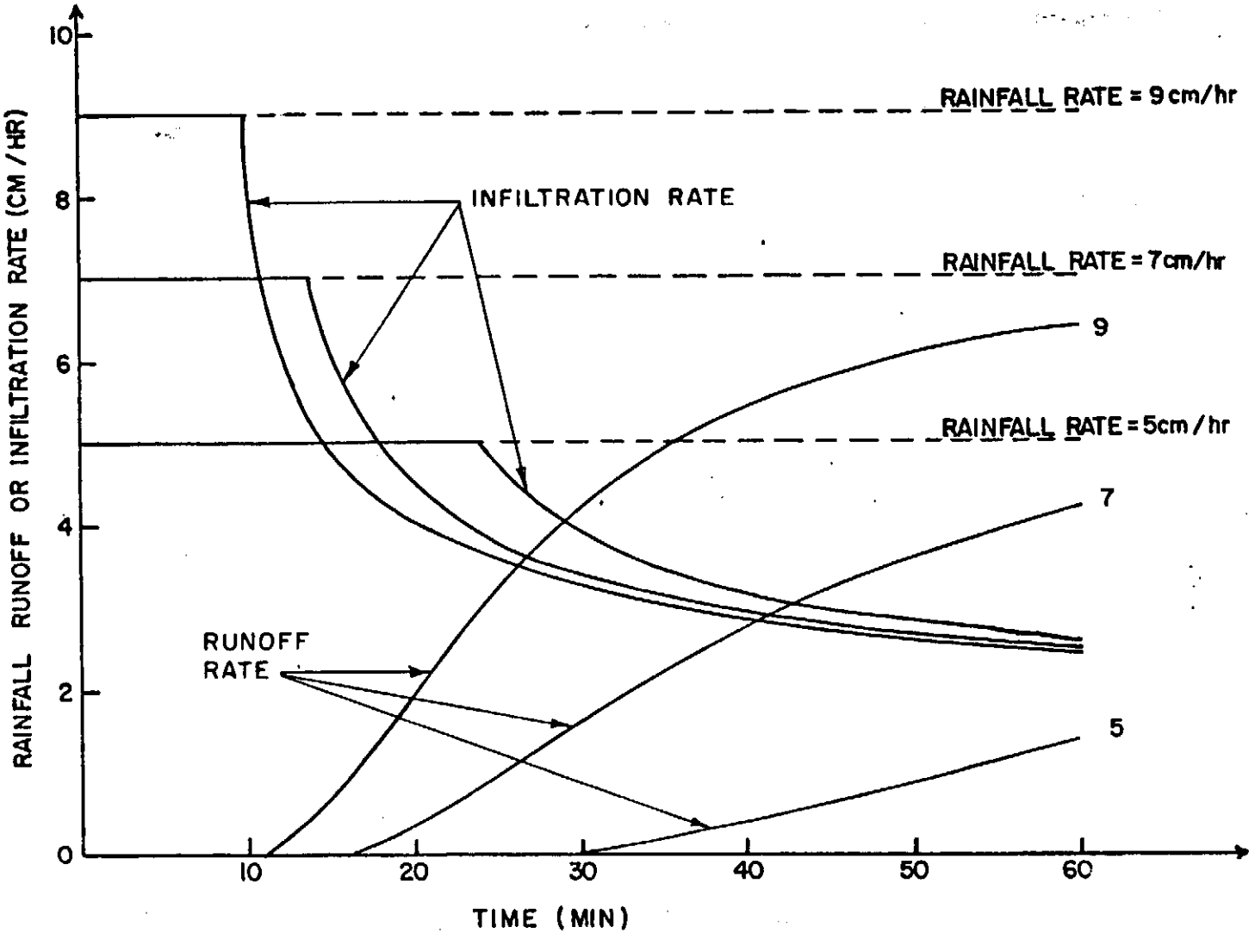

Figure 9.3 Effect of rainfall rate on infiltration and runoff rates

Table 9.1 Runoff Test Input Data

Variable	Dimension	Variable Description (Units)
Rain	1	Rainfall Rate (cm/hr)
TS	1	Simulation Time (min)
DTM	1	Time Step (min)
TR	1	Rainfall Duration (min)
RR(1)	1	Random Roughness (cm)
IMD1	1	Initial Moisture Deficit (cc/cc)
IMD2	1	Initial Moisture Deficit (cc/cc)
SAV1	1	Average Suction Along Wetted Front (cm-H_2O)
SAV2	1	Average Suction Along Wetted Front (cm-H_2O)
KFS1	1	Field Saturated Hydraulic Condition (cm/hr)
KFS2	1	Field Saturated Hydraulic Condition (cm/hr)
EF	1	Infiltration Rate Criterion (cm/hr)
EN	1	Infiltrated Volume Criterion (cm)
SO(1)	1	Plot Slope (m/m)

A fourth variable checked was the upper layer depth. The effect of this variable was influenced by the other parameters. In this case, the effect of a change in upper layer thickness was quite noticeable because the upper layer was dominating the infiltration process, as shown in Figure 9.4.

The next parameters checked were the initial-moisture deficits of each layer. The results were affected by the depth of the upper layer and other factors, but for a reasonably thin upper layer, both layers were important as shown in Figures 9.5a and 9.5b.

The limited sensitivity analysis shown in the above figures all indicated that the trends were correct. It was then necessary to show accuracy using measured data, if available. D from Idike et al. (1980) was available to check the infiltration routine. A comparison of predicted and observed values in Figure 9.6 shows that the infiltration routine works very well for the Idike et al. data.

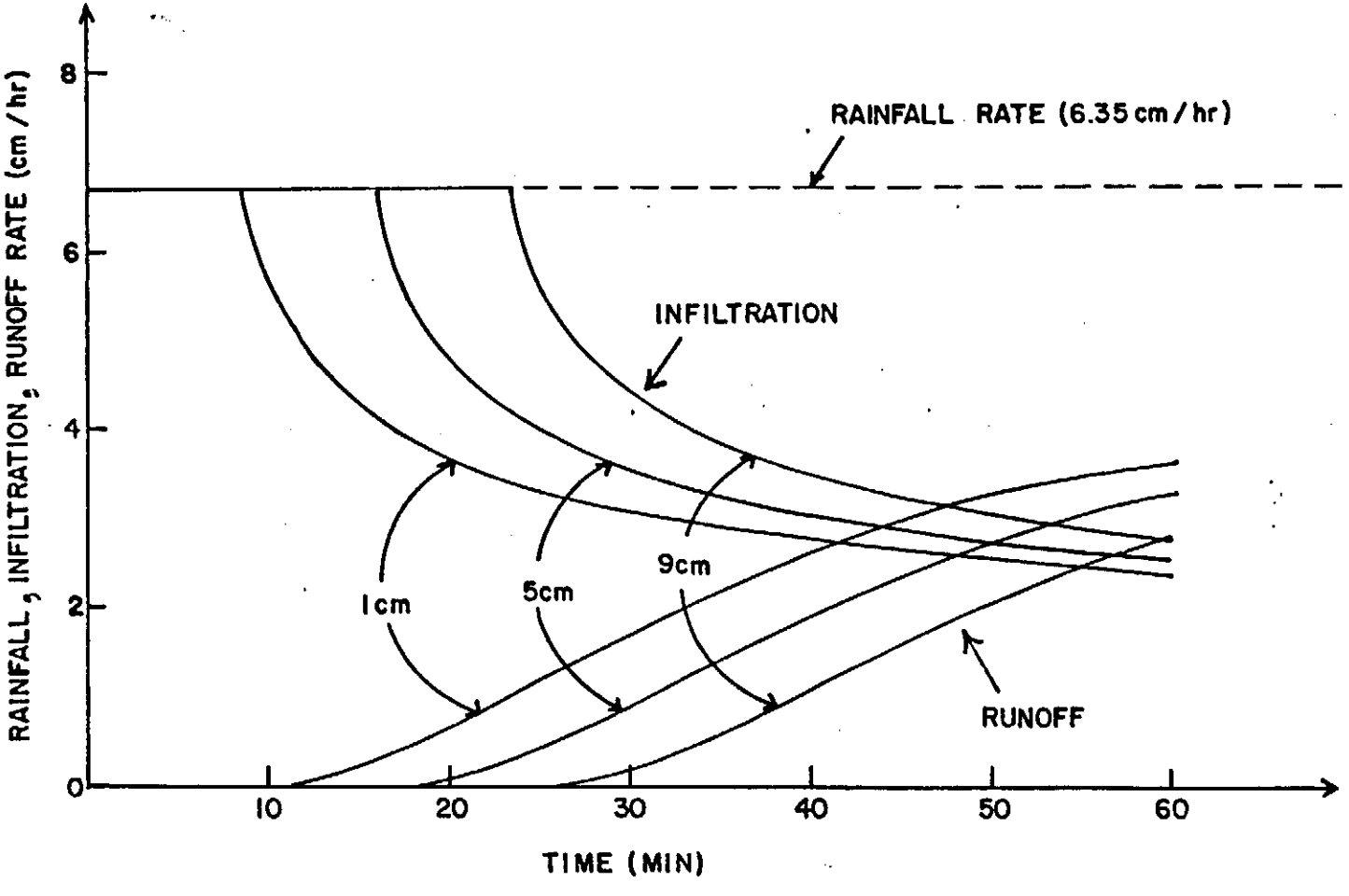

Figure 9.4 Effect of upper layer depth on infiltration and runoff rates

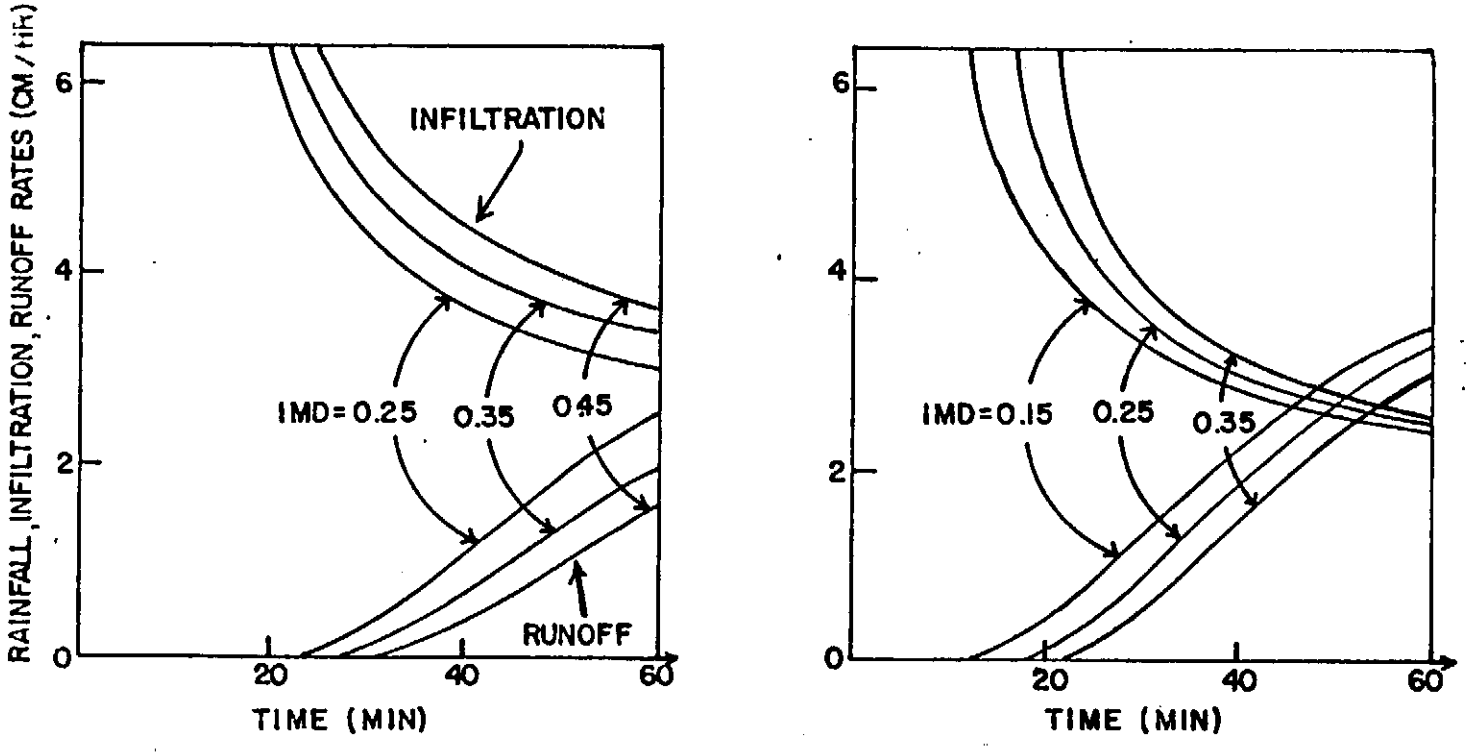

Figure 9.5 Effect of initial moisture deficit on infiltration and runoff for lower (a) and upper (b) layers

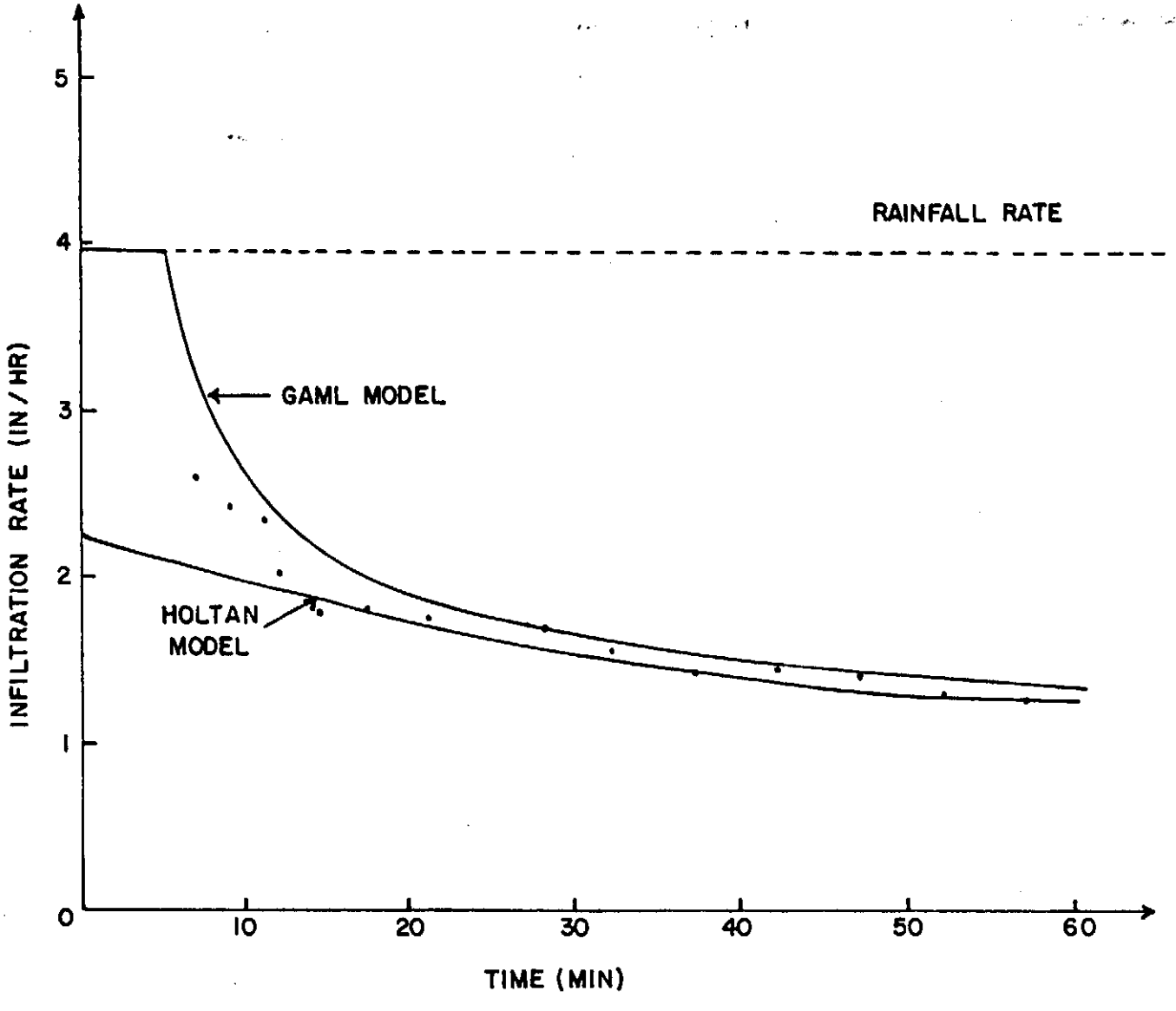

Figure 9.6 Comparison of GAML and Holtan models with Run "B-1" data of Idike et al. (1981)

Runoff Routing Component

The runoff routing component in this model has been checked for stability and continuity. The methodology itself has been checked for accuracy by others. In Figure 9.7. the 4-point kinematic routing prediction of streamflow was compared with the inflow data of Rice and Larson (1972) and predictions by the method of characteristics. Note the good agreement between the two prediction methods and the appropriate shift from the inflow hydrograph.

The runoff routing component was linked to the runoff generation component to examine the sensitivity of routing to varying inputs. A plot of the moisture balance for a 9 percent plot is shown in Figure 9.8. The first input varied was plot slope. The plot slope should affect both the runoff rate (due to higher surface storage for a given roughness), and the rill flow rates as calculated using Manning's This effect is shown in Figure 9.9. On high slopes where surface storage is essentially zero, there is very little difference due to different slopes because flow is limited by the delivery rate. Note the good continuity performance listed in Figure 9.9.

The next parameter varied was the rainfall rate. The major item of interest was the flow continuity. In Figure 9.10 the routing for four rainfall rates, with one hour durations is shown. The continuity performance was excellent for each.

The third parameter varied was the number of increments into which the plot was divided. The number of rills on each was set to 2 and the cross sections of all the rills were set to be identical. Flow was assumed to run straight down the rills with no junctions between rills.

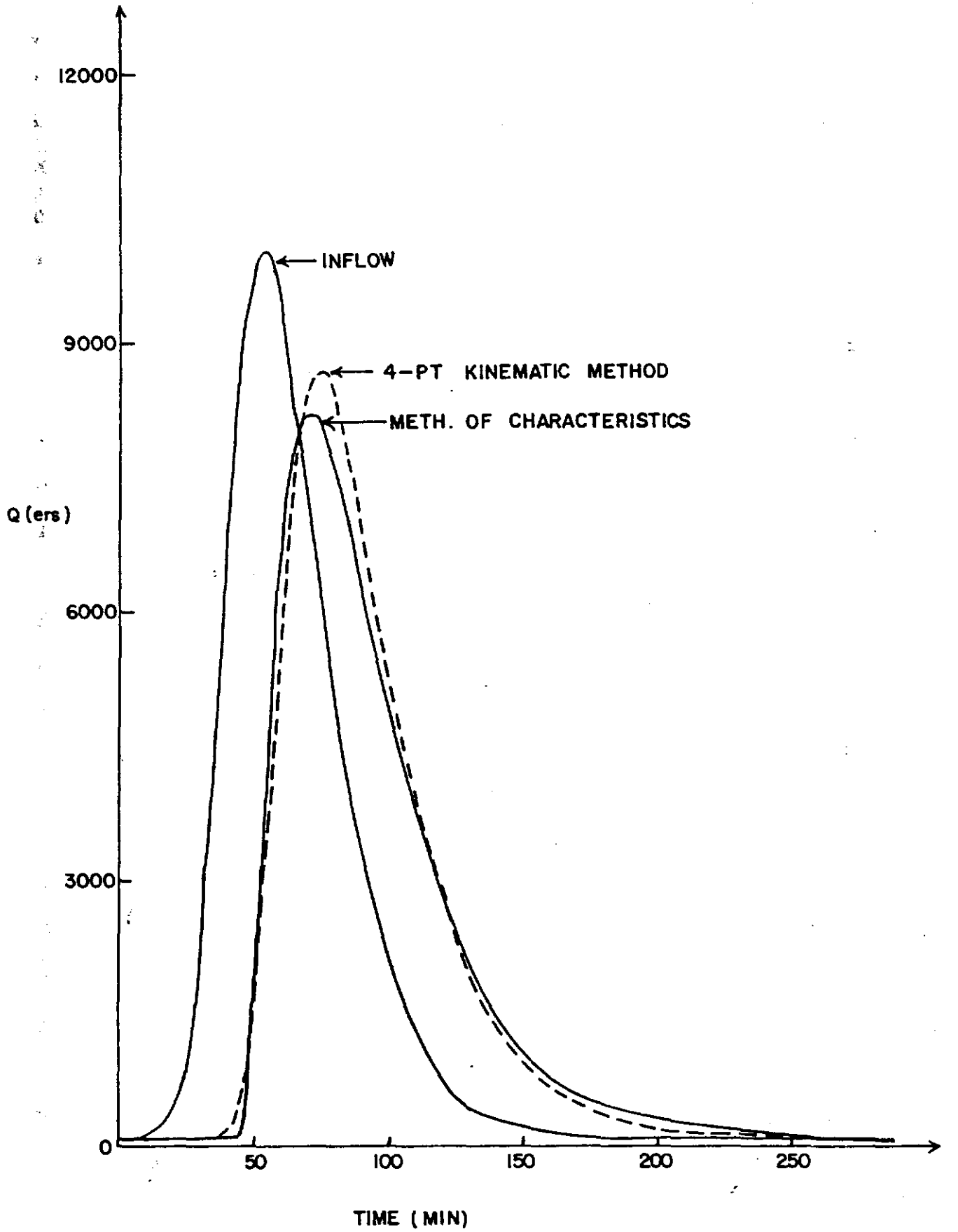

Figure 9.7 Performance of KYERMO routing method to inflow 12000 upstream & method of Characteristics (data from Rice and Larson (1972))

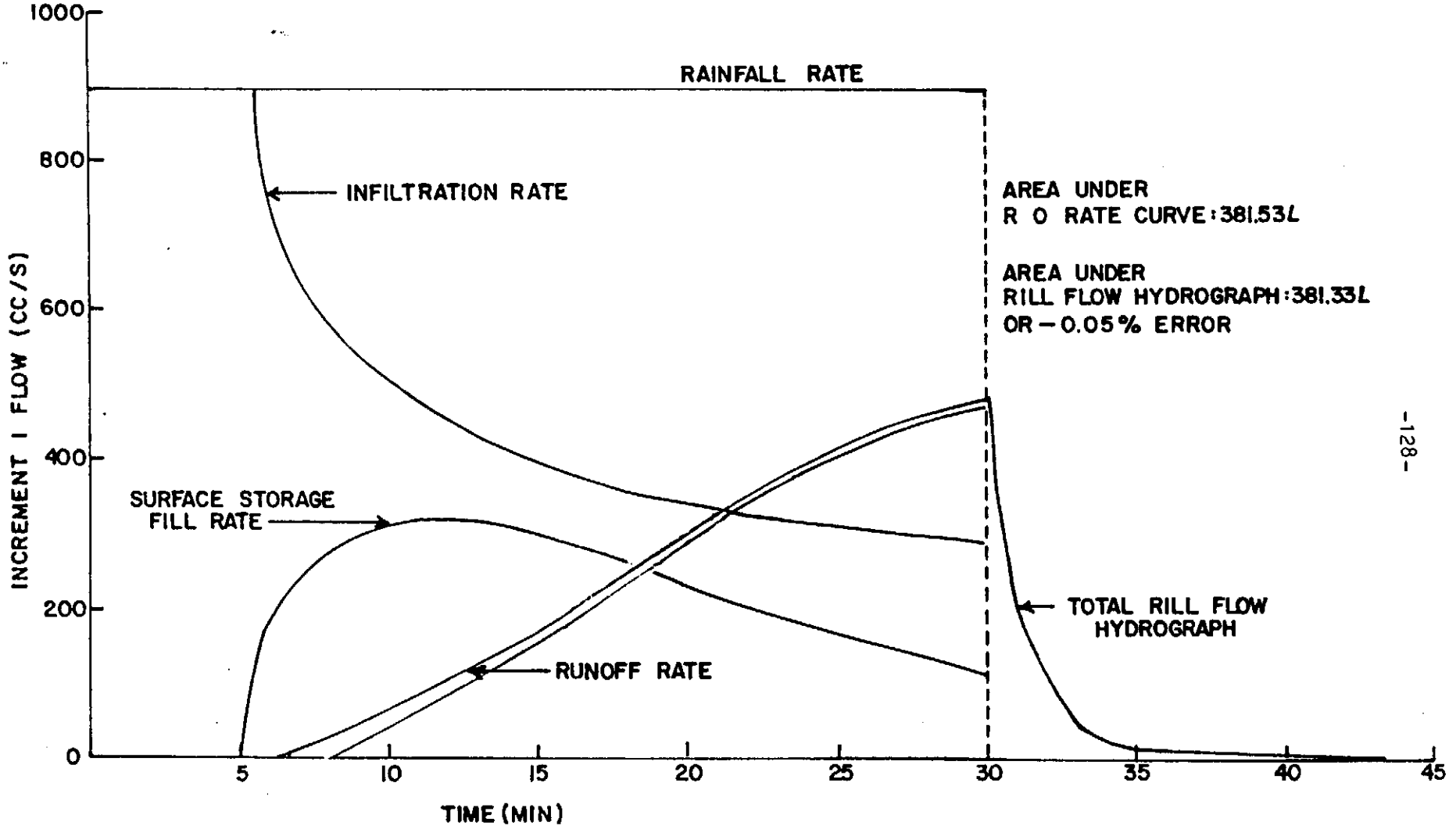

Figure 9.8 Joint output from runoff generation and runoff routing components (9% slope)

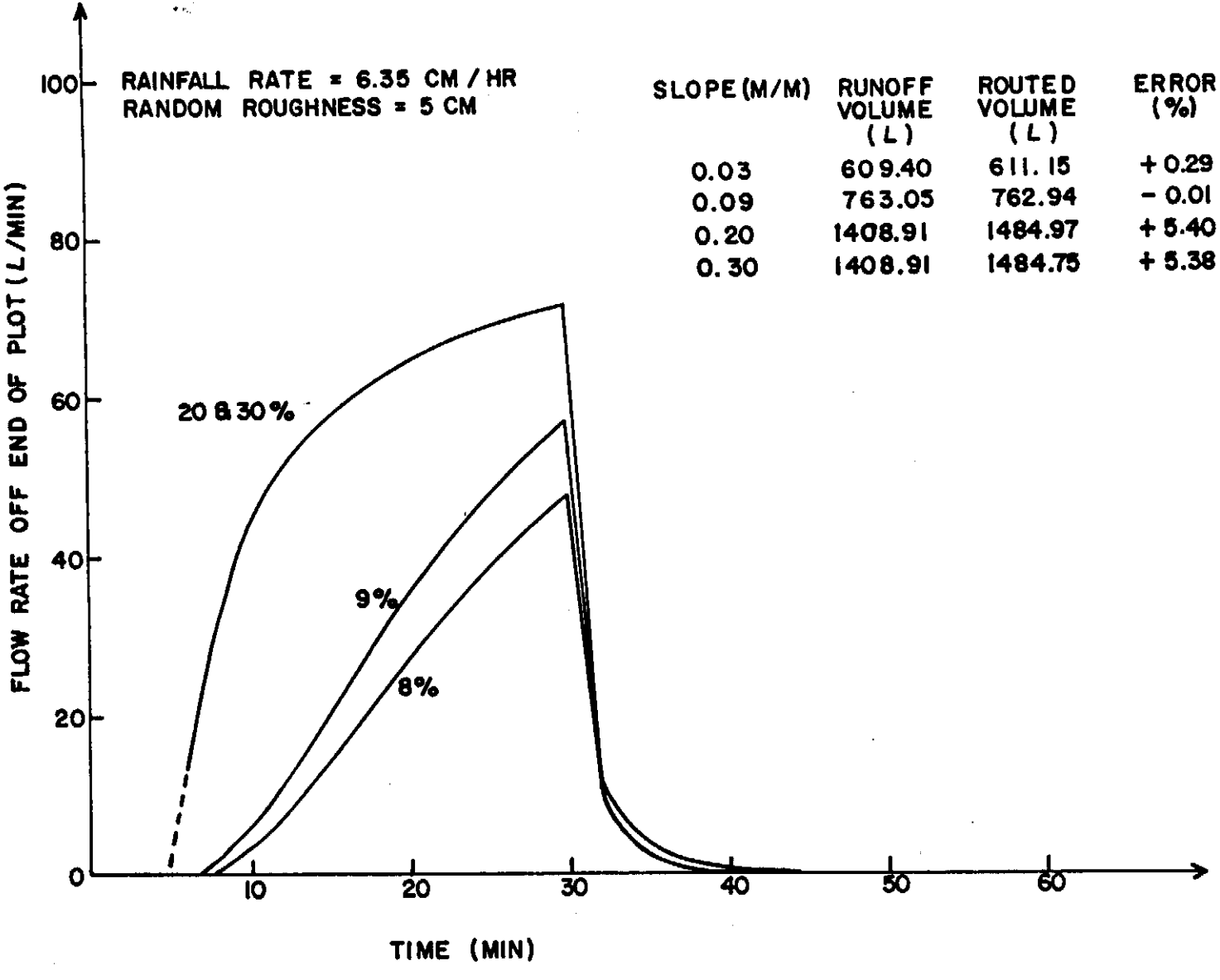

Figure 9.9 Effect of plot slope on plot end flow

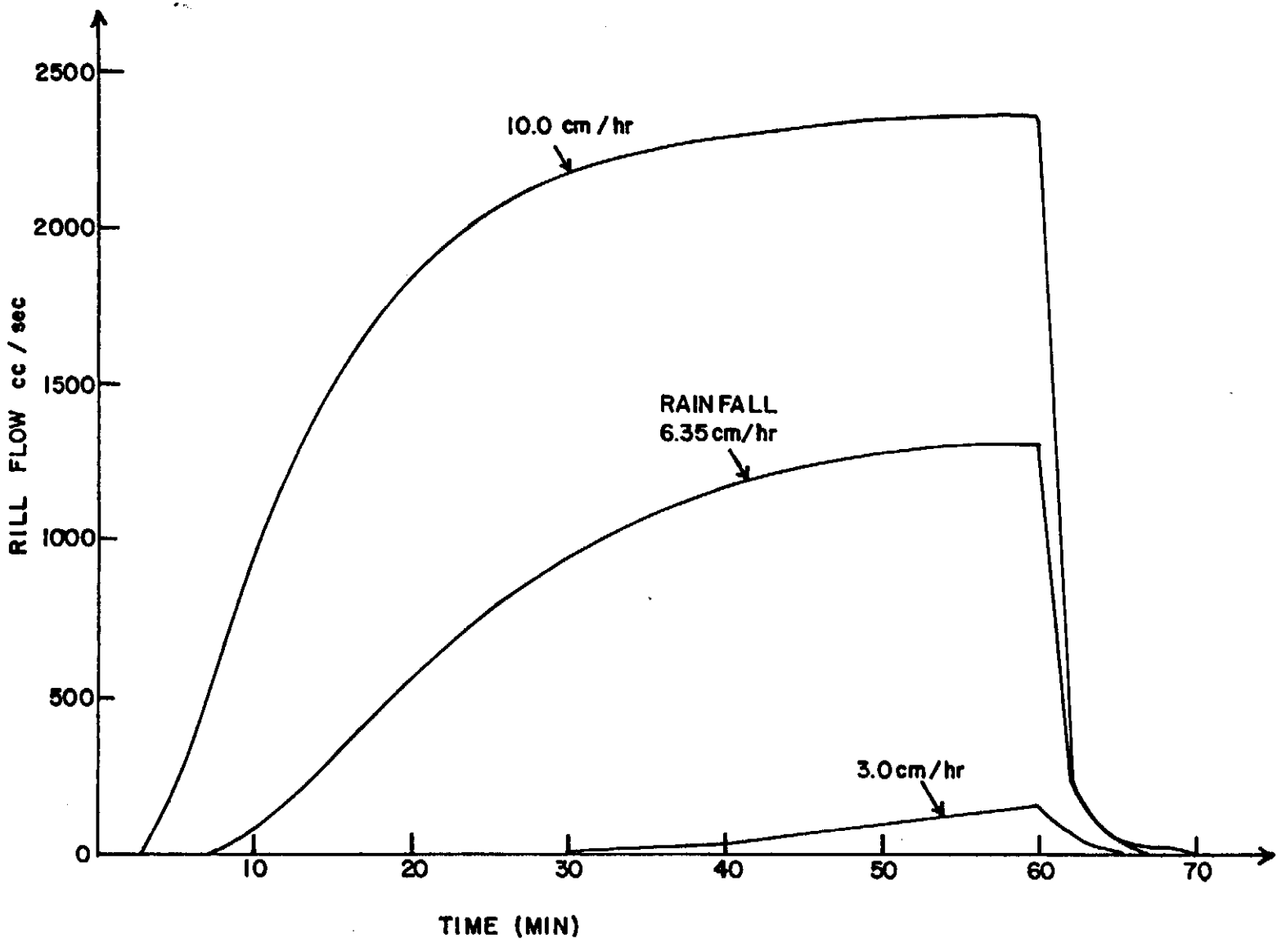

Figure 9.10 Effect of rainfall rate on rill flow routing

The results are shown in Table 9.2. It seems that if the rill number is constant, as few as 2 slope increments can be used and still maintain accuracy in the flow routing.

Sediment Generation Component

The major algorithms to be checked in the sediment generation component were the raindrop detachment, rill flow detachment, and the shear stress distribution algorithms. Each was examined individually for accuracy.

The detachment of soil by raindrops was calculated using a Bubenzer and Jones (1971) style equation tied to a "potential soil splash" function based on the Palmer (1965) data and the analysis of Massie (1980). The main relationship to be checked was the representation of the effect of a water layer on the surface. This effect was taken into account through the "potential soil splash" function. The function was:

$$PSS = C_1 \exp \left(C_2 \frac{D}{d}^3 + C_3 \frac{D}{d}^2 + C_4 \frac{D}{d}\right) \qquad (9.1)$$

where PSS is potenital soil splash, C_1, C_2, C_3, and C_4 are constants to be fitted, D is the surface water depth, and d is the raindrop diameter. The boundary conditions were as follows:

$$PSS = 1.0 \text{ when } D = 0 \qquad (9.2a)$$

$$PSS = K_1 \text{ when } D = R_o \qquad (9.2b)$$

$$PSS \text{ is a maximum when } D = R_o \qquad (9.2c)$$

$$PSS = K_2 \text{ when } D = 3 \qquad (9.2d)$$

where K_1 is the maximum value for PSS (= 1). R_o is the water depth-drop diameter ratio at which the maximum occurs, and K_2 is the value of PSS

Table 9.2 Effect of Number of Increments on Routing Continuity

# of Increments	Outlet Flow at 30 min (cc/s)	Outlet Flow at 60 min (cc/s)	Total Flow Volume (Cut off at 72 min)	Total Runoff Volume (ℓ)	Volume Error %
1	936.20	1319.68	2768.3	2838.0	2.4
2	939.70	1320.16	2927.9	2838.0	3.2
4	940.32	1320.31	2923.7	2838.0	3.0
10	941.27	1320.46	2923.5	2838.0	3.0

with a water layer depth of three drop diameters. These boundary conditions were adequate to solve for the constants in terms of the input parameters K_1, K_2, and R_o. If the maximum detachment was assumed to occur at a depth of one drop diameter, the constants were as follows:

$$C_1 = 1.0 \tag{9.3a}$$

$$C_2 = \frac{1}{12} \ln (K_1^3 K_2) \tag{9.3b}$$

$$C_3 = - \ln (K_1^{3/2} K_2^{1/6}) \tag{9.3c}$$

$$C_4 = \ln (K_1^{9/4} K_2^{1/12}) \tag{9.3d}$$

Predictions from equation 9.1 with constants defined in equations 9.3a through 9.3d are shown in Figure 9.11 for five different parameter combinations along with the Palmer (1965) data. The assumption of R_o equal to one is reasonably consistent with Palmer's data, although the data are quite scattered. However, Mutchler and Larson (1971) concluded that the maximum detachment would occur with a water layer of 1/5 of the drop diameter. Accordingly, Equation 9.1 was solved using R_o as an input. The equations are very complicated, but they will allow the user to specify the water layer-drop diameter ratio at which the maximum will occur. When R_o is set to 1, the new equations reduce to equations 9.3a

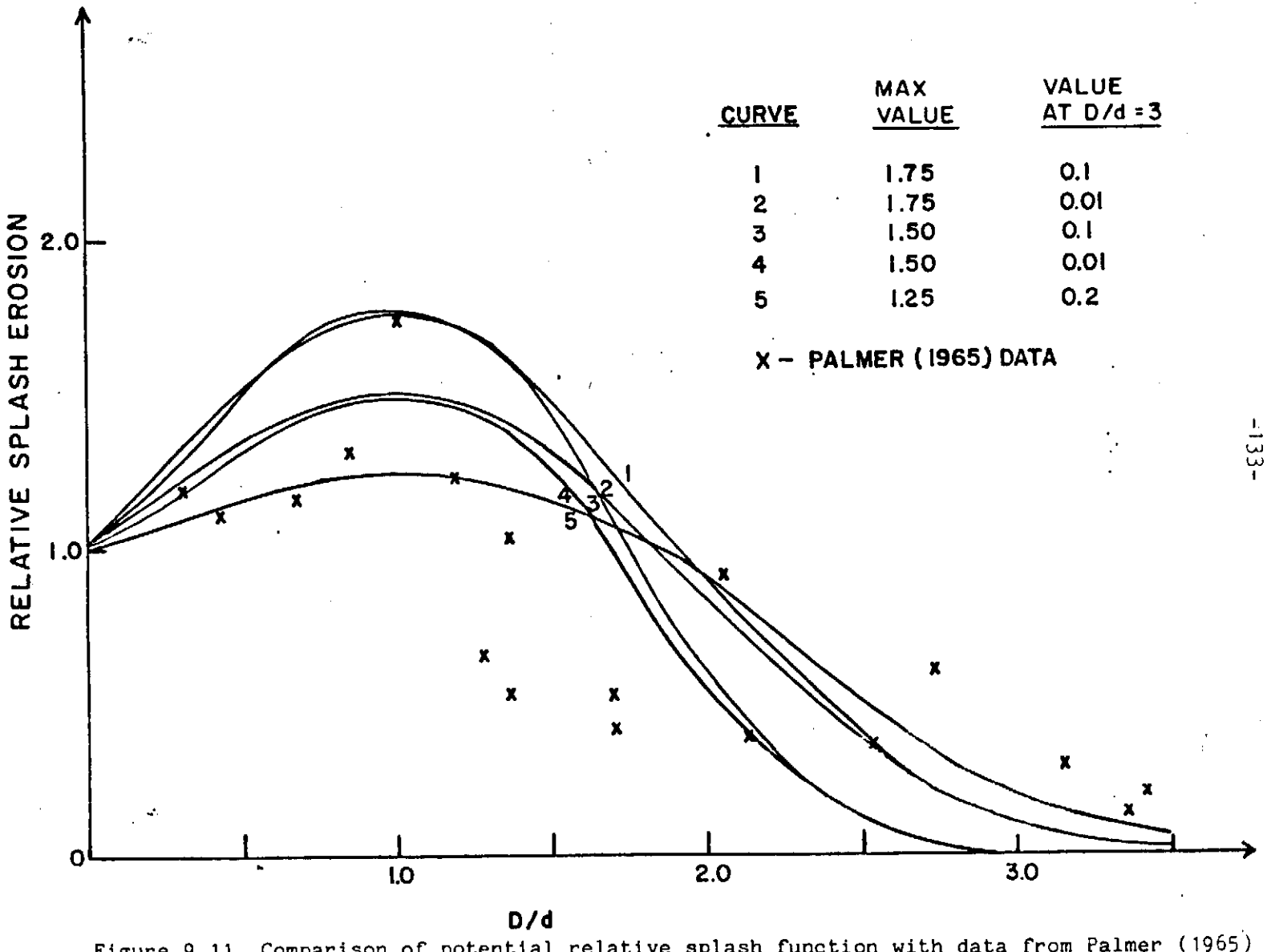

Figure 9.11 Comparison of potential relative splash function with data from Palmer (1965)

through 9.3d. as expected. Massie (1980) stated that Palmer's data should show the right shape, but the magnitude of his soil splash data is questionable due to lower kinetic energy during his experiments than that which would occur during natural rainfall.

The rill flow detachment equation used in KYERMO was presented by Foster (1982). The coefficient and exponent were fitted by Meyer et al. (1975) for furrow erosion with and without a canopy. The comparison presented by Foster (1982) is shown in Table 9.3. The agreement is excellent.

The shear stress distribution along a channel cross section was calculated in order to calculate the erosion on each channel cross section segment and to estimate the resulting geometry change. The relationship utilized was based upon the work of Lundgren and Jonsson (1964). In Figure 7.3 the algorithm results for the Replogle and Chow data were compared with the algorithm of Rohlf (1981) and Foster (1982). The agreement with measured data was very good.

Sediment Routing Component

The final component to be considered is the sediment routing component. The two sediment transport equations provided in KYERMO have already been shown as the best available for erosion work. The user can specify either the Yalin (1963) equation as modified by Foster and Meyer (1972) or a modification of the Yang (1973) equation for sheet flow transport and for rill flow transport. In Table 9.4 the results presented by Alonzo (1980) are shown and in Table 9.5 the results presented by Neibling and Foster (1980) are shown. The Z parameter in Table 9.4 is a dimensionsless flow depth. In each table a specific relationship is shown to be superior. In Table 9.4 the Yang (1973)

Table 9.3 Comparison of Observed Erosion Rates with Erosion Rates from Equation Fitted to Data From Rill Erosion Study of Meyer et al. (1975a) (From Foster, 1982)

Discharge x 10^4	Velocity*	Shear Stress	Rill Erosion Rate	
			Observed	Fitted
m^3/s	m/s	N/m^2	g/m rill length x m wetted permiter x s	
1.85	0.27	3.76	2.44	2.41
3.51	0.33	4.97	6.50	6.58
5.49	0.39	6.06	10.74	10.43
7.97	0.44	7.12	15.02	15.59
4.36§	0.36	5.48	2.88	3.02
8.22§	0.44	7.23	6.63	6.19
10.78§	0.48	8.17	8.50	9.56

*From Meyer et al. (1975a) velocity vs. discharge regression equation fitted to measured data.
§A three layer screen canopy just above the soil covered these rills.

equation is shown to be better, while in Table 9.5 the Yalin equation is shown to be better. Both equations can be utilized in the model.

Table 9.4 Sediment-Transport Equation Comparison of Alonzo (1980)

Formula	No. of tests	Ratio between predicted and measured load			Percentage of tests with ratio between 1/2 and 2
		Mean	95%-confidence limits of the mean	Standard deviation	
					Percent
		Field Data			
Ackers and White	40	1.27	1.05 1.48	0.68	87.8
Engelund and Hansen	40	1.46	1.28 1.64	.56	82.9
Laursen	40	.64	.49 .80	.48	56.1
MPME	40	.83	.50 1.15	1.02	58.5
Yang	40	1.00	.89 1.13	.39	92.7
Bagnold	40	.39	.31 .47	.26	32.0
Meyer-Peter & Muller	40	.24	.22 .27	.09	0
Yalin	40	2.59	2.08 3.11	1.62	46.3
		Flume data with Z < 70			
Ackers and White	177	1.34	1.24 1.54	1.29	73.0
Engelund and Hansen	177	.73	.63 .83	.68	51.1
Laursen	177	.81	.73 .88	.51	71.4
MPME	177	3.11	2.95 3.52	2.75	42.1
Yang	177	.99	.93 1.08	.60	79.8
Bagnold	177	.85	.81 1.22	2.50	20.8
Meyer-Peter & Muller	177	.40	.39 .47	.49	18.5
Yalin	177	1.62	1.38 2.23	4.08	32.6
		Flume Data with Z > 70			
Ackers and White	48	1.12	.93 1.28	.52	89.6
Engelund and Hansen	48	.75	.59 .90	.50	66.7
Laursen	48	1.04	.76 1.32	.99	79.2
MPME	48	1.34	1.04 1.64	1.04	66.7
Yang	48	.90	.79 1.05	.51	85.4
Bagnold	48	1.53	1.46 1.87	1.14	45.8
Meyer-Peter & Muller	48	1.03	1.00 1.27	.83	72.9
Yalin	48	1.92	1.45 2.41	1.65	64.6

Table 9.5 Percentage of Occurrences Where the Ratio of Calculated to Observed Sediment Discharge Was Between 0.75 and 1.5 (From Neibling and Foster, 1980)

Test	Specific		Method					
		(number)	(%)					
0.432 mm sand	2.64	22	0	0	23	32	10	10
0.265 mm sand	2.64	40	10	0	65	23	5	15
0.342 mm sand	2.64	42	0	0	25	0	78	13
0.342 mm coal	1.60	31	0	0	87	0	87	16
0.156 mm coal	1.67	38	3	0	71	29	45	0
Soil aggregates (D50 Approach)	1.8	3	33	0	67	0	67	0
Soil aggregates (7 size classes)	1.8	3	0	0	67	0	67	0

REFERENCES

1. Ackers, P. and W. R. White. 1973. Sediment transport: New approach and analysis. Journal of Hydraulics Division, ASCE 99(HY11):2041-2060.

2. Alberts, E. E., W. C. Moldenhauer and G. R. Foster. 1980. Soil aggregates and primary particles transported in rill and interrill flow. Soil Science Society of America Journal, 44(3):590-595.

3. Al-Durrah, M. and J. M. Bradford. 1981. New methods of studying soil detachment due to waterdrop impact. Soil Science Society of America Journal, 45:949-953.

4. Allmaras, R. R., R. E. Burwell, W. E. Larson, R. F. Holt and W. W. Nelson. 1966. Total porosity and random roughness of the interrow zone as influenced by tillage. USDA Cons. Rept. No. 7.

5. Alonso, C. V. 1980. Selecting a formula to estimate sediment transport capacity in nonvegetated channels. In CREAMS - A field scale model for Chemicals, Runoff, and Erosion from Agricultural Management Systems, Volume III, Supporting Documentation, Chapter 5, USDA-SEA, Conservation Report #28, pp. 426-439.

6. Alonso, C. V., W. H. Neibling and G. R. Foster. 1981. Estimating sediment transport capacity in watershed modeling. Transactions, ASAE 24(5): 1211-1220, 1226.

7. Barfield, B. J., R. C. Warner and C. T. Haan. 1981. Applied Hydrology and Sedimentology for Disturbed Lands. Oklahoma Technical Press, Stillwater, Oklahoma.

8. Bennett, J. P. 1974. Concepts of mathematical modeling of sedmient yield. Water Resources Research 10(3):485-492.

9. Bently, W. A. 1904. Studies of raindrops and raindrop phenomena. Monthly Weather Review, 32:450-456.

10. Biggerstaff, S. D. and I. D. Moore. 1983. Effect of surface mulching on infiltration, runoff, and erosion on reconstructed soils. Report No. IMMR83/ , Institute for Mining and Minerals Research, University of Kentucky, Lexington, Kentucky.

11. Bisal, F. 1950. Calibration of splash cups for soil erosion studies. Agricultural Engineering 31:621-622.

12. Bouwer, H. 1976. Infiltration into increasingly permeable soils. Proc. ASCE 102:IR1:127-136.

13. Brakensiek, D. L. 1966. Storage flood routing without coefficients. USDA-ARS, 41-122.

14. Bubenzer, G. D. and B. A. Jones, Jr. 1971. Drop size and impact velocity effects on the detachment of soils under simulated rainfall. ASAE Transactions, 14(4):625-628.

15. Campbell, G. S. 1974. A simple method for determining unsaturated conductivity from moisture retention data. Soil Sci. 117:6:311-314.

16. Campbell, K. L. and H. P. Johnson. 1975. Hydrologic simulation of watersheds with artifical drainage. Water Resources Research 11:1:120-126.

17. Carter, C. E., J. D. Greer, H. J. Brand, and J. M. Floyd. 1974. Raindrop characteristics in South Central United States. ASAE Transactions 17(6):1033-1037.

18. Cruse, R. M. and W. E. Larson. 1977. Effect of soil shear strength on soil detachment due to raindrop impact. Soil Science Society of America Journal, 41(4):777-781.

19. Currance, H. D. and W. G. Lovely. 1970. The analysis of soil surface roughness. Trans. ASAE 13(6):710-714.

20. Curtis, D. C. 1976. A deterministic urban storm water and sediment discharge model. National Symposium on Urban Hydrology, Hydraulics, and Sediment Control. UK Bulletin, University of Kentucky College of Engineering, Lexington, KY.

21. Davis, J. R. 1961. Estimating rate of advance for irrigation furrows. Trans. ASAE 4:1:52-54, 57.

22. Einstein, H. A. 1950. The bed-load function for sediment transportation in open channel flows. USDA-SCS Technical Bulletin # 1026, 78 pp.

23. Ekern, P. C. 1950. Raindrop impact as the force initiating soil erosion. Soil Sci. Soc. Amer. Proc. 15:7-10.

24. Ekern, P. C. 1953. Problems of raindrop impact erosion. Agric. Engrg. 34:1:23-25, 28.

25. Ellison, W. D. 1947. Soil erosion studies - Part II: Soil detachment hazard by raindrop splash. Agricultural Engineering, 28(5):197-201.

26. Ellison, W. D. and O. T. Ellison. 1947. Soil erosion studies - Part IV: Soil detachment by surface flow. Agricultural Engineering, 28(9): 402-405, 408.

27. Foster, G. R. 1982. Modeling the erosion process. In Hydraulic Modeling of Small Watersheds, C. T. Haan, editor, ASAE Monograph, pp.

28. Foster, G. R. and L. J. Lane. 1981. Discussion of modeling rill density. Jour. Irr. and Drain. Div., ASCE, 107(IR1):109-112.

29. Foster, G. R., L. J. Lane, J. D. Nowlin, J. M. Laflen and R. A. Young. 1980). A model to estimate sediment yield from field-sized areas: devlopment of model. In CREAMS - A field scale model for Chemicals, Runoff, and Erosion from Agricultural Management Systems. Volume I: Model Documentation, Chapter 3. USDA-SEA, Conservation Report #26, pp. 36-64.

30. Foster, G. R., L. J. Lane, J. D. Nowlin, J. M. Laflen, R. A. Young. 1981. Estimating erosion and sediment yield on field-sized areas. 24(5):1253-1262.

31. Foster, G. R., F. Lombardi and W. C. Moldenhauer. 1980. Evaluation of rainfall-runoff erosivity factors for individual storms. ASAE Transactions, 25(1):124-129.

32. Foster, G. R. and L. D. Meyer. 1972a. A closed-form soil erosion equation for upland areas. In Sedimentation: Symposium to Honor Professor H. A. Einstein. H. W. Shen, Editor, Fort Collins, Colorado, Chapter 12, 19 pp.

33. Foster, G. R. and L. D. Meyer. 1972b. Transport of soil particles by shallow flow. Transactions ASAE, 15(1):99-102.

34. Foster, G. R., L. D. Meyer and C. A. Onstad. 1977a. An erosion equation derived from basic erosion principles. Trans. ASAE 20(4):678=682.

35. Foster, G. R., L. D. Meyer, and C. A. Onstad. 1977b. A runoff erosivity factor and variable slope length exponents for soil loss estimates. Trans. ASAE, 20(4):683-687.

36. Foster, G. R. and W. H. Wischmeier. 1974. Evaluating irregular slopes for soil loss prediction. Trans. ASAE 17(2):305-309.

37. Frederick, R. H., V. A. Myers, and E. P. Auciello. 1977. Five-to-60-minute precipitation frequency for the eastern and central United States. NOAA Technical Memorandum NWS HYDRO-35, U.S. Department of Commerce, Washington, D.C.

38. Free, G. R. 1960. Erosion characteristics of rainfall. Agricultural Engineering 41(7):447-449, 455.

39. Gayle, G. A. and R. W. Skaggs. 1978. Surface storage on bedded cultivated lands. Trans. ASAE 21:1:101-104, 109.

40. Green, W. H., and G. A. Ampt. 1911. Studies on soil physics. 1. The flow of air and water through soils. J. Agric. Sci. 4:1-24.

41. Gregory, J. M. 1977. A land-phase hydraulic model for strip mined lands. Unpub. Ph.D. thesis, Iowa State University, Ames, Iowa.

42. Gunn, R. and G. D. Kinzer. 1949. The terminal velocity of fall for water droplets in stagnant air. Jour. of Meterology, 6(4):243-248.

43. Haan, C. T. and H. P. Johnson. 1967. Geometric properties of depressions in North-Central Iowa. Iowa State J. Sci. 42:2:149-160.

44. Hershfield, D. M. 1961. Rainfall frequency atlas of the United States. TP40, U.S. Department of COmmerce, Weather Building, Washington, D.C.

45. Hirschi, M. C. 1980. Hydraulic conductivity and degree of saturation during infiltration: A preliminary investigation. Unpub. M.S. paper, Department of Agricutlural Engineering, University of Minnesota, St. Paul, Minnesota.

46. Hirschi, M. C., C. L. Larson and D. C. Slack. 1980. Hydraulic conductivity and degree of saturation during infiltration. ASAE paper #80-2007, presented at the ASAE Summer Meeting, June 15-18, San Antonio, Texas.

47. Holtan, H. N. 1961. A concept for infiltration estimates in watershed engineering. U.S. Department of Agriculture (publication) ARS 41-51, 25 pp.

48. Horton, R. E. 1940. Approach toward a physical interpretation of infiltration capacity. Soil Science Society of American Proceedings 5:339-417.

49. Horton, R. E. 1945. Erosional development of streams and their drainage basis; hydrophysical approach to quantitative morphology. Geological Society of America Bulletin, 56:275-370.

50. Hudson, N. 1971. Soil Conservation, Cornell Univ. Press, Ithaca, NY.

51. Hudson, N. 1981. Soil Conservation, Cornell Univ. Press, Ithaca, NY.

52. Huff, F. A. 1967. Time distribution of rainfall in heavy storms. Water Resources Research 3(4):1007-1019.

53. Huggins, L. F. and E. J. Monke. 1967. A mathematical model for simulating the hydrologic response of a watershed. Water Resources Reserach 4:29-539.

54. Hughes, W. C. 1980. Scour velocities in ephemeral channels. Journal of Hydraulics Division, ASCE, 106(HY9):1435-1441.

55. Idike, F., C. L. Larson, D. C. Slack and R. A. Young. 1980. Experimental evaluation of two infiltration models. ASAE Transactions 23(6):1428-1433.

56. Kelly, W. E. and R. C. Gularte. 1981. Erosion resistance of cohesive soils. Journal of Hydraulics Division, ASCE, 107(HY10):1211-1224.

57. Lane, L. J. and G. R. Foster. 1980. Concentrated flow relationships. In. CREAMS - A Field Scale Model for Chemicals, Runoff, and Erosion from Agricultural Management Systems, Volume III, Supporting Documentation, Chapter 11, USDA-SEA, Conservation Report #26, pp. 474-485.

58. Lane, E. W. 1953. Progress Report on Studies in the Design of Stable Channels by the Bureau of Reclamation. ASCE Proceedings, Irrigation and Drainage Division, Separate No. 280, 31 pp.

59. Lane, E. W. 1955. Design of stable channels. ASCE Transactions. 120: 1234-1279.

60. Lattanzi, A. R., L. D. Meyer and M. F. Baumgardner. 1974. Influences of mulch rate and slope steepness on interrill erosion. Soil Science Society Proceedings 38(6):946-950.

61. Laurseh, E. M. 1958. The total sediment load of streams. Journal of Hydraulics Division, ASCE, 84(HY1):1530-1, 1530-36.

62. Laws, J. O. 1941. Measurements of the fall-velocity of water-drops and raindrops. Trans. Amer. Geo. Union, 22:709-721.

63. Laws, J. O. and D. A. Parsons. 1943. The relation of raindrop-size to intensity. Trans. American Geophysical Union, 24:452-460.

64. Leighly, J. B. 1932. Toward a theory of the morphologic significance of turbulence in the flow of water in streams. Univ. of Calif. Publications in Geography, 6(1):1-22.

65. Leopold, L. B., M. G. Wolman, and J. P. Miller. 1964. Fluvial Processes in Geomorphology. San Francisco: W. H. Freeman and Company, pp. 411-432.

66. Li, R., V. M. Ponce and D. B. Simons. 1980. Modeling rill density. Jour. Irr. and Drainage Div., ASCE, 106(IR1):63-67.

67. Li, R., R. K. Simons, and L. Y. Shiao. 1977. Mathematical modeling of on-site soil erosion. Proceedings of the International Symposium on Urban Hydrology, Hydraulics, and Sediment Control, July 18-21, Lexington, Kentucky, pp. 87-94.

68. Linden, D. R. 1979. A model to predict soil water storage as affected by tillage practices. Ph.D. Dissertation, Department of Soil Science, University of Minnesota, St. Paul, Minnesota.

69. Linsley, R. K., M. A. Kohler and J. L. H. Paulhus. 1949. Applied Hydrology. McGraw-Hill, New York.

70. Lundgren, H. and I. G. Jonsson. 1964. Shear and velocity distribution in shallow channels. Journal of Hydrualics Division, ASCE, 90(HY1):1-21.

71. Lyle, W. M. and E. T. Smerdon. 1965. Relation of compaction and other soil properties to erosion resistance of soils. Transactions ASAE, 8(3):419-422.

72. McGregor, K. C. and C. K. Mutchler. 1977. Status of the R-factor in Northern Mississippi. In Soil Erosion: Prediction and Control, SCSA Special Publication 321, pp. 135-142.

73. Mantz, P. A. 1977. Incipient transport in fine grains and flakes by fluids-extended Shields diagram. Journal of Hydraulics Division, ASCe, 103(HY6):601-615.

74. Massie, L. R. 1980. A soil splash model. ASAE Paper # 80-2501, presented at the ASAE Winter Meeting, December 2-5, Chicago, Illinois.

75. Mein, R. G. and C. L. Larson. 1971. Modeling the infiltration components of the rainfall-runoff process. WRRC, University of Minnesota Grad. School Bull. 43.

76. Mein, R. G. and C. L. Larson. 1973. Modeling infiltration during steady rain. Water Resources Research 9:2:384-394.

77. Meyer, L. D. 1982a. How rainfall intensity affects interrill erosion. Trans. ASAE 24(6):1472-1475.

78. Meyer, L. D. 1982b. Soil erosion research leading to the Universal Soil Loss Equation. Proceedings of the Workshop on estimating erosion and sediment yield on rangelands. USDA-ARS Publication ARM-W-26.

79. Meyer, L. D., G. R. Foster, and S. Nikolov. 1975. Effect of flow rate and canopy on rill erosion. Trans. ASAE 18(5):905-911.

80. Meyer, L. D. and D. L. McCune. 1958. Rainfall simulator for runoff plots. Agricultural Engineering 39(10):644-648.

81. Meyer, L. D. and W. H. Wischmeier. 1969. Mathematical simulation of the process of soil erosion by water. Transactions ASAE 12(6):754-758, 762.

82. Mihara, H. 1951. Raindrop and soil erosion. Bull. Nat. Inst. Agric. Sci. Series A, No. 1.

83. Mitchell, J. K. and B. A. Jones, Jr. 1976. Micro-relief surface depression storage:analysis of models to describe the depth-storage function. AWRA Water Resources Bull. 12:6:1205-1222.

84. Mitchell, J. K. and B. A. Jones, Jr. 1978. Micro-relief surface depression storage: changes during rainfall events and their application to rainfall-runoff models. AWRA Water Resources Bull. 14:4:777-802.

85. Moldenhauer, W. C. and D. C. Long. 1964. Influence of rainfall energy on soil loss and infiltration rates. I. Effect over a range of texture. Soil Sci. Soc. Amer. Proc. 28:813-817.

86. Monteith, N. H. 1974. The role of surface roughness in runoff. J. Soil Cons. New South Wales 30:42-45.

87. Moore, I. D. 1979. Infiltration into tillage affected soils. Unpub. Ph.D. thesis, University of Minnesota, St. Paul, Minnesota.

88. Moore, I. D. 1981. Infiltration equations modified for surface effects. Journal of the Irrigation and Drainage Division, ASCE, Vol. 107, No. IR1: 71-86.

89. Moore, I. D. 1982. Infiltration into multiple-layered soil profiles. Univ. of Kentucky Agr. Exp. Station. Unpub. J. Article No. 82-2-245. Univ. of Kentucky, Lexington, KY.

90. Moore, I. D. and J. D. Eigel. 1981. Infiltration into two-layered soil profiles. Transactions of the American Society of Agricultural Engineers 24(6):1496-1503.

91. Moore, I. D. and C. L. Larson. 1979. Effects of drainage projects on surface runoff from small depressional watersheds in the North Central region. WRRC, University of Minnesota Grad. School Bull. 99.

92. Moore, I. D., C. L. Larson and D. C. Slack. 1980. Predicting infiltration and micro-relief surface storage for cultivated soils. WRRC Bulletin 102, University of Minnesota Graduate School, Minneapolis, Minnesota.

93. Morel-Seytoux, H. J. 1973. Two-phase flows in porous media. Adv. Hydrosci. 9:119-202.

94. Morris, H. M. and J. M. Wiggert. 1972. Applied Hydraulics in Engineering. New York: Ronald Pless. 640 pp.

95. Mosley, M. P. 1972. An experimental study of rill erosion. M.S. Thesis, Department of Geology, Colorado State University, Ft. Collins, Colorado, 118 pp.

96. Mosley, M. P. 1974. Experimental study of rill erosion. Trans. ASAE 17(5):909-913, 196.

97. Mutchler, C. K. and C. L. Larson. 1971. Splash amounts from waterdrop impact on a smooth surface. Water Resources Research 7:1:195-200.

98. Neal, J. H. 1938. The effect of degree of slope and rainfall characteristics on runoff and soil erosion. Mo.Agric. Exp. Sta. Research Bull. 280, 47 pp.

99. Neibling, W. H. and G. R. Foster. 1980. Sediment transport capacity of overland flow. In CREAMS - A field Scale Model for Chemicals, Runoff, and Erosion from Agricultural Management Systems, Volume III, Supporting Documentation, Chapter 10, USDA-SEA, Conservation Report #26, pp. 463-473.

100. Onstad, C. A. and G. R. Foster. 1975. Erosion modeling on a watershed. Trans. ASAE 18(2):288-92.

101. Palmer, R. S. 1965. Waterdrop impact forces. Trans. ASAE 8:1:69-70, 72.

102. Park, S. W. and J. K. Mitchell. 1981. A dynamic system model for simulating sediment discharge. ASAE Paper #81-2037, presented at the ASAE Summer Meeting, June 21-24, Orlando, Florida.

103. Park, S. W., J. K. Mitchell and G. D. Bubenzer. 1982. Splash erosion modeling: Physical analysis. Transactions Amer. Soc. Agr. Engr. 25(2): 357-361.

104. Philip, J. R. 1957b. The theory of infiltration. 2: The profile at infinity. Soil Sci. 83:435-448.

105. Quansah, C. 1981. The effect of soil type, scope, rain intensity, and their interactions on splash detachment and transport. Journal of Soil Science 32:215-224.

106. Ranga Raju, K. G., R. J. Garde, and R. C. Bhardwaj. 1981. Total load transport in alluvial channels. Journal of Hydraulics Division, ASCE, 107(HY2):179-191.

107. Raudkivi, A. J. 1976. Loose Boundary Hydraulics. New York: Pergamon, 397 pp.

108. Replogle, J. A. and V. T. Chow. 1966. Tractive-force distribution in open channels. Jour. Hydraulics Division, ASCE, 92(HY2):169-191.

109. Rice, C. E. and C. L. Larson. 1972. Methods for routing hydrographs through open channels. Bulletin 51, Water Resources Research Center, University of Minnesota Graduate School, Minneapolis, Minnesota.

110. Rohlf, R. A. 1981. Development of a deterministic mathematical model for interrill and rill runoff and erosion. Unpublished M.S. Thesis, Department of Civil Engineering, University of Kentucky, Lexington, Kentucky, 84 pp.

111. Rose, C. W. 1960. Soil detachment caused by rainfall. Soil Science, 89(1):28-35.

112. Schwab, G. O., R. K. Frevert, T. W. Edminster, and K. K. Barnes. 1966. Soil and Water Conservation Engineering, 2nd Edition. New York: Wiley and Sons, 683 pp.

113. Seginer, I. 1968a. A model for surface drainage of cultivated fields. Technion, Israel Inst. Tech., Dept. Agric. Eng. Pub. No. 55.

114. Seginer, I. 1968b. Random walk and roughness models of drainage networks. Technion, Israel Inst. Tech., Dept. Agric. Eng. Pub. No. 56.

115. Seginer, I. 1971. A model for surface drainage of cultivated fields. J. Hydrol. 13:139-151.

116. Slack, D. C. 1978. Predicting ponding under moving irrigation systems. Journla of Irrig. and Drainage Div., ASCE, 104(IR4):446-451.

117. Smerdon, E. T. and R. P. Beasley. 1961. Critical tractive forces in cohesive soils. Agricultural Engineering 42(1):26-29.

118. Smith, D. D. and W. H. Wischmeier. 1957. Factors affecting sheet and rill erosion. Trans. Amer. Geophy. Union 38:889-896.

119. Soil Conservation Service. 1973. A method for estimating volume and rate of runoff in small watersheds. SCS-TP-149, U.S. Department of Agriculture, Soil Conservation Service, Washington, D.C.

120. Tholin, A. L. and C. J. Keifer. 1960. Hydrology of urban runoff. Transactions American Society of Civil Engineers 125:1308-1355.

121. Viesman, W., Jr. 1967. A linear model for synthesizing hydrographs for small drainage areas. Paper presented at the 48th Annual Meeting American Geophysical Union, Washington, D.C., April.

122. Whisler, F. D. and H. Bouwer. 1970. Comparison of methods for calculating vertical infiltration and drainage in soils. J. Hydrol. 10:1-19.

123. Williams, J. R. 1975. Sediment yield prediction with universal equation using runoff energy factor. USDA-ADS S-40 U.S. Department of Agriculture, Washington, D.C.

124. Williams, J. R. 1976. Sediment yield prediction with Universal Equation using runoff energy factor. In Present and Prospective Technology for Predicting Sediment Yields and Sources. Publication ARS-S-40, Agricultural Research Service, U.S. Department of Agriculture, Washington, D.C.

125. Wischmeier, W. H. 1976. Use and misuse of the Universal Soil Loss Equation. J. Soil and Water Cons. 31:5-9.

126. Wischmeier, W. H. and D. D. Smith. 1958. Rainfall energy and its relationship to soil loss. Trans. Amer. Geo. Union, 39(2):285-291.

127. Wischmeier, W. H. and D. D. Smith. 1965. Rainfall erosion losses from cropland east of the Rocky Mountains. Agriculture Handbook No. 282, U.S. Department of Agriculture, Washington, D.C.

128. Wischmeier, W. H. and D. D. Smith. 1978. Predicting rainfall erosion losses - a guide to conservation planning. USDA, AH-537.

129. Wright-McLaughlin Engineers. 1969. Urban storm drainage criteria manual. Denver Regional Council of Governments, Denver, Colorado, 1969 and 1975 revision.

130. Wu, T. H., K. W. Bedford, M. E. Mossaad, K. L. McCurdy, and E. M. Ali. 1982. A stochastic model of soil erosion. Water Resources Center, Ohio State University, Completion Report No. 711523, NTIS No. PB82-224734, 145 pp.

131. Yalin, M. S. 1963. An expressionfor bed-load transportation. Journal of the Hydraulic Division, ASCE 89(HY3):221-250.

132. Yalin, M. S. 1972. Mechanics of Sediment Transport. 2nd Edition. New York: Pergamon, 298 pp.

133. Yand, C. T. 1972. Unit stream power and sediment transport. Journal of Hydraulics Division, ASCE, 98(HY10):1805-1826.

134. Yang, C. T. 1973. Incipient motion and sediment transport. Journal of Hydraulics Division, ASCE, 99(HY10):1679-1704.

135. Young, R. A. and J. L. Wiersma. 1973. The role of rainfall impact in soil detachment and transport. Water Resources Research, 9(6):1629-1636.

APPENDIX I

MAIN AND SUPPORT

PROGRAM LISTINGS

```
C
C*****************************************************************
C*****************************************************************
C****                                                         *****
C****              KENTUCKY EROSION MODEL                     *****
C****                                                         *****
C****                        BY                               *****
C****                                                         *****
C****                MICHAEL C. HIRSCHI                       *****
C****               RESEARCH  SPECIALIST                      *****
C****                                                         *****
C****      DEPARTMENT OF AGRICULTURAL ENGINEERING             *****
C****              UNIVERSITY OF KENTUCKY                     *****
C****             LEXINGTON, KY 40546-0075                    *****
C****                                                         *****
C*****************************************************************
C*****************************************************************
C
      COMMON/SOILMP/KS(2),SMC(2),B(2),XI(2),MC(2),DS(2)
     X,SAV(2),KRFS(2)
      COMMON/PLOT1/NJ,NR(10),NRR,BD(2),HDDSL
      COMMON/SEDPAR/DMM(10),SS(10),FDMM(10),FDMMRD(10),
     XDEP(10,10,10)
      COMMON/TIMEP/T,DTM,DTS,TS,TRS,TRQ,TR,ITRS
      COMMON/RAINP/RAIN,EKRAIN,EK,RDMM(20),FRDMM(20),RTOT
      COMMON/INFISP/KFS1,KFS2,SAV1,SAV2,IMD1,IMD2,EF,EV
     X,LI(10)
      COMMON/INFP/F(10),V(10)
      COMMON/SURFAC/RR(10),SSTO(10),FCOV(10),STOD,DBURF,STO(10)
      COMMON/PLOT/HPL,PW,SLINC(10),SO(10),SINE(10),COSINE(10)
     X,PCL(2),HLINC(10)
      COMMON/ENVIR/G,TCELS,VK,SF,PI
      COMMON/FLOW/QRILL(10,10),YRILL(10,10),HRRILL(10,10)
     X,PWRILL(10,10),ARILL(10,10,2)
      COMMON/PRINT/PO0,PO1,PO2,PO3
      COMMON/RILLP/IK1(10),IK2(10),IK3(10),K1(10,10),K2(10,10)
     X,K3(10,10)
      COMMON/RADP/PSM,PS3,CC,E1,E2,E3,GSO,RDET(10,10)
      COMMON/RLDP/ARDET(2),BRDET(2),SHEAR(10,10,10),RSH,CSH
     X,DRILL(10,10),EXS,DRR(10)
      COMMON/WATER/RO(10),QRO,QSHEET(10,10),ROP(10)
      COMMON/SHEF/ST(10,10),FCD(10,10,10)
      COMMON/STATS/VWF,SEDR,SEDVR,SEDRTO,TSPWFR
     X,ROTCM,ROTL,SDKS,SDMTHA,SDTAC,WSDL,RTOTL
      COMMON/RLSL/QSR(10),QSRILL(10,2,10),RT(10,10),RTR(10)
      COMMON/SHEEF/ISED,NS(10,10)
      COMMON/NAME/SEDEQ(2)
      COMMON/INTE/QO,QI
      COMMON/RILLPA/IRSD,N(10,10),Z(10,10,10),RWSW(10,10)
     X,LAYER(10,10,10),NSES(10,10),NSS(10,10,10)
      COMMON/SEDDIS/PFW(10),NUM(10),SEDDMM(10)
```

```
      COMMON/DETR/DETOTD(10,10,10),DETOTM(10,10,10)
      COMMON/BEDDEP/FDMMB(10,10,100)
      COMMON/RLSHA/RX(10,10,30),RY(10,10,30),XDL(10,10)
      COMMON/SLUF/XSR(10,10),YSR(10,10),XSL(10,10),YSL(10,10)
      COMMON/RLSH/X(10,10),YB(10),Y(10,10),XL(10),XR(10),IL(10)
     X,IR(10),XB(10)
      COMMON/RLLINE/SLO(10,10),YIN(10,10)
      COMMON/MISC/IIN,IIIN,SUMQ,SUMQP
      REAL N,NS,MC,KRFS,KS,KRI,KFS1,KFS2,IMD1,IMD2,LI,L1
      INTEGER T,TR,TRQ,TRS,DTM,TS,PO0,PO1,PO2,PO3,DTS,TCH,TO
      OPEN(5,FILE='RUNDAT')
      OPEN(6,FILE='PRN')
C
C*** INITIALIZE PROGRAM AND INPUT PARAMETERS
C
      CALL INITIA
      ROTL=0.0
      RTOT=0.0
C
C*** BEGIN SIMULATION
C
      DO 10 T=DTM,TS,DTM
C
C*** CHECK TIME FOR RAINFALL AND INPUT IF NECESSARY
C
      IF(T.LT.TRS)GOTO20
      CALL RAINFA
   20 CONTINUE
      RTOT=RTOT+RAIN*DTM/60.
      SDKG=0.0
      WSDL=0.0
C
C*** BEGIN AT TOP OF PLOT
C
   25 CONTINUE
      HDDSL=0.0
      DO 30 J=1,NJ
      NRR=NR(J)
      RORTOT=0.0
C
C*** CALCULATE RUNOFF GENERATION DUE TO RAINFALL
C
      CALL RUNGEN(J)
C
C*** ROUTE RUNOFF
C
      CALL RUNROT(J)
C
C*** CALCULATE SEDIMENT GENERATION
C
      CALL SEDGEN(J)
C
```

```
C*** ROUTE SEDIMENT
C
      CALL SEDROT(J)
C
C*** PREPARE TO MOVE TO NEXT INCREMENT
C
      CALL MOVE(J)
      IF(PO1.NE.1)GOTO30
C
C*** PRINT INTERMEDIATE SLOPE RESULTS IF DESIRED
C
      CALL PRINT1(J)
C
C*** INCREMENT SLOPE
C
   30 CONTINUE
      IF(PO2.NE.1)GOTO10
C
C*** PRINT INTERMEDIATE TIME RESULTS AT BOTTOM OF PLOT
C*** IF DESIRED
C
      CALL PRINT2
   10 CONTINUE
      IF(PO3.NE.1)GOTO40
C
C*** PRINT SIMULATION SUMMARY IF DESIRED
C
      CALL PRINT3
   40 CONTINUE
      STOP
      END
```

```
C
C*****************************************************************
C*****************************************************************
      SUBROUTINE INITIA
C*****************************************************************
C*****************************************************************
C
      COMMON/SOILMP/KS(2),SMC(2),B(2),XI(2),MC(2),DS(2)
     X,SAV(2),KRFS(2)
      COMMON/PLOT1/NJ,NR(10),NRR,BD(2),HDDSL
      COMMON/SEDPAR/DMM(10),SS(10),FDMM(10),FDMMRD(10),
     XDEP(10,10,10)
      COMMON/TIMEP/T,DTM,DTS,TS,TRS,TRQ,TR,ITRB
      COMMON/RAINP/RAIN,EKRAIN,EK,RDMM(28),FRDMM(28),RTOT
      COMMON/INFISP/KFS1,KFS2,SAV1,SAV2,IMD1,IMD2,EF,EV
     X,LI(10)
      COMMON/INFP/F(10),V(10)
      COMMON/SURFAC/RR(10),SSTO(10),FCOV(10),STOD,DSURF,STO(10)
      COMMON/PLOT/HPL,PW,SLINC(10),SD(10),SINE(10),COSINE(10)
     X,PCL(2),HLINC(10)
      COMMON/ENVIR/G,TCELS,VK,SF,PI
      COMMON/FLOW/QRILL(10,10),YRILL(10,10),HRRILL(10,10)
     X,PWRILL(10,10),ARILL(10,10,2)
      COMMON/PRINT/PO0,PO1,PO2,PO3
      COMMON/RILLP/IK1(10),IK2(10),IK3(10),K1(10,10),K2(10,10)
     X,K3(10,10)
      COMMON/RADP/PSM,PS3,CC,E1,E2,E3,SSO,RDET(10,10)
      COMMON/RLDP/ARDET(2),BRDET(2),SHEAR(10,10,10),RSH,CSH
     X,DRILL(10,10),EXS,DRR(10)
      COMMON/WATER/RO(10),QRO,QSHEET(10,10),ROP(10)
      COMMON/SHEF/ST(10,10),FCD(10,10,10)
      COMMON/STATS/VWF,SEDR,SEDVR,SEDRTO,TSPWFR
     X,ROTCM,ROTL,SDKG,SDMTHA,SDTAC,WSDL,RTOTL
      COMMON/RLSL/QSR(10),QSRILL(10,2,10),RT(10,10),RTR(10)
      COMMON/SHEEF/ISSD,NS(10,10)
      COMMON/NAME/SEDEQ(2)
      COMMON/INTE/QO,QI
      COMMON/RILLPA/IRSD,N(10,10),Z(10,10,10),RWSW(10,10)
     X,LAYER(10,10,10),NSES(10,10),NSS(10,10,10)
      COMMON/SEDDIS/PFW(10),NUM(10),SEDDMM(10)
      COMMON/DETR/DETOTD(10,10,10),DETOTM(10,10,10)
      COMMON/BEDDEP/FDMMB(10,10,100)
      COMMON/RLSHA/RX(10,10,30),RY(10,10,30),XDL(10,10)
      COMMON/SLUF/XSR(10,10),YSR(10,10),XSL(10,10),YSL(10,10)
      COMMON/RLSH/X(10,10),YB(10),Y(10,10),XL(10),XR(10),IL(10)
     X,IR(10),XB(10)
      COMMON/RLLINE/SLO(10,10),YIN(10,10),SLNB(10,10)
      COMMON/MISC/IIN,IIIN,SUMQ,SUMQP
      REAL N,NS,MC,KRFS,KS,KRI,KFS1,KFS2,IMD1,IMD2,LI,L1
      INTEGER T,TR,TRQ,TRS,DTM,TS,PO0,PO1,PO2,PO3,DTS,TCH,TO
      OPEN(5,FILE='RUNDAT')
      OPEN(6,FILE='PRN')
```

```
      OPEN(4,FILE='BURDAT')
      OPEN(7,FILE='CON')
      READ(5,1)HPL,PW
    1 FORMAT(2F7.2)
      READ(5,12)NJ
   12 FORMAT(I2)
      READ(5,13)(NR(J),J=1,NJ)
      DO 107 J=1,NJ
      READ(5,13)(NSEB(J,M),M=1,NR(J))
      DO 107 M=1,NR(J)
      READ(5,13)(NBB(J,M,MJ),MJ=1,NSEB(J,M))
  107 CONTINUE
   13 FORMAT(10I3)
      READ(5,4)(BD(J),J=1,NJ)
      READ(5,4)(HLINC(J),J=1,NJ)
      READ(5,2)TB,DTM,ITRB,TCELB
    2 FORMAT(3I5,F5.2)
      READ(5,3)(KB(L),BMC(L),B(L),XI(L),L=1,2)
    3 FORMAT(8F7.4)
      BD(1)=(1.-BMC(1))*2.65
      BD(2)=(1.-BMC(2))*2.65
      READ(5,4)(DMM(I),I=1,10)
      READ(5,4)(BS(I),I=1,10)
      READ(5,4)(FDMM(I),I=1,10)
      READ(5,4)(FDMMRD(I),I=1,10)
    4 FORMAT(10F7.4)
      READ(5,5)(DB(L),MC(L),PCL(L),L=1,2),EF,EV
    5 FORMAT(8F7.3)
      READ(5,6)(LI(J),J=1,NJ)
      DO 130 J=1,NJ
      NRR=NR(J)
      READ(5,10)(N(J,M),M=1,NRR)
      READ(5,10)(NB(J,M),M=1,NRR)
      READ(5,6)(RWBW(J,M),M=1,NRR)
  130 CONTINUE
    6 FORMAT(10F7.2)
      READ(5,7)IBBD,IRBD
    7 FORMAT(2I5)
      READ(5,4)(RR(J),J=1,NJ)
      READ(5,9)CC,E1,E2,E3,PBM,PB3
      READ(5,8)(ARDET(L),BRDET(L),L=1,2)
    8 FORMAT(4F7.4)
    9 FORMAT(6F7.4)
   10 FORMAT(10F5.3)
      READ(5,11)P00,P01,P02,P03
   11 FORMAT(4I2)
      NR1=NR(1)
      DO 100 M=1,NR1
      K1(1,M)=0
      K2(1,M)=0
      K3(1,M)=0
      XDL(1,M)=0.0
```

```
100 CONTINUE
    DO 101 J=2,NJ
    NRR=NR(J)
    READ(5,15)(K1(J,M),K2(J,M),K3(J,M),M=1,NRR)
 15 FORMAT(10(1X,3I1))
    DO 101 M=1,NRR
    NSG=NSEG(J,M)
    XDL(J,M)=0.0
    DO 101 MJ=1,NSG
    FCD(J,M,MJ)=0.0
    JM=10*M+MJ
101 CONTINUE
    DO 102 J=1,NJ
    F(J)=0.0
    V(J)=0.0
    STO(J)=0.0
    RO(J)=0.0
    ROP(J)=0.0
    SINE(J)=SIN(ATAN(SO(J)))
    COSINE(J)=COS(ATAN(SO(J)))
    SLINC(J)=HLINC(J)/COSINE(J)
102 CONTINUE
    DO 103 I=1,10
    DO 103 J=1,NJ
    NRR=NR(J)
    DO 103 M=1,NRR
    DETOTM(I,J,M)=0.0
    DETOTD(I,J,M)=0.0
    DEP(I,J,M)=0.0
    QSRILL(I,1,M)=0.0
    QSRILL(I,2,M)=0.0
    ST(I,M)=0.0
    RT(I,M)=0.0
103 CONTINUE
    G=981.
    DO 110 L=1,2
    SAE=10.**XI(L)*SMC(L)**(-B(L))
    E=2.*B(L)+3.
    A=(B(L)+3.)/E
    DSI=MC(L)/SMC(L)
    DSF=DS(L)
    KRI=DSI**E
    KRFS(L)=DSF**E
    SAV(L)=SAE*(KRFS(L)**A-KRI**A)/A/(KRFS(L)-KRI)
110 CONTINUE
    SAV1=SAV(1)
    SAV2=SAV(2)
    KFS1=KRFS(1)*KS(1)
    KFS2=KRFS(2)*KS(2)
    IMD1=DS(1)*SMC(1)-MC(1)
    IMD2=DS(2)*SMC(2)-MC(2)
    WRITE(7,151)IMD1,IMD2
```

```
151 FORMAT(5X,2(F8.4))
    VK=0.02908*TCELS**(-0.3784)
    SF=1.06143+(TCELS+273.)*(-2.183E-04)
    RTOT=0.0
    ROTL=0.00
    TRS=ITRS
    SUMQ=0.0
    SUMQP=0.0
    IIN=0
    IIIN=0
    PI=3.14159
    IF(SF.GT.1.0)SF=1.0
    DO 105 J=1,NJ
    NRR=NR(J)
    DO 105 M=1,NRR
    QRILL(J,M)=0.0
    QSHEET(J,M)=0.0
    RX(J,M,1)=0.0
    NSG=NSEG(J,M)+1
    READ(4,20)(RX(J,M,MJ),RY(J,M,MJ),MJ=2,NSG+1)
    RY(J,M,1)=RY(J,M,2)
105 CONTINUE
 20 FORMAT(20(F5.1))
    IF(POO.NE.1)GOTO120
    CALL PRINTO
120 CONTINUE
    END
```

```
C
C*****************************************************************
C*****************************************************************
      SUBROUTINE PRINTO
C*****************************************************************
C*****************************************************************
C
      COMMON/PLOT1/NJ,NR(10),NRR,BD(2),HDDBL
      COMMON/SEDPAR/DMM(10),SS(10),FDMM(10),FDMMRD(10)
     X,DEP(10,10,10)
      COMMON/PLOT/HPL,PW,SLINC(10),SO(10),SINE(10),COSINE(10)
     X,PCL(2),HLINC(10)
      COMMON/SOILMP/KS(2),SMC(2),B(2),XI(2),MC(2),DS(2)
     X,SAV(2),KRFS(2)
      COMMON/TIMEP/T,DTM,DTS,TS,TRS,TRQ,TR,ITRS
      COMMON/INFISP/KFS1,KFS2,SAV1,SAV2,IMD1,IMD2,EF,EV
     X,LI(10)
      COMMON/SURFAC/RR(10),SSTO(10),FCOV(10),STOD,DSURF,STO(10)
      COMMON/ENVIR/G,TCELS,VK,SF,PI
      COMMON/PRINT/PO0,PO1,PO2,PO3
      COMMON/RILLP/IK1(10),IK2(10),IK3(10),K1(10,10),K2(10,10)
     X,K3(10,10)
      COMMON/RILLPA/IRSD,N(10,10),Z(10,10,10),RWSW(10,10)
     X,LAYER(10,10,10),NSEG(10,10),NSS(10,10,10)
      COMMON/RADP/PSM,PS3,CC,E1,E2,E3,SSO,RDET(10,10)
      COMMON/RLDP/ARDET(2),BRDET(2),SHEAR(10,10,10),RSH,CSH
     X,DRILL(10,10),EXS,DRR(10)
      COMMON/SHEEF/ISSD,NS(10,10)
      COMMON/RLSHA/RX(10,10,30),RY(10,10,30),XDL(10,10)
      COMMON/NAME/SEDEQ(2)
      CHARACTER*5 SEDEQ
      CHARACTER*5 PO(2),POP(4)
      INTEGER TS,DTM,PO0,PO1,PO2,PO3,DTS
      REAL KS,MC,LI,N,NS
      OPEN(6,FILE='PRN')
      WRITE(6,1)
      WRITE(6,1)
    1 FORMAT(1X,71('*'))
      WRITE(6,2)
    2 FORMAT(' *',23X,'INPUT PARAMETERS:',29X,'*')
      WRITE(6,1)
      WRITE(6,1)
      WRITE(6,3)
    3 FORMAT(' *',69X,'*')
      WRITE(6,100)HPL
      WRITE(6,110)PW
      WRITE(6,120)NJ
      WRITE(6,130)TS
      WRITE(6,140)DTM
      WRITE(6,143)ITRS
      WRITE(6,150)TCELS
  100 FORMAT(' *',10X,'HORIZ. PLOT LENGTH (M):  ',F6.2,28X,'*')
```

```
110 FORMAT(' *',10X,'PLOT WIDTH (M):  ',F5.2,37X,'*')
120 FORMAT(' *',10X,'NUMBER OF PLOT INCREMENTS:  ',I2,29X,'*')
130 FORMAT(' *',10X,'TOTAL SIMULATION TIME (MIN):  ',I4,25X,'*')
140 FORMAT(' *',10X,'TIME STEP (MIN):  ',I2,39X,'*')
143 FORMAT(' *',10X,'INITIAL RAINFALL START TIME (MIN):  ',I3,20X
   X,'*')
150 FORMAT(' *',10X,'AMBIENT TEMPERATURE (DEG. CELSIUS):  ',F4.1,18X
   X,'*')
    WRITE(6,3)
    WRITE(6,5)
  5 FORMAT(' * PLOT INCREMENT PARAMETERS:',42X,'*')
    WRITE(6,3)
    WRITE(6,160)
    WRITE(6,170)
    WRITE(6,180)
    WRITE(6,3)
151 FORMAT('+ ',69X,'*')
160 FORMAT(' *',18X,'HORIZ      # OF',6X,'TOP LAYER',7X,'RANDOM',9X
   X,'*')
170 FORMAT(' * INCR   SLOPE    LENGTH     RILLS',7X,'DEPTH',7X
   X,'ROUGHNESS',8X,'*')
180 FORMAT(' *',8X,'(M/M)',6X,'(M)',18X,'(CM)',11X,'(CM)',10X,'*')
    DO 40 J=1,NJ
    WRITE(6,36)J,SO(J),HLINC(J),NR(J),LI(J),RR(J)
 40 CONTINUE
 36 FORMAT(' *  ',I3,3X,F5.3,4X,F6.3,6X,I3,8X,F4.1,11X,F4.1,10X,'*')
    WRITE(6,3)
    WRITE(6,37)
    WRITE(6,3)
    WRITE(6,38)
    WRITE(6,39)(M,M=1,10)
    DO 50 J=1,NJ
    NRJ=NR(J)
    WRITE(6,41)J,(NSEG(J,M),M=1,NRJ)
    WRITE(6,151)
 50 CONTINUE
 37 FORMAT(' *',18X,'# OF RILL CHANNEL SEGMENTS:',24X,'*')
 38 FORMAT(' *',28X,'RILL',37X,'*')
 39 FORMAT(' * INCR ',10(I5),13X,'*')
 41 FORMAT(' *  ',I2,2X,10(I5))
    WRITE(6,3)
    WRITE(6,42)
 42 FORMAT(' *',18X,'# OF RILL CHANNEL SEGMENT SUB-SEGMENTS:',12X
   X,'*')
    WRITE(6,3)
    DO 80 J=1,NJ
    WRITE(6,45)J
 45 FORMAT(' * INCR #:',I3,58X,'*')
    WRITE(6,3)
    WRITE(6,38)
    WRITE(6,47)(M,M=1,10)
 47 FORMAT(' * SEG  ',10(I5),13X,'*')
```

```
      NRJ=NR(J)
      DO 60 M=1,NRJ
      NSS=NSES(J,M)
      WRITE(6,41)M,(NSS(J,M,MJ),MJ=1,NSS)
      WRITE(6,151)
   60 CONTINUE
      WRITE(6,3)
   80 CONTINUE
      WRITE(6,3)
      WRITE(6,43)
      WRITE(6,3)
      WRITE(6,38)
      WRITE(6,48)(M,M=1,10)
      DO 70 J=1,NJ
      NRJ=NR(J)
      WRITE(6,44)J,(RWSW(J,M),M=1,NRJ)
      WRITE(6,151)
   70 CONTINUE
   43 FORMAT(' *',18X,'RILL WATERSHED WIDTH (CM):',25X,'*')
   44 FORMAT(' *',I4,2X,10F6.1,'   *')
      WRITE(6,3)
      WRITE(6,6)
    6 FORMAT(' *',18X,'RILL FLOW MANNING N:',31X,'*')
      WRITE(6,3)
      WRITE(6,38)
      WRITE(6,48)(M,M=1,10)
   48 FORMAT(' * INCR    ',10(I2,4X),'*')
      WRITE(6,3)
      DO 90 J=1,NJ
      NRJ=NR(J)
      WRITE(6,46)J,(N(J,M),M=1,NRJ)
      WRITE(6,151)
   90 CONTINUE
   46 FORMAT(' *',I4,2X,10F6.3,'   *')
      WRITE(6,3)
      WRITE(6,7)
    7 FORMAT(' *',18X,'SHEET FLOW MANNING N:',30X,'*')
      WRITE(6,3)
      WRITE(6,38)
      WRITE(6,48)(M,M=1,10)
      WRITE(6,3)
      DO 95 J=1,NJ
      NRJ=NR(J)
      WRITE(6,46)J,(NS(J,M),M=1,NRJ)
      WRITE(6,151)
   95 CONTINUE
      WRITE(6,3)
      WRITE(6,4)
    4 FORMAT(' *',18X,'FLOW JUNCTION INDICATORS:',26X,'*')
      WRITE(6,3)
      WRITE(6,38)
      WRITE(6,49)(M,M=1,10)
```

```
 49 FORMAT(' *     ',10I6,5X,'*')
    WRITE(6,51)
 51 FORMAT(' * INCR',10('   LCR'),4X,'*')
    WRITE(6,3)
    DO 105 J=1,NJ
    NRJ=NR(J)
    WRITE(6,52)J,(K1(J,M),K2(J,M),K3(J,M),M=1,NRJ)
    WRITE(6,151)
105 CONTINUE
 52 FORMAT(' *  ',I2,1X,10(3X,3I1))
    WRITE(6,3)
    WRITE(6,53)
 53 FORMAT(' *',18X,'RILL WATERSHED SURFACE COORDINATES:',16X,'*')
    WRITE(6,3)
    DO 115 J=1,NJ
    WRITE(6,45)J
    WRITE(6,55)
    WRITE(6,54)(M,M=1,10)
 54 FORMAT(' * RILL ',10I6,'   *')
    NRJ=NR(J)
 55 FORMAT(' *',33X,'SEGMENT',29X,'*')
    DO 125 M=1,NRJ
    NSG=NSEG(J,M)+2
    WRITE(6,56)M,(RX(J,M,MJ),MJ=2,NSG)
    WRITE(6,151)
    WRITE(6,57)(RY(J,M,MJ),MJ=2,NSG)
    WRITE(6,151)
125 CONTINUE
115 CONTINUE
 56 FORMAT(' * ',I2,'  X: ',10F6.1)
 57 FORMAT(' *     Y: ',10F6.1)
    WRITE(6,3)
    WRITE(6,58)
 58 FORMAT(' * SOIL LAYER PARAMETERS:',23X,'LAYER 1',6X
   X,'LAYER 2   *')
    WRITE(6,3)
    WRITE(6,59)ARDET(1),ARDET(2)
    WRITE(6,61)BRDET(1),BRDET(2)
    WRITE(6,62)KS(1),KS(2)
    WRITE(6,63)SMC(1),SMC(2)
    WRITE(6,64)B(1),B(2)
    WRITE(6,65)
    WRITE(6,69)XI(1),XI(2)
    WRITE(6,71)
    WRITE(6,66)DS(1),DS(2)
    WRITE(6,67)MC(1),MC(2)
    WRITE(6,68)PCL(1),PCL(2)
 59 FORMAT(' * RILL DETACHMENT EQ. COEFF. (G/CM/CM/MIN):    ',
   XF7.3,6X,F7.3,'   *')
 61 FORMAT(' * RILL DETACHMENT EXPONENT',21X,F7.3,6X,F7.3,'   *')
 62 FORMAT(' * LAB SATURATED HYDRAULIC COND. (CM/HR):',7X,F7.3,6X
   X,F7.3,'   *')
```

```
 63 FORMAT(' * LAB SATURATED MOIST. CONT. (CC/CC):',10X,F7.3,6X,F7.3,
   X'   *')
 64 FORMAT(' * ABS OF L-L SLOPE OF MOIST. REL. CURVE:',7X,F7.3,6X
   X,F7.3,'   *')
 65 FORMAT(' *',6X,'(LOG(CM-WATER)/LOG(CC/CC))',37X,'*')
 69 FORMAT(' * INTERCEPT OF L-L MOIST. REL. CURVE:',10X,F7.3,6X
   X,F7.3,'   *')
 71 FORMAT(' *',6X,'(LOG(CM-WATER))',48X,'*')
 66 FORMAT(' * FINAL DEGREE OF SATURATION:',18X,F7.3,6X,F7.3,'   *')
 67 FORMAT(' * INITIAL MOISTURE CONTENT (CC/CC)',13X,F7.3,6X,F7.3
   X,'   *')
 68 FORMAT(' * CLAY FRACTION (%)',28X,F7.3,6X,F7.3,'   *')
    WRITE(6,3)
    WRITE(6,72)
 72 FORMAT(' * SEDIMENT PARTICLE PARAMETERS:',39X,'*')
    WRITE(6,3)
    WRITE(6,73)
    WRITE(6,74)
    WRITE(6,3)
    DO 135 I=1,10
    WRITE(6,75)I,DMM(I),SS(I),FDMM(I),FDMMRD(I)
135 CONTINUE
 73 FORMAT(' *',8X,'DIAMETER     SPEC. GRAV.',7X,'MATRIX',10X
   X,'RAINDROP DET. *')
 74 FORMAT(' * TYPE     (MM)',24X,'FRACTION',11X,'FRACTION    *')
 75 FORMAT(' *  ',I2,5X,F6.3,8X,F5.2,11X,F7.3,12X,F7.3,'    *')
    WRITE(6,3)
    PO(1)=' NO'
    PO(2)='YES'
    POP(2)=PO(PO1+1)
    POP(3)=PO(PO2+1)
    POP(4)=PO(PO3+1)
    WRITE(6,76)
    WRITE(6,3)
    WRITE(6,77)CC
    WRITE(6,78)E1
    WRITE(6,79)E2
    WRITE(6,81)E3
    WRITE(6,82)PBM
    WRITE(6,83)PB3
    WRITE(6,84)EF
    WRITE(6,85)EV
    WRITE(6,3)
    WRITE(6,86)
    WRITE(6,3)
    WRITE(6,87)POP(2)
    WRITE(6,88)POP(3)
    WRITE(6,89)POP(4)
    WRITE(6,3)
    SEDEQ(1)='YALIN'
    SEDEQ(2)=' YANG'
    IX=1
```

```
      IF(ISSD.EQ.1)IX=2
      WRITE(6,91)SEDEQ(IX)
      IX=1
      IF(IRSD.EQ.1)IX=2
      WRITE(6,92)SEDEQ(IX)
      WRITE(6,3)
      WRITE(6,1)
      WRITE(6,1)
   76 FORMAT(' * SOIL SPLASH AND INFILTRATION PARAMETERS:',28X,'*')
   77 FORMAT(' *',10X,'SPLASH EQUATION COEFFICIENT (G/CM/CM/MIN):  ',
     XF7.3,8X,'*')
   78 FORMAT(' *',10X,'SPLASH EQ. INTENSITY EXPONENT:  ',F7.3,20X,'*')
   79 FORMAT(' *',10X,'SPLASH EQ. ENERGY EXPONENT:  ',F7.3,23X,'*')
   81 FORMAT(' *',10X,'SPLASH EQ. CLAY PERCENTAGE EXPONENT:  ',F7.3,14X
     X,'*')
   82 FORMAT(' *',10X,'MAXIMUM POTENTIAL SOIL SPLASH:  ',F5.2,22X,'*')
   83 FORMAT(' *',10X,'POT. SOIL SPLASH AT 3 DROP DIAMETER DEPTH:  '
     X,F6.3,9X,'*')
   84 FORMAT(' *',10X,'INFILT. RATE CONVERG. CRITERION (CM/HR):  ',F7.4
     X,10X,'*')
   85 FORMAT(' *',10X,'INFILT. VOL. CONVERG. CRITERION (CM):  ',F7.4
     X,13X,'*')
   86 FORMAT(' * RUN PARAMETERS:',53X,'*')
   87 FORMAT(' *',10X,'PRINT AFTER EACH SLOPE INCREMENT?',6X,A3
     X,17X,'*')
   88 FORMAT(' *',10X,'PRINT AFTER EACH TIME INCREMENT?',7X,A3,17X,'*')
   89 FORMAT(' *',10X,'PRINT FINAL SUMMARY?',19X,A3,17X,'*')
   91 FORMAT(' *',10X,'SHEET FLOW SED. TRANSPORT EQUATION?  ',A5,17X
     X,'*')
   92 FORMAT(' *',10X,'RILL FLOW SED. TRANSPORT EQUATION?  ',A5,17X
     X,'*')
      END
```

```
C
C*****************************************************************
C*****************************************************************
      SUBROUTINE RAINFA
C*****************************************************************
C*****************************************************************
C
      COMMON/RAINP/RAIN,EKRAIN,EK,RDMM(28),FRDMM(28),RTOT
      COMMON/TIMEP/T,DTM,DTS,TS,TRS,TRQ,TR,ITRS
      INTEGER TR,TRQ,TRS,T,DTM
      READ(5,1)RAIN,EKRAIN,TR,TRS
      TRQ=T+TR-DTM
      EK=EKRAIN*RAIN*DTM/60.
      DO 10 K=1,28
      RDMM(K)=K*0.25-0.125
   10 CONTINUE
      READ(5,2)(FRDMM(K),K=1,12)
      READ(5,2)(FRDMM(K),K=13,24)
      READ(5,3)(FRDMM(K),K=25,28)
      CALL PRINTR
    1 FORMAT(2F6.2,2I6)
    2 FORMAT(12F6.3)
    3 FORMAT(4F6.3)
      END
C
C*****************************************************************
C*****************************************************************
      SUBROUTINE PRINTR
C*****************************************************************
C*****************************************************************
C
      COMMON/RAINP/RAIN,EKRAIN,EK,RDMM(28),FRDMM(28),RTOT
      COMMON/TIMEP/T,DTM,DTS,TS,TRS,TRQ,TR,ITRS
      INTEGER TR,TRQ,TRS,T,DTM
      OPEN(6,FILE='PRN')
      WRITE(6,1)
      WRITE(6,1)
      WRITE(6,5)T
      WRITE(6,1)
      WRITE(6,1)
      WRITE(6,3)
      WRITE(6,10)RAIN
      WRITE(6,20)EKRAIN
      WRITE(6,30)TR
      WRITE(6,40)TRS
      WRITE(6,3)
      WRITE(6,50)
      WRITE(6,3)
      WRITE(6,55)
      DO 100 K=1,28
      WRITE(6,60)K,RDMM(K),FRDMM(K)*100.
  100 CONTINUE
```

```
      WRITE(6,3)
      WRITE(6,1)
      WRITE(6,1)
    1 FORMAT(1X,71('*'))
    3 FORMAT(' *',69X,'*')
    5 FORMAT(' *',19X,'RAINFALL INPUTS AT TIME ',I3,' MIN',19X,'*')
   10 FORMAT(' *',10X,'RAINFALL RATE (CM/HR):',F5.2,32X,'*')
   20 FORMAT(' *',10X,'RAINFALL ENERGY (JOULES/CM/CM):',F5.3,23X,'*')
   30 FORMAT(' *',10X,'RAINFALL DURATION (MIN):',I3,32X,'*')
   40 FORMAT(' *',10X,'NEXT RAINFALL START TIME (MIN):',I3,25X,'*')
   50 FORMAT(' *',10X,'DROP SIZE DISTRIBUTION:',36X,'*')
   55 FORMAT(' *',10X,'SIZE CLASS',11X,'DIA. (MM)',11X,'% VOLUME'
     X,10X,'*')
   60 FORMAT(' *',14X,I2,17X,F5.2,14X,F5.1,12X,'*')
      END
```

```
C
C*****************************************************************
C*****************************************************************
      SUBROUTINE MOVE(J)
C*****************************************************************
C*****************************************************************
C
      COMMON/PLOT1/NJ,NR(10),NRR,BD(2),HDDSL
      COMMON/RAINP/RAIN,EKRAIN,EK,RDMM(28),FRDMM(28),RTOT
      COMMON/STATS/VWF,SEDR,SEDVR,SEDRTO,TSPWSR,ROTCM
     X,ROTL,SDKG,SDMTHA,SDTAC,WSDL,RTOTL
      COMMON/FLOW/QRILL(10,10),YRILL(10),HRRILL(10,10)
     X,PWRILL(10,10),ARILL(10,10,2)
      COMMON/RLSL/QSR(10),QSRILL(10,2,10),RT(10,10),RTR(10)
      COMMON/SEDDIS/PFW(10),NUM(10),SEDDMM(10)
      COMMON/SEDPAR/DMM(10),SS(10),FDMM(10),FDMMRD(10)
     X,DEP(10,10,10)
      COMMON/PLOT/HPL,PW,SLINC(10),SO(10),SINE(10),COSINE(10)
     X,PCL(2),HLINC(10)
      COMMON/ENVIR/G,TCELS,VK,SF,PI
      DIMENSION DM(10)
      IF(J.EQ.NJ)GOTO20
      DO 10 M=1,NRR
      DO 10 I=1,10
      QSRILL(I,1,M)=QSRILL(I,2,M)
   10 CONTINUE
      HDDSL=HDDSL+HLINC(J)
      GOTO40
   20 DO 30 M=1,NRR
      DO 30 I=1,10
      QSRILL(I,1,M)=0.0
      SEDDMM(I)=0.0
   30 CONTINUE
      HDDSL=HDDSL+HLINC(J)
      VWF=0.0
      SEDR=0.0
      SEDVR=0.0
      DO 102 M=1,NRR
      DO 103 I=1,10
      SEDDMM(I)=SEDDMM(I)+QSRILL(I,2,M)/1000.*DTM
      SEDR=SEDR+QSRILL(I,2,M)/1000.
      SEDVR=SEDVR+QSRILL(I,2,M)/SS(I)/GF/1000.
  103 CONTINUE
      VWF=VWF+QRILL(J,M)
  102 CONTINUE
      SEDRTO=SEDR
      TSPWFR=VWF+SEDVR
      ROTCM=ROTL/10./HPL/PW
      SDKG=SDKG+SEDRTO*DTM
      SDMTHA=SDKG/HPL/PW
      SDTAC=SDMTHA*2.2046/2.47105
      WSDL=WSDL+TSPWFR*DTM
```

```
      RTOTL=RTOT*HPL*PW*10.
      WSDKG=SDKG+ROTL*SF
      DO 110 I=1,10
      DM(I)=DMM(I)
      NUM(I)=I
  110 CONTINUE
      DO 120 I=1,9
      JI=10-I
      DO 130 JK=1,JI
      IF(DM(JK).LT.DM(JK+1))GOTO130
      TE=DM(JK)
      DM(JK)=DM(JK+1)
      DM(JK+1)=TE
      TEN=NUM(JK)
      NUM(JK)=NUM(JK+1)
      NUM(JK+1)=TEN
  130 CONTINUE
  120 CONTINUE
      PFW(1)=SEDDMM(1)/SDKG*100.
      DO 140 I=2,10
      PFW(I)=SEDDMM(I)/SDKG*100.+PFW(I-1)
  140 CONTINUE
   40 CONTINUE
      END
```

```
C
C*****************************************************************
C*****************************************************************
      SUBROUTINE PRINT1(J)
C*****************************************************************
C*****************************************************************
C
      COMMON/STATS/VWF,SEDR,SEDVR,SEDRTO,TSPWFR,ROTCM,ROTL
     X,SDKG,SDMTHA,SDTAC,WSDL,RTOTL
      COMMON/TIMEP/T,DTM,DTS,TS,TRS,TRO,TR,ITRS
      COMMON/INFP/F(10),V(10)
      COMMON/SURFAC/RR(10),SSTO(10),FCOV(10),STOD,DSURF,STO(10)
      COMMON/RLSL/QSR(10),QSRILL(10,2,10),RT(10,10),RTR(10)
      COMMON/SHEF/ST(10,10),FCD(10,10,10)
      COMMON/INTE/QO,QI
      COMMON/WATER/RO(10),QRO,QSHEET(10,10),ROP(10)
      COMMON/FLOW/QRILL(10,10),YRILL(10,10),HRRILL(10,10)
     X,PWRILL(10,10),ARILL(10,10,2)
      COMMON/RADP/PSM,PS3,CC,E1,E2,E3,SBO,RDET(10,10)
      COMMON/RLDP/ARDET(2),BRDET(2),SHEAR(10,10,10),RSH,CSH
     X,DRILL(10,10),EXS,DRR(10)
      COMMON/PLOT1/NJ,NR(10),NRR,BD(2),HDDSL
      COMMON/PLOT/HPL,PW,SLINC(10),SO(10),SINE(10),COSINE(10)
     X,PCL(2),HLINC(10)
      COMMON/SEDPAR/DMM(10),SS(10),FDMM(10),FDMMRD(10)
     X,DEP(10,10,10)
      COMMON/DETR/DETOTD(10,10,10),DETOTM(10,10,10)
      INTEGER T
      WRITE(6,1)
      WRITE(6,1)
    1 FORMAT(1X,71('*'))
      WRITE(6,2)J,T
      WRITE(6,1)
      WRITE(6,1)
    2 FORMAT(' *',18X,'INCREMENT',I3,' RESULTS AT TIME ',I3,' MIN'
     X,15X,'*')
      WRITE(6,3)
    3 FORMAT(' *',69X,'*')
      WRITE(6,4)HDDSL
    4 FORMAT(' *',10X,'HORIZ. DISTANCE DOWNSLOPE (M):  ',F6.2,21X,'*')
      WRITE(6,5)F(J)
      WRITE(6,6)V(J)
      WRITE(6,7)QI
      WRITE(6,8)QO
      WRITE(6,9)RO(J)
      WRITE(6,10)SSTO(J)
      WRITE(6,11)STO(J)
      WRITE(6,3)
    5 FORMAT(' *',10X,'INFILTRATION RATE (CM/HR):  ',F6.2,25X,'*')
    6 FORMAT(' *',10X,'INFILTRATED VOLUME (CM):  ',F6.2,27X,'*')
    7 FORMAT(' *',10X,'INTERFLOW INTO INCREMENT (CM/HR):  ',F6.2,18X
     X,'*')
```

```
  8 FORMAT(' *',10X,'INTERFLOW OUT OF INCREMENT (CM/HR):  ',F6.2,16X
   X,'*')
  9 FORMAT(' *',10X,'RUNOFF RATE (CM/HR):  ',F6.2,31X,'*')
 10 FORMAT(' *',10X,'POTENTIAL SURFACE STORAGE (CM):  ',F6.2,20X,'*')
 11 FORMAT(' *',10X,'SURFACE STORAGE FILLED (CM):  ',F6.2,23X,'*')
    WRITE(6,3)
    IF(ROTL.GT.0.0)GOTO170
    WRITE(6,171)
171 FORMAT(' *',31X,'NO FLOW',31X,'*')
    GOTO300
170 WRITE(6,12)
 12 FORMAT(' *',10X,'FLOW RATES (CC/SEC): RILL     SHEET FLOW
   X,'RILL FLOW',5X,'*')
    NRJ=NR(J)
    DO 100 M=1,NRJ
    WRITE(6,13)M,QSHEET(J,M)*2,QRILL(J,M)
100 CONTINUE
 13 FORMAT(' *',31X,I2,8X,F6.2,9X,F6.2,7X,'*')
    WRITE(6,3)
    WRITE(6,14)
 14 FORMAT(' *',8X,'DETACHMENT RATES (G/MIN):',36X,'*')
    WRITE(6,3)
    WRITE(6,15)
 15 FORMAT(' *',26X,'PARTICLE TYPE:',29X,'*')
    WRITE(6,22)(I,I=1,10)
 22 FORMAT(' *',6X,10I6,'   *')
    WRITE(6,16)(RDET(I,J),I=1,10)
 16 FORMAT(' *  RAIN ',10F6.0,'  *')
    WRITE(6,3)
    WRITE(6,17)
 17 FORMAT(' * MATRIX',62X,'*')
    WRITE(6,18)
 18 FORMAT(' *  RILL',63X,'*')
    DO 110 M=1,NRJ
    WRITE(6,19)M,(DETOTM(I,J,M),I=1,10)
110 CONTINUE
 19 FORMAT(' *   ',I2,2X,10F6.0,'  *')
    WRITE(6,3)
    WRITE(6,20)
 20 FORMAT(' * DEPOS.',62X,'*')
    WRITE(6,18)
    DO 120 M=1,NRJ
    WRITE(6,19)M,(DETOTD(I,J,M),I=1,10)
120 CONTINUE
    WRITE(6,3)
    WRITE(6,21)
 21 FORMAT(' *',8X,'TRANSPORT RATES (G/MIN)',38X,'*')
    WRITE(6,3)
    WRITE(6,15)
    WRITE(6,22)(I,I=1,10)
    WRITE(6,23)
 23 FORMAT(' *  SHEET',62X,'*')
```

```
      WRITE(6,18)
      DO 130 M=1,NRJ
      WRITE(6,19)M,(ST(I,M),I=1,10)
  130 CONTINUE
      WRITE(6,3)
      WRITE(6,18)
      DO 140 M=1,NRJ
      WRITE(6,19)M,(RT(I,M),I=1,10)
  140 CONTINUE
      WRITE(6,3)
      WRITE(6,24)
   24 FORMAT(' *',8X,'DEPOSITION RATE (G/MIN):',37X,'*')
      WRITE(6,3)
      WRITE(6,15)
      WRITE(6,25)(I,I=1,10)
   25 FORMAT(' *  RILL',10I6,'   *')
      DO 150 M=1,NRJ
      WRITE(6,19)M,(DEP(I,J,M),I=1,10)
  150 CONTINUE
      WRITE(6,3)
      WRITE(6,26)
   26 FORMAT(' *',8X,'SEDIMENT DELIVERY DOWNSLOPE (G/MIN):',25X,'*')
      WRITE(6,3)
      WRITE(6,15)
      WRITE(6,25)(I,I=1,10)
      DO 160 M=1,NRJ
      WRITE(6,19)M,(QSRILL(I,2,M),I=1,10)
  160 CONTINUE
  300 WRITE(6,3)
      WRITE(6,1)
      WRITE(6,1)
      RETURN
      END
```

APPENDIX II

RUNOFF GENERATION

COMPONENT LISTINGS

```
C
C*****************************************************************
C*****************************************************************
      SUBROUTINE RUNGEN(J)
C*****************************************************************
C*****************************************************************
C
      COMMON/STATS/VWF,SEDR,SEDVR,SEDRTO,TSPWSR,ROTCH,ROTL
     X,SDKB,SDMTHA,SDTAC,WSDL,RTOTL
      COMMON/PLOT1/NJ,NR(10),NRR,BD(2),HDDSL
      COMMON/TIMEP/T,DTM,DTS,TB,TRB,TRQ,TR,ITRS
      COMMON/RAINP/RAIN,EKRAIN,EK,RDMM(28),FRDMM(28),RTOT
      COMMON/INFIBP/KFB1,KFB2,SAV1,SAV2,IMD1,IMD2,EF,EV
     X,LI(10)
      COMMON/INFP/F(10),V(10)
      COMMON/SURFAC/RR(10),SSTO(10),FCOV(10),STOD,DSURF,STO(10)
      COMMON/PLOT/HPL,PW,SLINC(10),SO(10),SINE(10),COSINE(10)
     X,PCL(2),HLINC(10)
      COMMON/WATER/RO(10),QRO,QSHEET(10,10),ROP(10)
      COMMON/INTE/QO,QI
      REAL KFB1,KFB2,IMD1,IMD2,LI
      INTEGER DTM
C
C*** CALCULATE SURFACE STORAGE
C
      CALL SURSTO(J)
C
C*** CALCULATE INFILTRATION RATE AND INFILTRATED VOLUME
C
      CALL INFILT(J)
C
C*** CALCULATE RUNOFF RATE
C
      CALL RUNOFF(J)
      ROTL=ROTL+RO(J)*DTM/60.*HPL*PW
      RORTOT=RORTOT+RO(J)
      RETURN
      END
```

```
C
C*****************************************************************
C*****************************************************************
      SUBROUTINE SURSTO(J)
C*****************************************************************
C*****************************************************************
C
C
C*****************************************************************
C*** THIS SUBROUTINE USES A RELATIONSHIP DEVELOPED BY     **
C*** LINDEN(1979) TO EVALUATE POTENTIAL SURFACE STORAGE   **
C*** VOLUME AS A FUNCTION OF LAND SLOPE AND SURFACE       **
C*** RANDOM ROUGHNESS.  THIS RELATIONSHIP IS STATE-OF-THE-**
C*** ART AND HAS NOT BEEN WIDELY TESTED.  THIS SUBROUTINE **
C*** WILL BE REVISED IN THE FUTURE.                       **
C*****************************************************************
C
      COMMON/PLOT1/NJ,NR(10),NRR,BD(2),HDDSL
      COMMON/PLOT/HPL,PW,SLINC(10),SO(10),SINE(10),COSINE(10)
     X,PCL(2),HLINC(10)
      COMMON/SURFAC/RR(10),SSTO(10),FCOV(10),STOD,DSURF,STO(10)
      DIMENSION RRE(6)
      DATA RRE(1),RRE(2),RRE(3),RRE(4),RRE(5),RRE(6)/
     X0.,.8,1.6,2.4,3.2,4./
C
C*** LINDEN (1979) PRESENTED CURVES FOR SURFACE STORAGE
C*** VERSUS LAND SLOPE FOR EACH OF THE RANDOM ROUGHNESS
C*** VALUES IN THE ARRAY RRE.  THESE CURVES WERE FIT
C*** USING A LAGRANGIAN TECHNIQUE, MATCHING AT FOUR POINTS.
C*** THE FUNCTION SE OUTPUTS THE APPROPRIATE SURFACE STORAGE
C*** VALUES FOR LINEAR INTERPOLATION BETWEEN THE CURVES
C
      S=SO(J)*100.
      II=INT(RR(J)+1)
      IF(II.LT.1)II=1
      IF(II.GT.5)II=5
      SSTO(J)=(RR(J)-RRE(II))/(RRE(II+1)-RRE(II))*(SE(II+1,S)
     X-SE(II,S))+SE(II,S)
   10 CONTINUE
      END
C
C*****************************************************************
      FUNCTION SE(II,S)
C*****************************************************************
C
      DIMENSION C1(6),C2(6),C3(6),C4(6),C5(6)
      DATA C1(1),C1(2),C1(3),C1(4),C1(5),C1(6)/
     X0.,1.042E-03,8.396E-04,6.008E-04,5.167E-04,3.056E-04/
      DATA C2(1),C2(2),C2(3),C2(4),C2(5),C2(6)/0.,1.208E-02,
     X1.319E-02,1.146E-02,1.165E-02,8.528E-03/
      DATA C3(1),C3(2),C3(3),C3(4),C3(5),C3(6)/0.,5.E-05,8.018E-03,
     X5.163E-04,3.833E-03,-3.278E-03/
```

```
 DATA C4(1),C4(2),C4(3),C4(4),C4(5),C4(6)/0.,0.2,0.4,0.62
X,0.84,1.06/
 DATA C5(1),C5(2),C5(3),C5(4),C5(5),C5(6)/0.,8.,10.,12.,15.
X,19./
 SE=C1(II)*S**3.-C2(II)*S*S+C3(II)*S+C4(II)
 IF(S.GT.C5(II))SE=0.0
 RETURN
 END
```

```
C
C*****************************************************************
C*****************************************************************
      SUBROUTINE INFILT(J)
C*****************************************************************
C*****************************************************************
C
C
C*****************************************************************
C*** THIS SUBROUTINE UTILIZES A MODIFIED GREEN-AMPT-MEIN- **
C*** LARSON INFILTRATION MODEL TO CALCULATE INFILTRATION  **
C*** ON EACH INCREMENT AT A GIVEN TIME.  THE MODIFICATION **
C*** INVOLVES USING A TWO-LAYER SYSTEM AS DEFINED BY      **
C*** MOORE (1981) AND THE FIELD SATURATION CONCEPTS       **
C*** UTILIZED BY HIRSCHI, LARSON, AND BLACK (1980) FOR    **
C*** THE MODEL PARAMETERS.                               **
C*****************************************************************
C
      COMMON/TIMEP/T,DTM,DTS,TS,TRS,TRQ,TR,ITRS
      COMMON/RAINP/RAIN,EKRAIN,EK,RDMM(28),FRDMM(28),RTOT
      COMMON/INFISP/KFS1,KFS2,SAV1,SAV2,IMD1,IMD2,EF,EV
     X,LI(10)
      COMMON/INFP/F(10),V(10)
      COMMON/INTE/QO,QI
      REAL IMD1,IMD2,KFS1,KFS2,LI
      INTEGER DTM
      IF(RAIN.GT.0.0)GOTO80
      F(J)=0.0
      GOTO90
   80 DTH=DTM/60.
      LI=LI(J)
      FI=F(J)
      VI=V(J)
      V1=IMD1*LI(J)
C
C*** BRANCH FOR WETTED FRONT IN UPPER OR LOWER LAYER
C
      IF(VI.GE.V1)GOTO40
C
C*** DETERMINE INFILTRATION RATE AND VOLUME FOR END OF TIME
C*** STEP WITH WETTED FRONT IN UPPER LAYER BY CONVERGING
C*** SUCCESSIVE APPROXIMATIONS WITHIN PRESCRIBED LIMITS FOR
C*** RATE AND VOLUME
C
   45 VN=VI+FI*DTH
      FN=KFS1*(1.+IMD1*SAV1/VN)
C
C*** COMPARE INFILTRATION RATE AND RAINFALL RATE AND SET
C*** INFILTRATION RATE TO LESSER VALUE
C
      IF(FN.GT.RAIN)FN=RAIN
      DO 10 I1=1,10
```

```
      VN1=VI+(FI+FN)/2.*DTH
      FN1=KFS1*(1.+IMD1*SAV1/VN1)
C
C*** COMPARE INFILTRATION RATE AND RAINFALL RATE AND SET
C*** INFILTRATION RATE TO LESSER VALUE
C
      IF(FN1.GT.RAIN)FN1=RAIN
      IF(ABS(FN1-FN)/FN.GT.EF)GOTO20
      IF(ABS(VN1-VN)/VN.GT.EV)GOTO20
      GOTO30
   20 VN=VN1
      FN=FN1
   10 CONTINUE
C
C*** PRINT MESSAGE IF CONVERGENCE DOES NOT OCCUR WITHIN 10
C*** TRIALS AND ACCEPT FINAL APPROXIMATION AS CLOSE ENOUGH
C
      WRITE(6,1000)
      WRITE(6,1010)
      WRITE(6,1020)J
   30 VN=VN1
      FN=FN1
      GOTO100
C
C*** DETERMINE INFILTRATION RATE AND VOLUME FOR END OF TIME
C*** STEP WITH WETTED FRONT IN LOWER LAYER BY CONVERGING
C*** SUCCESSIVE APPROXIMATIONS WITHIN PRESCRIBED LIMITS FOR
C*** RATE AND VOLUME
C
   40 VN=VI+FI*DTH
      FN=KFS2*(IMD2*(L1+SAV2)+VN-V1)/(L1*IMD2*KFS2/KFS1+VN-V
     X1)
C
C*** COMPARE INFILTRATION RATE AND RAINFALL RATE AND SET
C*** INFILTRATION RATE TO LESSER VALUE
C
      IF(FN.GT.RAIN)FN=RAIN
      DO 50 I1=1,10
      VN1=VI+(FI+FN)/2.*DTH
      FN1=KFS2*(IMD2*(L1+SAV2)+VN-V1)/(L1*IMD2*KFS2/KFS1+VN-
     XV1)
C
C*** COMPARE INFILTRATION RATE AND RAINFALL RATE AND SET
C*** INFILTRATION RATE TO LESSER VALUE
C
      IF(FN1.GT.RAIN)FN1=RAIN
      IF(ABS(FN1-FN)/FN.GT.EF)GOTO70
      IF(ABS(VN1-VN)/VN.GT.EV)GOTO70
      GOTO60
   70 VN=VN1
      FN=FN1
   50 CONTINUE
```

```
C
C*** PRINT MESSAGE IF CONVERGENCE DOES NOT OCCUR WITHIN 10
C*** TRIALS AND ACCEPT FINAL APPROXIMATION AS CLOSE ENOUGH
C
      WRITE(6,1000)
      WRITE(6,1010)
      WRITE(6,1020)J
   60 VN=VN1
      FN=FN1
C
C*** CHECK FOR INSTABILITY DUE TO ARTIFICIAL LAYER INTERFACE
C*** AND USE UPPER LAYER SEQUENCE IF FOUND
C
      IF(FN.GT.FI)GOTO45
C
C*** ACCOUNT FOR INTERFLOW IN APPARENT INFILTRATED VOLUME
C
  100 CALL INTERF
      F(J)=FN
      V(J)=VN+(QI-QO)*DTH
   90 RETURN
 1000 FORMAT(5(/),5X,5('*'),'RATE AND/OR VOLUME DID NOT CONV
     XERGE')
 1010 FORMAT(10X,'WITHIN PRESCRIBED LIMITS AFTER 10 ITERATIO
     XNS.')
 1020 FORMAT(10X,'VALUES AFTER 10 ITERATIONS USED FOR SEGMEN
     XT ',I2,2X,5('*'),5(/))
      END
```

```
C
C*****************************************************************
C*****************************************************************
      SUBROUTINE INTERF
C*****************************************************************
C*****************************************************************
C
C*** DUMMY SUBROUTINE TO BE FULLY DEVELOPED AT A LATER DATE
C
      COMMON/INTE/QO,QI
      QI=1.0
      QO=1.0
      RETURN
      END
```

```
C
C*************************************************************
C*************************************************************
      SUBROUTINE RUNOFF(J)
C*************************************************************
C*************************************************************
C
C
C*************************************************************
C*** THIS SUBROUTINE USES A RELATIONSHIP PRESENTED BY     **
C*** BARFIELD,WARNER,AND HAAN (1981) TO CALCULATE THE     **
C*** RUNOFF SUPPLY RATE ON A GIVEN SLOPE INCREMENT AT A   **
C*** GIVEN TIME.  IT USES AN EXPONENTIAL RELATIONSHIP TO  **
C*** REPRESENT THE SURFACE STORAGE DETENTION.             **
C*************************************************************
C
      COMMON/TIMEP/T,DTM,DTS,TS,TRS,TRQ,TR,ITRS
      COMMON/RAINP/RAIN,EKRAIN,EK,RDMM(28),FRDMM(28),RTOT
      COMMON/INFP/F(10),V(10)
      COMMON/SURFAC/RR(10),SSTO(10),FCOV(10),STOD,DSURF,STO(10)
      COMMON/WATER/RO(10),QRO,QSHEET(10,10),ROP(10)
      INTEGER DTM
      IF(SSTO(J).LT.0.1)GOTO10
      RO(J)=(RAIN-F(J))*(1.-EXP(-(RTOT-V(J))/SSTO(J)))
      STO(J)=STO(J)+(RAIN-F(J)-RO(J))*DTM/60.
      FCOV(J)=STO(J)/SSTO(J)
      GOTO20
   10 RO(J)=RAIN-F(J)
      FCOV(J)=0.0
      STO(J)=0.0
   20 CONTINUE
      RETURN
      END
```

APPENDIX III

RUNOFF ROUTING

COMPONENT LISTINGS

```
C
C*****************************************************************
C*****************************************************************
      SUBROUTINE RUNROT(J)
C*****************************************************************
C*****************************************************************
C
      COMMON/PLOT1/NJ,NR(10),NRR,BD(2),HDDSL
      COMMON/TIMEP/T,DTM,DTS,TS,TRS,TRQ,TR,ITRS
      COMMON/PLOT/HPL,PW,SLINC(10),SO(10),SINE(10),COSINE(10)
     X,PCL(2),HLINC(10)
      COMMON/ENVIR/G,TCELS,VK,SF,PI
      COMMON/FLOW/QRILL(10,10),YRILL(10,10),HRRILL(10,10)
     X,PWRILL(10,10),ARILL(10,10,2)
      COMMON/RILLP/IK1(10),IK2(10),IK3(10),K1(10,10),K2(10,10)
     X,K3(10,10)
      COMMON/WATER/RO(10),QRO,QSHEET(10,10),ROP(10)
      COMMON/STATS/VWF,SEDR,SEDVR,SEDRTO,TSPWFR
     X,ROTCM,ROTL,SDKG,SDMTHA,SDTAC,WSDL,RTOTL
      COMMON/RILLPA/IRSD,N(10,10),Z(10,10,10),RWSW(10,10)
     X,LAYER(10,10,10),NSEG(10,10),NSS(10,10,10)
      COMMON/RLSHA/RX(10,10,30),RY(10,10,30),XDL(10,10)
      REAL N
      INTEGER T,DTM,DTS
C
C*** CALCULATE WATER FLOW IN RILLS
C
      CALL RILLFL(J)
      RETURN
      END
```

```
C
C*****************************************************************
C*****************************************************************
      SUBROUTINE RILLFL(J)
C*****************************************************************
C*****************************************************************
C
C
C*****************************************************************
C*** THIS SUBROUTINE CALCULATES THE FLOW IN EACH RILL USING*
C*** MANNING'S EQUATION AND A SPECIFIED SEGMENTED CHANNEL  *
C*** CONFIGURATION.  IT THEN CALLS UP A SEPARATE SUBROUTINE*
C*** TO ROUTE THE FLOW THROUGH THE RILLS.                  *
C*****************************************************************
C
      COMMON/STATS/VWF,SEDR,SEDVR,SEDRTO,TSPWFR
     X,ROTCM,ROTL,SDKG,SDMTHA,SDTAC,WSDL,RTOTL
      COMMON/PLOT1/NJ,NR(10),NRR,BD(2),HDDSL
      COMMON/MISC/IIN,IIIN,SUMQ,SUMQP
      COMMON/RILLPA/IRSD,N(10,10),Z(10,10,10),RWSW(10,10)
     X,LAYER(10,10,10),NSEG(10,10),NSS(10,10,10)
      COMMON/RILLP/IK1(10),IK2(10),IK3(10),K1(10,10),K2(10,10)
     X,K3(10,10)
      COMMON/PLOT/HPL,PW,SLINC(10),SO(10),SINE(10),COSINE(10)
     X,PCL(2),HLINC(10)
      COMMON/ENVIR/G,TCELS,VK,SF,PI
      COMMON/TIMEP/T,DTM,DTS,TS,TRS,TRQ,TR,ITRS
      COMMON/WATER/RO(10),QRO,QSHEET(10,10),ROP(10)
      COMMON/FLOW/QRILL(10,10),YRILL(10,10),HRRILL(10,10)
     X,PWRILL(10,10),ARILL(10,10,2)
      INTEGER DTM,T,DTS
      IF(ROTL.EQ.0.0)GOTO200
      IF(IIN.EQ.1)GOTO75
      QMS=0.0
      AMS=0.0
      YMS=0.0
      DO 50 M=1,NRR
      QMS=QMS+QRILL(J,M)
      AMS=AMS+ARILL(J,M,2)
      YMS=YMS+YRILL(J,M)
   50 CONTINUE
      QM=QMS/NRR
      AM=AMS/NRR
      YM=YMS/NRR
      SI=SINE(J)
      IF(IIIN.EQ.1)GOTO60
      IF(YM.LE.0.0)GOTO75
      IF(VM.LE.0.0)GOTO75
      VM=QM/AM
      DTS=INT(SLINC(J)*100./(VM+SQRT(G*YM)))
      IF(DTS.GT.DTM*60)DTS=DTM*60
   65 CONTINUE
```

```
      IF(DTS.LT.1)DTS=1
      IA=INT(DTM*60./DTS)
      IF(IA.EQ.DTM*60./DTS)GOTO70
      DTS=DTS-1
      GOTO65
   60 DTS=10
      IIIN=1
   70 CONTINUE
      ITS=(T-DTM)*60+DTS
      ITST=T*60
      DO 80 IT=ITS,ITST,DTS
      ROP(J)=RO(J)
      CALL RLFLOW(J)
      SUMQ=0.0
      DO 110 M=1,NRR
      SUMQ=SUMQ+QRILL(J,M)*60.
  110 CONTINUE
   80 CONTINUE
      GOTO150
   75 CONTINUE
      DTS=DTM*60
      CALL RLFLOW(J)
      ROP(J)=RO(J)
  120 CONTINUE
  140 CONTINUE
      SUMQ=0.0
      DO 145 M=1,NRR
      SUMQ=SUMQ+QRILL(J,M)*60.
  145 CONTINUE
  150 CONTINUE
      DO 160 M=1,NRR
      ARILL(J,M,1)=ARILL(J,M,2)
      IF(J.EQ.1)GOTO160
      QRILL(J-1,M)=0.0
  160 CONTINUE
      IIN=0
      IF(SUMQ.LE.0.0)GOTO200
      IF(ABS(1.-SUMQP/SUMQ).LE.0.001)IIN=1
  200 CONTINUE
      SUMQP=SUMQ
      RETURN
      END
```

```
C
C*****************************************************************
C*****************************************************************
      SUBROUTINE RLFLOW(J)
C*****************************************************************
C*****************************************************************
C
C
C*****************************************************************
C*** THIS SUBROUTINE USES A FOUR-POINT KINEMATIC ROUTING  **
C*** PROCEDURE AS DESCRIBED BY BRAKENSIEK (1967) TO ROUTE **
C*** THE RUNOFF THROUGH THE RILLS.  THIS IS THE ONLY      **
C*** SUBROUTINE THAT USES DTS AS ITS PRIMARY TIME-STEP.   **
C*****************************************************************
C
      COMMON/PLOT1/NJ,NR(10),NRR,BD(2),HDDSL
      COMMON/FLOW/QRILL(10,10),YRILL(10,10),HRRILL(10,10)
     X,PWRILL(10,10),ARILL(10,10,2)
      COMMON/RILLP/IK1(10),IK2(10),IK3(10),K1(10,10),K2(10,10)
     X,K3(10,10)
      COMMON/PLOT/HPL,PW,SLINC(10),SO(10),SINE(10),COSINE(10)
     X,PCL(2),HLINC(10)
      COMMON/WATER/RO(10),QRO,QSHEET(10,10),ROP(10)
      COMMON/TIMEP/T,DTM,DTS,TS,TRS,TRQ,TR,ITRS
      COMMON/RILLPA/IRSD,N(10,10),Z(10,10,10),RWSW(10,10)
     X,LAYER(10,10,10),NSEG(10,10),NSS(10,10,10)
      INTEGER DTS
      REAL LHS,LAM,N
      LAM=DTS/SLINC(J)/100.
      DO 10 M=1,NRR
      QRO=RO(J)*RWSW(J,M)*HLINC(J)*100./3600.
      Q4IN=0.0
      IF(J.EQ.1)GOTO15
      ALPHA=(ARILL(J,M,1)+K2(J,M)*ARILL(J-1,M,1)-K2(J,M)
     X*ARILL(J-1,M,2))/2.
      IF(M.EQ.1)GOTO25
      IF(M.EQ.NRR)GOTO30
      Q4IN=(K1(J,M)*QRILL(J-1,M-1)+K3(J,M)*QRILL(J-1,M+1))
      GOTO35
   25 Q4IN=K3(J,M)*QRILL(J-1,M+1)
      GOTO35
   30 Q4IN=K1(J,M)*QRILL(J-1,M-1)
      GOTO35
   15 ALPHA=0.0
      BETA=LAM*QRO
      GOTO17
   35 BETA=LAM*(QRILL(J-1,M)*K2(J,M)+Q4IN+QRO)
   17 RHS=ALPHA+BETA
      IF(RHS.LE.0.0)GOTO43
      CALL RLCSSH(J,M,D,RHS,LHS,LAM)
      GOTO45
   43 Y4=0.0
```

```
      A4=0.0
      P4=0.0
      HRRILL(J,M)=0.0
      PWRILL(J,M)=0.0
      YRILL(J,M)=0.0
      QRILL(J,M)=0.0
      GOTO50
   45 A4=ARILL(J,M,2)
      P4=PWRILL(J,M)
      QRILL(J,M)=1./N(J,M)*(A4/P4/100.)**(2./3.)*SQRT(SINE(J))*A4*
     X100.
   50 CONTINUE
   10 CONTINUE
      RETURN
      END
```

```
C
C*****************************************************************
C*****************************************************************
      SUBROUTINE RLCSSH(J,M,D,RHS,LHS,LAM)
C*****************************************************************
C*****************************************************************
C
C
C*****************************************************************
C*** THIS SUBROUTINE UTILIZES THE FINAL CHANNEL NODAL PTS  **
C*** FROM THE PREVIOUS TIME STEP TO CALCULATE THE DEPTH OF **
C*** FLOW FOR A 4-PT KINEMATIC ROUTING PROCEDURE.  THE     **
C*** CHANNEL EDGE PTS ARE THEN RESET TO THE NEW WATER EDGE **
C*** AND THE OLD PTS ABOVE THE WATER ARE SAVED TO CHECK THE**
C*** STABILITY OF THE EXPOSED SLOPE.  A NEWTON-RAPHSON     **
C*** TECHNIQUE IS USED TO CONVERGE TO THE NEW FLOW DEPTH.  **
C*** THE CONVERGENCE CRITERION IS 0.0001.                  **
C*****************************************************************
C
      COMMON/RLSHA/RX(10,10,30),RY(10,10,30),XDL(10,10)
      COMMON/SLUF/XSR(10),YSR(10),XSL(10),YSL(10)
      COMMON/RLSH/X(10),YB(10),Y(10),XL(10),XR(10)
     X,IL(10),IR(10),XB(10)
      COMMON/FLOW/QRILL(10,10),YRILL(10,10),HRRILL(10,10)
     X,PWRILL(10,10),ARILL(10,10,2)
      COMMON/RILLPA/IRSD,N(10,10),Z(10,10,10),RNSW(10,10)
     X,LAYER(10,10,10),NSEG(10,10),NSS(10,10,10)
      COMMON/PLOT/HPL,PW,BLINC(10),BO(10),SINE(10),COSINE(10)
     X,PCL(2),HLINC(10)
      REAL N,LHS,LAM,LHSO
      NSP=NSEG(J,M)+2
      JI=0
      DO 5 I=1,30
      IF (RX(J,M,I).LT.XDL(J,M))GOTO 5
      JI=JI+1
      YB(JI)=RY(J,M,I)
      XB(JI)=RX(J,M,I)
      X(JI)=XB(JI)-XB(1)
      IF(JI.EQ.NSP+1)GOTO 7
    5 CONTINUE
    7 RS=SQRT(SINE(J))/N(J,M)
      YO=YB(1)
      IO=1
      DO 10 I=2,NSP
      IF(YB(I).GT.YO)GOTO10
      IO=I
      YO=YB(I)
   10 CONTINUE
      DO 20 I=1,NSP
      Y(I)=YB(I)-YO
   20 CONTINUE
      D=1.0
```

```
      DO=2.0
      LHSO=0.5
   25 I=IO
   30 I=I-1
      IF(I.LE.0)GOTO70
      IF(Y(I).LT.D)GOTO30
      IF(Y(I).EQ.D)GOTO40
      IF(Y(I+1).LT.D)GOTO50
   70 WRITE(*,1500)I,Y(I),Y(I+1),D
 1500 FORMAT(5X,'** UNUSUAL PROBLEM, I=',I3,3F8.3,' **')
      STOP
   40 IL(M)=I
      XL(M)=X(I)
      GOTO60
   50 IL(M)=I+1
      XL(M)=ABS(D*(X(I+1)-X(I))/(Y(I+1)-Y(I)))
   60 CONTINUE
      DO 80 I=IL(M),NSP
      IF(Y(I).LT.D)GOTO80
      IF(Y(I).EQ.D)GOTO90
      IF(Y(I-1).LT.D)GOTO100
      WRITE(*,1500)I,Y(I),Y(I-1),D
      STOP
   90 IR(M)=I
      XR(M)=X(I)
      GOTO110
  100 IR(M)=I-1
      XR(M)=ABS(D*(X(I)-X(I-1))/(Y(I)-Y(I-1)))
      GOTO110
   80 CONTINUE
      WRITE(*,1500)I,Y(I),Y(I-1),D
  110 CONTINUE
      WRITE(*,211)J,M,IR(M),IL(M)
      WRITE(*,212)XR(M),XL(M),D,DO
  211 FORMAT(5X,4I10)
  212 FORMAT(5X,4F10.4)
      AREA=0.0
      WP=0.0
      DO 120 I=IL(M),IR(M)-1
      YD=D-Y(I)
      XD=X(I)
      YD1=D-Y(I+1)
      XD1=X(I+1)
      AREA=AREA+(XD1-XD)*YD+0.5*(XD1-XD)*(YD1-YD)
      WP=WP+SQRT((XD1-XD)*(XD1-XD)+(YD1-YD)*(YD1-YD))
  120 CONTINUE
      YDL=D-Y(IL(M))
      YDR=D-Y(IR(M))
      AREA=AREA+0.5*(XL(M)*YDL+XR(M)*YDR)
      WP=WP+SQRT(XL(M)*XL(M)+YDL*YDL)+SQRT(XR(M)*XR(M)+YDR*YDR)
      RH=AREA/WP*0.01
      LHS=LAM*100.*RH**(2./3.)*AREA*RS+AREA/2.
```

```
      IF(ABS((RHS-LHS)/RHS).LT.0.0001)GOTO130
      F=RHS-LHS
      FP=(LHSO-LHS)/(D-DO)
      LHSO=LHS
      QPO=QP
      DO=D
      D=DO-F/FP
      GOTO25
  130 CONTINUE
      IF(IL(M).EQ.1)GOTO210
      DO 200 MJ=1,IL(M)-1
      XSL(MJ)=X(MJ)
      YSL(MJ)=Y(MJ)
  200 CONTINUE
      IF(IR(M).EQ.NSEG(J,M)+1)GOTO230
  210 DO 220 MJ=IR(M)+1,NSEG(J,M)+1
      XSR(MJ)=X(MJ)
      YSR(MJ)=Y(MJ)
  220 CONTINUE
  230 CONTINUE
      YRILL(J,M)=D
      HRRILL(J,M)=RH
      PWRILL(J,M)=WP
      ARILL(J,M,2)=AREA
      DO 140 I=1,NSP-1
      Z(J,M,I)=(Y(I+1)-Y(I))/(X(I+1)-X(I))
  140 CONTINUE
      NSE=IR(M)-IL(M)+3
      DO 150 MJ=2,NSE-1
      X(MJ)=X(MJ+IL(M)-1)
      Y(MJ)=Y(MJ+IL(M)-1)
      RX(J,M,MJ)=X(MJ)
      RY(J,M,MJ)=Y(MJ)
  150 CONTINUE
      X(1)=0.0
      Y(1)=D
      RX(J,M,1)=0.0
      RY(J,M,1)=D
      X(NSE)=X(NSE-1)+XR(M)
      RX(J,M,NSE)=X(NSE)
      Y(NSE)=D
      RY(J,M,NSE)=D
      NSEG(J,M)=NSE-1
      RETURN
      END
```

APPENDIX IV

SEDIMENT GENERATION

COMPONENT LISTINGS

```
C
C*****************************************************************
C*****************************************************************
      SUBROUTINE SEDGEN(J)
C*****************************************************************
C*****************************************************************
C
      COMMON/BEDDEP/FDMMB(10,10,100)
      COMMON/RLSH/X(10,10),YB(10),Y(10,10),XL(10),XR(10),IL(10)
     X,IR(10),XB(10)
      COMMON/PLOT1/NJ,NR(10),NRR,BD(2),HDDSL
      COMMON/SEDPAR/DMM(10),SS(10),FDMM(10),FDMMRD(10),
     XDEP(10,10,10)
      COMMON/TIMEP/T,DTM,DTS,TS,TRS,TRQ,TR,ITRS
      COMMON/RAINP/RAIN,EKRAIN,EK,RDMM(28),FRDMM(28),RTOT
      COMMON/INFP/F(10),V(10)
      COMMON/SURFAC/RR(10),SSTO(10),FCOV(10),STOD,DSURF,STO(10)
      COMMON/PLOT/HPL,PW,SLINC(10),SO(10),SINE(10),COSINE(10)
     X,PCL(2),HLINC(10)
      COMMON/ENVIR/G,TCELS,VK,SF,PI
      COMMON/FLOW/QRILL(10,10),YRILL(10,10),HRRILL(10,10)
     X,PWRILL(10,10),ARILL(10,10,2)
      COMMON/RADP/PSM,PSJ,CC,E1,E2,E3,SSO,RDET(10,10)
      COMMON/RLDP/ARDET(2),BRDET(2),SHEAR(10,10,10),RSH,CSH
     X,DRILL(10,10),EXS,DRR(10)
      COMMON/SHEF/ST(10,10),FCD(10,10,10)
      COMMON/RILLPA/IRSD,N(10,10),Z(10,10,10),RWSW(10,10)
     X,LAYER(10,10,10),NSEB(10,10),NSS(10,10,10)
      INTEGER DTM
C
C*** CALCULATE RAINDROP DETACHMENT
C
      CALL RADET(J)
C
C*** CALCULATE RILL FLOW SEDIMENT DETACHMENT
C
      CALL RLDET(J)
C
C*** CALCULATE NEW RILL SHAPES
C
      CALL RLBHAP(J)
C
C*** CALCULATE RILL WALL SLOUGHING SEDIMENT DETACHMENT
C
      CALL BLUFF(J)
      RETURN
      END
```

```
C
C*****************************************************************
C*****************************************************************
      SUBROUTINE RADET(J)
C*****************************************************************
C*****************************************************************
C
C
C*****************************************************************
C*** THIS SUBROUTINE CALCULATES THE SOIL DETACHMENT DUE TO**
C*** RAINDROP IMPACT. IT UTILIZES A BUBENZER AND JONES    **
C*** (1971) STYLE EQUATION TO CALCULATE BARE-SOIL SOIL    **
C*** SPLASH AND A POTENTIAL SOIL SPLASH FRACTION TO ADJUST**
C*** FOR PONDED CONDITIONS.  THE POND-DEPTH-TO-DROP-      **
C*** DIAMETER RATIO IS UTILIZED TO ACCOUNT FOR DIFFERING  **
C*** SOIL SPLASH BETWEEN THE 28 RAINDROP DIAMETER CLASSES.**
C*** THE TOTAL POTENTIAL SOIL SPLASH IS TAKEN AS A        **
C*** WEIGHTED AVERAGE OF THE SPLASH DUE TO EACH RAINDROP  **
C*** SIZE CLASS.                                          **
C*****************************************************************
C
      COMMON/RAINP/RAIN,EKRAIN,EK,RDMM(28),FRDMM(28),RTOT
      COMMON/SURFAC/RR(10),SSTO(10),FCOV(10),STOD,DSURF,STO(10)
      COMMON/PLOT/HPL,PW,SLINC(10),SO(10),SINE(10),COSINE(10)
     X,PCL(2),HLINC(10)
      COMMON/SEDPAR/DMM(10),SS(10),FDMM(10),FDMMRD(10)
     X,DEP(10,10,10)
      COMMON/BEDDEP/FDMMB(10,10,100)
      COMMON/TIMEP/T,DTM,DTS,TS,TRS,TRQ,TR,ITRS
      COMMON/RADP/PSM,PS3,CC,E1,E2,E3,SSO,RDET(10,10)
      INTEGER DTM
      STOD=STO(J)
      IF (FCOV(J).EQ.0.0)THEN
      DSURF=0.0
      GOTO10
      ENDIF
      DSURF=STOD/FCOV(J)*10.
   10 SSO=CC*RAIN**E1*EK**E2*PCL(1)**E3
      TPSS=1.
      IF(DSURF.LT.0.01)GOTO30
      TPSS=0.
      DO 25 K=1,28
      PSSI=FRDMM(K)*PSS(RDMM(K),DSURF,PSM,PS3)
      TPSS=TPSS+PSSI
   25 CONTINUE
   30 CONTINUE
      DO 40 I=1,10
      RDET(I,J)=((1.-FCOV(J))*SSO+SSO*FCOV(J)*TPSS)*FDMMRD(I)
   40 CONTINUE
      RETURN
      END
C
```

```
C*************************************************************
      FUNCTION PSS(RDMM,DSURF,PSM,PS3)
C*************************************************************
C
      DR=DSURF/RDMM
      C6=ALOG(PSM**3.*PS3)/12.
      C7=-ALOG(PS3**(1./6.)*PSM**1.5)
      C8=ALOG(PS3**(1./12.)*PSM**2.25)
      P=C6*DR**3.+C7*DR*DR+C8*DR
      IF(P.LT.-10.)GOTO10
      PS=EXP(C6*DR**3.+C7*DR*DR+C8*DR)
      GOTO20
   10 PS=0.0
   20 PSS=PS
      RETURN
      END
```

```
C
C*****************************************************************
C*****************************************************************
      SUBROUTINE RLDET(J)
C*****************************************************************
C*****************************************************************
C
C
C*****************************************************************
C*** THIS SUBROUTINE CALCULATES RILL FLOW DETACHMENT USING**
C*** THE EXCESS SHEAR EQUATION OF FOSTER (1982).  THE     **
C*** COEFFICIENT AND EXPONENT ARE USER-SUPPLIED AND THE   **
C*** CRITICAL SHEAR STRESS IS ESTIMATED FROM THE PERCENT  **
C*** CLAY USING A RELATIONSHIP OF SMERDON AND BEASLEY     **
C*** (1961).                                             **
C*****************************************************************
C
      COMMON/SHEF/ST(10,10),FCD(10,10,10)
      COMMON/PLOT1/NJ,NR(10),NRR,BD(2),HDDSL
      COMMON/RILLPA/IRSD,N(10,10),Z(10,10,10),RWSW(10,10)
     X,LAYER(10,10,10),NSEG(10,10),NSS(10,10,10)
      COMMON/ENVIR/G,TCELS,VK,SF,PI
      COMMON/PLOT/HPL,PW,SLINC(10),SD(10),SINE(10),COSINE(10)
     X,PCL(2),HLINC(10)
      COMMON/FLOW/QRILL(10,10),YRILL(10),HRRILL(10,10)
     X,PWRILL(10,10),ARILL(10,10,2)
      COMMON/SEDPAR/DMM(10),SS(10),FDMM(10),FDMMRD(10)
     X,DEP(10,10,10)
      COMMON/DETR/DETOTD(10,10,10),DETOTM(10,10,10)
      COMMON/BEDDEP/FDMMB(10,10,100)
      COMMON/RLDP/ARDET(2),BRDET(2),SHEAR(10,10,10),RSH,CSH
     X,DRILL(10,10,10),EXS,DRR(10)
      DO 10 M=1,NRR
      NSE=NSEG(J,M)
      CALL SHDIST(J,M)
      DO 10 MJ=1,NSE
      L=LAYER(J,M,MJ)
      CSH=0.493*10.**(0.0183*PCL(L))
      EXS=SHEAR(J,M,MJ)-CSH
      IF(EXS.LT.0.0)GOTO20
      DETOTM(J,M,MJ)=(1.-FCD(J,M,MJ))*ARDET(L)*EXS**BRDET(L)
      DETOTD(J,M,MJ)=FCD(J,M,MJ)*ARDET(L)*(SHEAR(J,M,MJ)
     X-0.5)**BRDET(L)
      GOTO30
   20 DETOTM(J,M,MJ)=0.0
      IF(SHEAR(J,M,MJ).LE.0.5)GOTO25
      DETOTD(J,M,MJ)=FCD(J,M,MJ)*ARDET(L)*(SHEAR(J,M,MJ)
     X-0.5)**BRDET(L)
      GOTO30
   25 DETOTD(J,M,MJ)=0.0
      JM=10*M+MJ
   30 DO 15 I=1,10
```

```
      DRILL(I,M,MJ)=DETOTM(J,M,MJ)*FDMM(I)+DETOTD(J,M,MJ)
     X*FDMMB(I,J,JM)
   15 CONTINUE
   10 CONTINUE
      RETURN
      END
```

```
C
C*****************************************************************
C*****************************************************************
      SUBROUTINE SHDIST(J,M)
C*****************************************************************
C*****************************************************************
C
C
C*****************************************************************
C*** THIS SUBROUTINE CALCULATES THE SHEAR STRESS DISTRI-  **
C*** BUTION IN A RILL USING THE "AREA METHOD" OF          **
C*** LUNDGREN AND JONSSON (1964). THE CROSS-SECTION OF THE**
C*** RILL CAN BE REPRESENTED BY UP TO 9 STRAIGHT-LINE     **
C*** SEGMENTS.                                            **
C*****************************************************************
C
      COMMON/RLLINE/SLO(10,10),YIN(10,10)
      COMMON/RLSH/X(10,10),YB(10),Y(10,10),XL(10),XR(10),IL(10)
     X,IR(10),XB(10)
      COMMON/RLDP/ARDET(2),BRDET(2),SHEAR(10,10,10),RSH,CSH
     X,DRILL(10,10,10),EXS,DRR(10)
      COMMON/RILLPA/IRSD,N(10,10),Z(10,10,10),RWSW(10,10)
     X,LAYER(10,10,10),NSEG(10,10),NSS(10,10,10)
      COMMON/ENVIR/G,TCELS,VK,SF,PI
      COMMON/PLOT/HPL,PW,SLINC(10),SD(10),SINE(10),COSINE(10)
     X,PCL(2),HLINC(10)
      DIMENSION SLOPE(10),YINT(10),BETA(10),GAMMA(10),SLN(10)
      DIMENSION ALPHA(10),DN(10),SLEN(10),SNINT(10),SAREA(10)
      DIMENSION XS(10),IO(10),IND(11),XINTT(11),SL(11),AR(10)
      DIMENSION INDN(10),DET(10),SH(10),YX(10)
      D=Y(1)
      NSG=NSEG(J,M)
      DO 10 MJ=1,NSG
      DY=Y(MJ+1)-Y(MJ)
      DX=X(MJ+1)-X(MJ)
      SLOPE(MJ)=DY/DX
      SLO(M,MJ)=SLOPE(MJ)
      YINT(MJ)=Y(MJ)-SLOPE(MJ)*X(MJ)
      YIN(M,MJ)=YINT(MJ)
      IND(MJ)=0
      INDN(MJ)=0
      SLEN(MJ)=SQRT(DY*DY+DX*DX)
   10 CONTINUE
      XS(1)=X(1)
      XS(NSG+1)=X(NSG+1)
      SLN(1)=0.0
      SLN(NSG+1)=0.0
      SNINT(1)=D
      SNINT(NSG+1)=D
      BETA(1)=ATAN(SLOPE(1))
      DO 20 MJ=2,NSG
      BETA(MJ)=ATAN(SLOPE(MJ))
```

```
      GAMMA(MJ)=BETA(MJ-1)
      ALPHA(MJ)=PI-(BETA(MJ)-GAMMA(MJ))
      DN(MJ)=(D-Y(MJ))/COS(ALPHA(MJ)/2.+BETA(MJ)-PI/2.)
      IF(ABS(ALPHA(MJ)/2.+BETA(MJ)-PI/2.).LT.0.01) GOTO30
      SLN(MJ)=TAN(ALPHA(MJ)/2.+BETA(MJ))
      SNINT(MJ)=Y(MJ)-SLN(MJ)*X(MJ)
      XS(MJ)=(D-SNINT(MJ))/SLN(MJ)
      YX(MJ)=D
      GOTO20
   30 INDN(MJ)=1
      SLN(MJ)=999.999
      SNINT(MJ)=-99.999
      XS(MJ)=X(MJ)
      YX(MJ)=D
   20 CONTINUE
      DO 40 MJ=1,NSG
      DO 50 MJJ=MJ,NSG
      IF(XS(MJ).LE.XS(MJJ)) GOTO50
      XS(MJ)=(SNINT(MJ)-SNINT(MJJ))/(SLN(MJ)-SLN(MJJ))
      XS(MJJ)=XS(MJ)
      YX(MJ)=SLN(MJ)*XS(MJ)+SNINT(MJ)
      YX(MJJ)=YX(MJ)
   50 CONTINUE
   40 CONTINUE
      DO 60 MJ=1,NSG
      NSSS=NSS(J,M,MJ)
      SAREA(MJ)=0.0
      X1=X(MJ)
      Y1=Y(MJ)
      X3=X(MJ)
      Y3=Y(MJ)
      DX=(X(MJ+1)-X(MJ))/NSSS
      DY=SLOPE(MJ)*DX
      XINTT(1)=SNINT(MJ)
      XINTT(NSSS+1)=SNINT(MJ+1)
      SL(1)=SLN(MJ)
      SL(NSSS+1)=SLN(MJ+1)
      DO 70 MJJ=2,NSSS+1
      IND(MJJ)=0
      IF(MJJ.EQ.NSSS+1) GOTO80
      X2=X1+DX
      Y2=Y1+DY
      GOTO90
   80 X2=X(MJ+1)
      Y2=Y(MJ+1)
      SL(MJJ)=SLN(MJ+1)
      XINTT(MJJ)=SNINT(MJ+1)
      GOTO100
   90 IF(SLOPE(MJ).EQ.0.0)GOTO110
      SL(MJJ)=-1./SLOPE(MJ)
      XINTT(MJJ)=Y2-SL(MJJ)*X2
  100 Y4=D
```

```
      IF(MJ.EQ.NSG)THEN
      IF(MJJ.EQ.NSSS+1)THEN
      GOTO120
      ENDIF
      ENDIF
      X4=(D-XINTT(MJJ))/SL(MJJ)
      GOTO130
  120 X4=X(NSG-1)
      GOTO130
  110 SL(MJJ)=999.999
      XINTT(MJJ)=-99.999
      IND(MJJ)=1
      Y4=D
      X4=X2
      XYR=X2
      XYL=X2
      GOTO140
  130 IF(SLN(MJ).EQ.999.999)GOTO150
      XYL=(XINTT(MJJ)-SNINT(MJ))/(SLN(MJ)-SL(MJJ))
  140 YXL=SLN(MJ)*XYL+SNINT(MJ)
      GOTO160
  150 XYL=X(MJ)
      YXL=SL(MJJ)*XYL+XINTT(MJJ)
  160 IF(YXL.GT.D)YXL=D
      IF(YXL.LT.Y2)YXL=D
      IF(IND(MJJ).EQ.1)GOTO170
      IF(MJJ.EQ.NSSS+1)GOTO180
      IF(SLN(MJ+1).EQ.999.999)GOTO190
      XYR=(XINTT(MJJ)-SNINT(MJ+1))/(SLN(MJ+1)-SL(MJJ))
      GOTO170
  190 XYR=X(MJ+1)
      YXR=SL(MJJ)*XYR+XINTT(MJJ)
      GOTO200
  180 XYR=XS(MJ+1)
  170 YXR=SLN(MJ+1)*XYR+SNINT(MJ+1)
  200 IF(YXR.GT.D)YXR=D
      IF(YXR.LT.Y2)YXR=D
      Y4=AMIN1(YXL,YXR)
      IF(Y4.EQ.D)THEN
      IF(MJJ.EQ.2)THEN
      IF(SLN(MJ).NE.0.0)THEN
      GOTO210
      ENDIF
      ENDIF
      ENDIF
      GOTO220
  210 Y3=D
      IF(INDN(MJ).EQ.1)GOTO230
      X3=(Y3-SNINT(MJ))/SLN(MJ)
      GOTO220
  230 X3=X1
  220 IF(MJJ.EQ.NSSS+1)THEN
```

```
      IF(X3.EQ.X(MJ+1))THEN
      Y4=Y3
      ENDIF
      ENDIF
      IF(IND(MJJ).EQ.1)GOTO240
      IF(MJ.EQ.NSB)THEN
      IF(MJJ.EQ.NSB+1)THEN
      GOTO250
      ENDIF
      ENDIF
      IF(SL(MJJ).EQ.999.999)GOTO260
      X4=(Y4-XINTT(MJJ))/SL(MJJ)
      GOTO270
  250 X4=X(NSB+1)
      GOTO270
  260 X4=X(MJ+1)
  270 IF(ABS(X4-X3).LE.0.01)GOTO280
  240 SLS=(Y4-Y3)/(X4-X3)
      XINTS=Y4-SLS*X4
      GOTO290
  280 XINTS=0.0
      SLS=0.0
  290 XINT1=SL(MJJ-1)/2.*(X3*X3-X1*X1)+XINTT(MJJ-1)*(X3-X1)
      XINT2=SLS/2.*(X4*X4-X3*X3)+XINTS*(X4-X3)
      XINT3=SL(MJJ)/2.*(X4*X4-X2*X2)+XINTT(MJJ)*(X4-X2)
      XINT4=SLOPE(MJ)/2.*(X2*X2-X1*X1)+YINT(MJ)*(X2-X1)
      IF(IND(MJJ).EQ.1)XINT3=0.0
      IF(IND(MJJ-1).EQ.1)XINT1=0.0
      AR(MJJ-1)=XINT1+XINT2-XINT3-XINT4
      SAREA(MJ)=SAREA(MJ)+AR(MJJ-1)
      X1=X2
      X3=X4
      Y1=Y2
      Y3=Y4
   70 CONTINUE
      SHEAR(J,M,MJ)=SAREA(MJ)*SF*G/SLEN(MJ)*SO(J)
   60 CONTINUE
      RETURN
      END
```

```
C
C*****************************************************************
C*****************************************************************
      SUBROUTINE RLSHAP(J)
C*****************************************************************
C*****************************************************************
C
C
C*****************************************************************
C***THIS SUBROUTINE CALCULATES NEW BED COORDINATES DUE TO  **
C***FLOW REMOVAL OF MATRIX MATERIAL.  THE COORDINATES WILL **
C***ALSO BE CHANGED BY SIDESLOPE SLOUGHING.                **
C*****************************************************************
C
      COMMON/RLSH/X(10,10),YB(10),Y(10,10),XL(10),XR(10),IL(10)
     X,IR(10),XB(10)
      COMMON/DEPR/DETOTD(10,10,10),DETOTM(10,10,10)
      COMMON/PLOT1/NJ,NR(10),NRR,BD(2),HDDSL
      COMMON/TIMEP/T,DTM,DTS,TS,TRS,TRQ,TR,ITRS
      COMMON/RLLINE/SLO(10,10),YIN(10,10)
      DIMENSION YN(10)
      DO 10 M=1,NRR
      Y3=Y(M,1)
      DO 20 MJ=1,NSEG(J,M)
      L=LAYER(J,M,MJ)
      AREA=DETOTM(J,M,MJ)*DTM*60.*BD(L)
      X1=X(M,MJ)
      X2=X(M,MJ+1)
      X3=X1
      X4=X2
      Y1=Y(M,MJ)
      Y2=Y(M,MJ+1)
      XINT4=SLO(M,MJ)/2.*(X2*X2-X1*X1)+YIN(M,MJ)*(X2-X1)
      Y4=(AREA+XINT4+Y3*(X4-X3)/2.)*2./(X4-X3)
      YN(MJ)=Y4
      Y3=Y4
   20 CONTINUE
      IF(Y4.EQ.Y(M,NSEG(J,M)+1))GOTO15
      DY=(Y(M,NSEG(J,M)+1)-Y4)/NSEG(J,M)
      DO 30 MJ=2,NSEG(J,M)
      YN(MJ)=YN(MJ)+DY
   30 CONTINUE
   15 CONTINUE
      DO 10 MJ=2,NSEG(J,M)
      Y(M,MJ)=YN(MJ)
   10 CONTINUE
      RETURN
      END
```

```
C
C*****************************************************************
C*****************************************************************
      SUBROUTINE SLUFF(J)
C*****************************************************************
C*****************************************************************
C
C
C*****************************************************************
C*** THIS SUBROUTINE CALCULATES THE SEDIMENT CONTRIBUTION **
C*** DUE TO RILL WALL SLOUGHING.  IT ASSUMES THAT THE     **
C*** RILL WALLS HAVE A SET ANGLE, WHICH WHEN EXCEEDED,    **
C*** CAUSES SLOUGHING OF THE RILL WALL DOWN TO A STABLE   **
C*** ANGLE.  THIS SLOUGHED MATERIAL IS TREATED AS         **
C*** DETACHED MATERIAL OF THE SAME PARTICLE MAKEUP AS THE **
C*** MATRIX MATERIAL.                                     **
C*****************************************************************
C
      COMMON/RLSHA/RX(10,10,30),RY(10,10,30),XDL(10,10)
      COMMON/SLUF/XSR(10,10),YSR(10,10),XSL(10,10),YSL(10,10)
      COMMON/RLSH/X(10),YB(10),Y(10),XL(10),XR(10),IL(10)
     X,IR(10),XB(10)
      COMMON/PLOT1/NJ,NR(10),NRR,BD(2),HDDSL
      COMMON/RLLINE/SLO(10,10),YIN(10,10),SLNG(10,10)
      COMMON/RILLPA/IRSD,N(10,10),Z(10,10,10),RWSW(10,10)
     X,LAYER(10,10,10),NSEG(10,10),NSS(10,10,10)
      COMMON/DETR/DETOTD(10,10,10),DETOTM(10,10,10)
      COMMON/SLOUGH/SLOO,SSLO
      DIMENSION XSS(10),SSL(10),YSS(10)
      DO 10 M=1,NR(J)
      NSG=NSEG(J,M)
      DO 20 MJ=1,IL(M)-1
      IF(XSL(M,MJ).EQ.999.999)GOTO15
      ZS=(Y(MJ+1)-Y(MJ))/(X(MJ+1)-X(MJ))
      IF(ZS.GT.SSLO)GOTO15
      GOTO20
   15 CONTINUE
      DO 5 JM=1,MJ
      XCHK=(YIN(M,JM)-YINO)/(SLOO-SLO(M,JM))
      YCHK=SLOO*XCHK+YINO
      IF (XCHK.LT.X(JM))GOTO5
      IF(XCHK.GT.X(JM+1))GOTO5
      IHIGHL=JM
      GOTO7
    5 CONTINUE
      WRITE(*,6)
    6 FORMAT(5X,'SLOUGHING PROBLEM ON LEFT SIDE')
      STOP
      SMASS=0.0
      MJL=MJ
      DO 8 JM=IHIGHL,MJ-1
      ARE=0.5*(SLO(M,JM)-SLOO)*(X(M,JM+1)**2.-X(M,MJ)**2.)+
```

```
     X(YIN(M,JM)-YINO)*(X(M,JM+1)-X(M,JM))
      SMASS=SMASS+ARE*SLINC(J)*BD(LAYER(J,M,JM))
    8 CONTINUE
      DETOTM(J,M,JM)=DETOTM(J,M,JM)+SMASS
   20 CONTINUE
      DO 30 MJ=IR(M)+1,NSS
      IF(XSR(M,MJ).EQ.999.999)GOTO12
      ZS=(Y(M,MJ+1)-Y(M,MJ))/(X(M,MJ+1)-X(M,MJ))
      IF(ZS.GT.SSLO)GOTO31
      GOTO30
   31 CONTINUE
      DO 11 JM=MJ,NSS
      XCHK=(YIN(M,JM)-YINO)/(SLOO-SLO(M,JM))
      YCHK=SLOO*XCHK+YINO
      IF(XCHK.GT.X(M,JM+1)GOTO11
      IF(XCHK.LT.X(M,JM))GOTO11
      GOTO12
   11 CONTINUE
      WRITE(*,13)
   13 FORMAT(5X,'SLOUGHING PROBLEM ON RIGHT SIDE')
      STOP
   12 SMASS=0.0
      MJR=MJ
      DO 14 JM=MJ+3,IHIGHR
      ARE=0.5*(SLO(M,JM-SLOO)*(X(M,JM+1)**2.-X(M,JM)**2.)+
     X(YIN(M,JM)-YINO)*(X(M,JM+1)-X(M,JM))
      SMASS=SMASS+ARE*SLINC(J)*BD(LAYER(J,M,JM))
   14 CONTINUE
      DETOTM(J,M,JM)=DETOTM(J,M,JM)+SMASS
      NSEG(J,M)=NSEG(J,M)-(IHIGHR-MJR)-(MJL-IHIGHL)
   30 CONTINUE
      RETURN
      END
```

APPENDIX V

SEDIMENT ROUTING

COMPONENT LISTINGS

```
C
C*************************************************************
C*************************************************************
      SUBROUTINE SEDROT(J)
C*************************************************************
C*************************************************************
C
      COMMON/PLOT1/NJ,NR(10),NRR,BD(2),HDDSL
      COMMON/SEDPAR/DMM(10),SS(10),FDMM(10),FDMMRD(10),
     XDEP(10,10,10)
      COMMON/TIMEP/T,DTM,DTS,TS,TRS,TRQ,TR,ITRS
      COMMON/PLOT/HPL,PW,SLINC(10),SO(10),SINE(10),COSINE(10)
     X,PCL(2),HLINC(10)
      COMMON/ENVIR/B,TCELS,VK,SF,PI
      COMMON/FLOW/QRILL(10,10),YRILL(10,10),HRRILL(10,10)
     X,PWRILL(10,10),ARILL(10,10,2)
      COMMON/RILLP/IK1(10),IK2(10),IK3(10),K1(10,10),K2(10,10)
     X,K3(10,10)
      COMMON/RADP/PSM,PS3,CC,E1,E2,E3,SSO,RDET(10,10)
      COMMON/RLDP/ARDET(2),BRDET(2),SHEAR(10,10,10),RSH,CSH
     X,DRILL(10,10),EXS,DRR(10)
      COMMON/WATER/RO(10),QRO,QSHEET(10,10),ROP(10)
      COMMON/SHEF/ST(10,10),FCD(10,10,10)
      COMMON/RLSL/QSR(10),QSRILL(10,2,10),RT(10,10),RTR(10)
      COMMON/SHEEF/ISSD,NS(10,10)
      COMMON/RILLPA/IRSD,N(10,10),Z(10,10,10),RWSW(10,10)
     X,LAYER(10,10,10),NSES(10,10),NSS(10,10,10)
      INTEGER DTM
C
C*** CALCULATE SHEET SEDIMENT TRANSPORT
C
      CALL SHEET(J)
C
C*** CALCULATE RILL FLOW SEDIMENT TRANSPORT AND LIMIT BY
C*** SEDIMENT LOAD AND DETACHMENT
C
      CALL RILLTR(J)
      RETURN
      END
```

```
C
C*****************************************************************
C*****************************************************************
      SUBROUTINE SHEET(J)
C*****************************************************************
C*****************************************************************
C
C
C*****************************************************************
C*** THIS SUBROUTINE CALCULATES THE SHEET FLOW AND ITS    **
C*** SEDIMENT LOAD CARRIED TO THE RILLS.  THE TRANSPORT   **
C*** RATE OF EACH SEDIMENT TYPE CAN BE CALCULATED BY THE  **
C*** MODIFIED YALIN OR THE MODIFIED YANG EQUATION AND IS  **
C*** LIMITED BY THE RAINDROP DETACHMENT RATE.             **
C*****************************************************************
C
      COMMON/SHEF/ST(10,10),FCD(10,10,10)
      COMMON/PLOT1/NJ,NR(10),NRR,BD(2),HDDBL
      COMMON/SEDPAR/DMM(10),SB(10),FDMM(10),FDMMRD(10)
     X,DEP(10,10,10)
      COMMON/ENVIR/G,TCELS,VK,SF,PI
      COMMON/PLOT/HPL,PW,BLINC(10),SO(10),SINE(10),COSINE(10)
     X,PCL(2),HLINC(10)
      COMMON/SHEEF/ISSD,NS(10,10)
      COMMON/WATER/RD(10),QRD,QSHEET(10,10),ROP(10)
      COMMON/RADP/PSM,PS3,CC,E1,E2,E3,SSO,RDET(10,10)
      DIMENSION D(10),QSJ(10),QSH(10),SQQ(10),STT(10)
      REAL NS
      SOO=SO(J)/2.
      SSINE=SIN(ATAN(SOO))
      DO 40 M=1,NRR
      QSHEET(J,M)=RD(J)*RWSW(J,M)*HLINC(J)/3600./2.
      YSHEET=(NS(J,M)*QSHEET(J,M)/SQRT(SSINE)*SQRT(3.)/RWSW(J,M))
     X**0.6
      WP=2.*YSHEET+RWSW(J,M)/SQRT(3.)
      QSH(M)=QSHEET(J,M)/1000.
   40 CONTINUE
      DO 50 M=1,NRR
      DO 10 I=1,10
      D(I)=RDET(I,J)/RWSW(J,M)/2.
      QSJ(I)=0.0
      SQQ(I)=0.0
   10 CONTINUE
      IF(ISSD.NE.1)GOTO20
      CALL YANGSE(YSHEET,SSINE,SQQ,D,QSJ,QSH,SOO,NS,STT)
      GOTO30
   20 CALL SEDTRA(YSHEET,SSINE,SQQ,D,QSJ,WP,STT)
   30 CONTINUE
      DO 60 I=1,10
      ST(I,M)=STT(I)
   60 CONTINUE
   50 CONTINUE
```

```
RETURN
END
```

```
C
C*****************************************************************
C*****************************************************************
      SUBROUTINE RILLTR(J)
C*****************************************************************
C*****************************************************************
C
C
C*****************************************************************
C*** THIS SUBROUTINE USES EITHER THE MODIFIED YALIN (1963)**
C*** OR THE MODIFIED YANG (1973) EQUATION FOR RILL        **
C*** SEDIMENT TRANSPORT.  THE TRANSPORT IS LIMITED BY THE **
C*** SEDIMENT DELIVERED TO THE RILL PLUS THE DETACHMENT BY**
C*** FLOW IN THE RILL.                                    **
C*****************************************************************
C
      COMMON/TIMEP/T,DTM,DTS,TS,TRS,TRQ,TR,ITRS
      COMMON/PLOT1/NJ,NR(10),NRR,BD(2),HDDSL
      COMMON/PLOT/HPL,PW,SLINC(10),SD(10),SINE(10),COSINE(10)
     X,PCL(2),HLINC(10)
      COMMON/SHEF/ST(10,10),FCD(10,10,10)
      COMMON/FLOW/QRILL(10,10),YRILL(10,10),HRRILL(10,10)
     X,PWRILL(10,10),ARILL(10,10,2)
      COMMON/RLSL/QSR(10),QSRILL(10,2,10),RT(10,10),RTR(10)
      COMMON/RILLPA/IRSD,N(10,10),Z(10,10,10),RWSW(10,10)
     X,LAYER(10,10,10),NSEB(10,10),NSS(10,10,10)
      COMMON/SEDPAR/DMM(10),SS(10),FDMM(10),FDMMRD(10)
     X,DEP(10,10,10)
      COMMON/ENVIR/G,TCELS,VK,SF,PI
      COMMON/RLDP/ARDET(2),BRDET(2),SHEAR(10,10,10),RSH,CSH
     X,DRILL(10,10),EXS,DRR(10)
      DIMENSION PD(10),SQ(10)
      INTEGER DTM
      SI=SINE(J)
      DO 10 M=1,NRR
      IF(M.EQ.1)GOTO13
      IF(M.EQ.NR(J))GOTO16
      DO 15 I=1,10
      QSR(I)=QSRILL(I,1,M)*K1(J,M)+QSRILL(I,1,M-1)*K2(J,M)
     X+QSRILL(I,1,M+1)*K3(J,M)
      DRR(I)=DRILL(I,M)
      PD(I)=QSR(I)+DRR(I)
      SQ(I)=ST(I,M)
   15 CONTINUE
      GOTO19
   13 DO 14 I=1,10
      DRR(I)=DRILL(I,M)
      QSR(I)=QSRILL(I,1,M)*K1(J,M)+QSRILL(I,1,M+1)*K3(J,M)
      PD(I)=QSR(I)+DRR(I)
      SQ(I)=ST(I,M)
   14 CONTINUE
      GOTO19
```

```
 16 DO 17 I=1,10
    DRR(I)=DRILL(I,M)
    QSR(I)=QSRILL(I,1,M)*K1(J,M)+QSRILL(I,1,M-1)*K2(J,M)
    SQ(I)=ST(I,M)
    PD(I)=QSR(I)+DRR(I)
 17 CONTINUE
 19 QR=QRILL(2,M)
    WP=WPRILL(J,M)
    HRR=HRRILL(J,M)
    IF(IRSD.NE.1)GOTO20
    CALL YANGSE(HRR,SI,QSR,DRR,SQ,QR,SO,N,RTR)
    GOTO30
 20 CALL SEDTRA(HRR,SI,QSR,DRR,SQ,WP,RTR)
 30 CONTINUE
    DO 40 I=1,10
    QSRILL(I,2,M)=QSR(I)
    RT(I,M)=RTR(I)
    DEP(I,J,M)=PD(I)-QSR(I)
 40 CONTINUE
    SFCD=0.0
    DO 100 I=1,10
    SFCD=SFCD+DEP(I,J,M)/SS(I)*3./4./DMM(I)*2.
100 CONTINUE
    FCD(J,M)=SFCD*DTM/10./HLINC(J)/BW(J,M)
    IF(FCD(J,M).GT.1.0)FCD(J,M)=1.0
 10 CONTINUE
    RETURN
    END
```

```
C
C*****************************************************************
C*****************************************************************
      SUBROUTINE SEDTRA(HR,SINE,QS,D,QSJ,WP,TC)
C*****************************************************************
C*****************************************************************
C
C
C*****************************************************************
C*** THIS SUBROUTINE CALCULATES THE SEDIMENT TRANSPORT    **
C*** DUE TO FLOWING WATER USING A MODIFIED YALIN (1963)   **
C*** EQUATION.  THE MODIFICATION INVOLVES DISTRIBUTING    **
C*** THE TRANSPORT CAPACITY BETWEEN DIFFERENT SEDIMENT    **
C*** TYPES.  THE MODIFICATION WAS PRESENTED BY FOSTER AND **
C*** MEYER (1972) AND IS USED IN THE CREAMS MODEL.        **
C*****************************************************************
C
      COMMON/SEDPAR/DMM(10),SS(10),FDMM(10),FDMMRD(10)
     X,DEP(10,10,10)
      COMMON/ENVIR/G,TCELS,VK,SF,PI
      DIMENSION PS(10),DEL(10),BR(10),TC(10),PE(10),WS(10)
      DIMENSION KK(10),LL(10)
      DIMENSION QS(10),D(10),QST(10),QSN(10),QSJ(10)
      TOTTF=0.0
C
C*** ITERATE THROUGH THE TOTAL NUMBER OF SEDIMENT TYPES TO
C*** ACCUMULATE OR CALCULATE ARRAYS FOR BOUNDARY REYNOLDS'
C*** NUMBER, CRITICAL LIFT FORCE, EXCESS DIMENSIONLESS LIFT,
C*** DIMENSIONLESS TRANSPORT, AND TOTAL EXCESS DIMENSIONLESS
C*** LIFT
C
      DO 10 I=1,10
      BR(I)=SQRT(G*HR*SINE)*DMM(I)/10./VK
      YC=YCR(BR(I))
      DEL(I)=HR*SINE/(SS(I)-SF)/DMM(I)/YC*10.-1.
      IF(DEL(I).LT.0.0)DEL(I)=0.0
      SIG=2.45*YC**0.5/SS(I)**0.4*DEL(I)
      IF(SIG.LE.0.0)GOTO15
      PS(I)=0.635*DEL(I)*(1.-ALOG(1.+SIG)/SIG)
      GOTO17
   15 PS(I)=0.0
   17 CONTINUE
      TOTTF=TOTTF+DEL(I)
   10 CONTINUE
      SMUS=0.0
C
C*** ITERATE THROUGH THE TOTAL NUMBER OF SEDIMENT TYPES TO
C*** ACCUMULATE OR CALCULATE ARRAYS FOR INDIVIDUAL
C*** DIMENSIONLESS TRANSPORT, INDIVIDUAL TRANSPORT CAPACITY,
C*** INDIVIDUAL SEDIMENT LOAD, AND REQUIRED TRANSPORT
C*** CAPACITY FRACTION
C
```

```
      DO 20 I=1,10
      PE(I)=PS(I)*DEL(I)/TOTTF
      WS(I)=PE(I)*SS(I)*SF*BR(I)*VK*WP
      QSN(I)=QS(I)+D(I)+QSJ(I)
      QST(I)=QSN(I)
      IF(PS(I).LE.0.0)GOTO20
      SMUS=SMUS+PE(I)/PS(I)
   20 CONTINUE
   30 SPT=0.0
      SDLT=0.0
C
C*** ITERATE THROUGH THE TOTAL NUMBER OF SEDIMENT TYPES TO
C*** CALCULATE THE EXCESS AND INSUFFICIENT TRANSPORT FOR
C*** EACH SEDIMENT TYPE.  SET FLAGS FOR NEEDS.
C
      DO 50 I=1,10
      KK(I)=0
      LL(I)=0
      IF(WS(I).GE.QST(I))KK(I)=1
      IF(WS(I).LT.QST(I))LL(I)=1
      IF(WS(I).LE.0.0)GOTO55
      SPT=SPT+QST(I)/WS(I)*KK(I)
   55 CONTINUE
      SDLT=SDLT+DEL(I)*LL(I)
   50 CONTINUE
      EXC=1.-SPT
      KI=0
      KJ=2
C
C*** ITERATE THROUGH THE TOTAL NUMBER OF SEDIMENT TYPES TO
C*** REDISTRIBUTE THE SEDIMENT TRANSPORT CAPACITY FROM THE
C*** TYPES THAT HAVE SUFFICIENT CAPACITY TO THOSE THAT
C*** REQUIRE MORE CAPACITY
C
      DO 40 I=1,10
      IF(LL(I).EQ.0)GOTO45
      IF(SDLT.LE.0.0)GOTO43
      TC(I)=DEL(I)/SDLT*EXC*PS(I)*SS(I)*SF*BR(I)*LL(I)
      GOTO44
   43 TC(I)=0.0
   44 CONTINUE
      IF(KK(I).EQ.0)GOTO47
   45 TC(I)=QST(I)*KK(I)
   47 CONTINUE
C
C*** CHECK FOR EQUILIBRIUM CONDITIONS (ALL FULFILLED OR ALL
C*** REQUIRING MORE CAPACITY AND SEND BACK THROUGH IF NEEDED
C
      IF(TC(I).GT.QST(I))KI=1
      IF(TC(I).LT.QST(I))KJ=1
      QST(I)=TC(I)
   40 CONTINUE
```

```
      IF(KI.EQ.KJ)GOTO30
      IF(KI.EQ.0)GOTO70
C
C*** IF ONE TYPE HAS ALL THE EXCESS TRANSPORT, LINEARLY
C*** DISTRIBUTE THE EXCESS AMONG ALL TYPES
C
      DO 60 I=1,10
      TC(I)=QST(I)/SMUS
   60 CONTINUE
   70 CONTINUE
C
C*** LIMIT TRANSPORT BY DETACHMENT AND DELIVERED LOAD
C*** AND INPUT TO THE ARRAY FOR OUTPUT TO THE MAIN PROGRAM
C
      DO 80 I=1,10
      QS(I)=TC(I)
      IF(TC(I).GT.QSN(I))QS(I)=QSN(I)
   80 CONTINUE
      RETURN
      END
C
C*****************************************************************
      FUNCTION YCR(R)
C*****************************************************************
C
C*** LINE SEGMENT REPRESENTATION OF MODIFIED SHIELD DIAGRAM
C
      IF(R.LT.1.0)Y=0.1/R**0.3
      IF(R.GE.1.0)Y=0.1/R**0.5
      IF(R.GE.10.8)Y=0.02*R**0.177
      IF(R.GE.120.)Y=0.047
      YCR=Y
      RETURN
      END
```

```
C
C*************************************************************
C*************************************************************
      SUBROUTINE YANGSE(HR,SINE,QS,D,QSJ,Q,SD,N,QT)
C*************************************************************
C*************************************************************
C
C
C*************************************************************
C*** THIS SUBROUTINE UTILIZES A MODIFIED YANG (1973)      **
C*** EQUATION TO CALCULATE THE SEDIMENT TRANSPORT DUE TO  **
C*** FLOWING WATER. THE MODIFICATION INVOLVES DISTRIBUTING**
C*** THE SEDIMENT TRANSPORT ASSUMING AN AVERAGE SEDIMENT  **
C*** TO CALCULATE THE TOTAL TRANSPORT AND THEN DISTRIBUT- **
C*** ING ACCORDING TO INDIVIDUAL SEDIMENT TYPE TRANSPORT  **
C*** AND AVAILABILITY.                                    **
C*************************************************************
C
      COMMON/ENVIR/G,TCELS,VK,SF,PI
      COMMON/SEDPAR/DMM(10),SS(10),FDMM(10),FDMMRD(10)
     X,DEP(10,10,10)
      REAL N
      DIMENSION QS(10),D(10),QSJ(10),C(10)
      DIMENSION CE(10),QT(10),QST(10),ICE(10)
      VS=G*HR*SINE
      STOT=0.0
      DTOT=0.0
      QSTOT=0.0
      CTOT=0.0
      V=1/N*(HR/100.)**(2./3.)*SINE**0.5*100.
C
C*** ITERATE THROUGH ALL SEDIMENT TYPES TO DEVELOP AVERAGE
C*** CHARACTERISTICS AND TO CALCULATE SEDIMENT CONCENTRATION
C*** RATIOS OF EACH TYPE RELATIVE TO TOTAL
C
      DO 10 I=1,10
      QST(I)=QS(I)+D(I)+QSJ(I)
      QSTOT=QSTOT+QST(I)
      DTOT=DTOT+QST(I)*DMM(I)
      STOT=STOT+QST(I)*SS(I)
      VF=DMM(I)**2.*(SS(I)-SF)/1800./VK
      RF=VF*DMM(I)/10./VK
      RS=VS*DMM(I)/10./VK
      VCR=(2.5/(ALOG10(RS)-0.06)+0.66)*VF
      IF(RS.LT.1.2)VCR=150.*VF
      IF(RS.GE.70.)VCR=2.05*VF
   30 CONTINUE
      CE(I)=10.**(5.435-0.286*ALOG10(RF)-0.457*ALOG10(VS/VF)
     X+(1.799-0.409*ALOG10(RF)-0.314*ALOG10(VS/VF))*(ALOG10(
     X(V-VCR)*SD/VF)))
      CTOT=CTOT+CE(I)
      ICE(I)=I
```

```
   10 CONTINUE
C
C*** SORT SUBSCRIPTS ACCORDING TO CE (DESCENDING ORDER)
C
      DO 15 I=1,9
      IN=10-I
      DO 17 IK=1,IN
      IF(CE(IK).GT.CE(IK+1))GOTO17
      IEC=ICE(IK)
      ICE(IK)=ICE(IK+1)
      ICE(IK+1)=IEC
   17 CONTINUE
   15 CONTINUE
C
C*** DETERMINE TOTAL TRANSPORT ASSUMING AVERAGE PROPERTIES
C
      IF(QSTOT.EQ.0.0)GOTO100
      D50=DTOT/QSTOT
      S50=STOT/QSTOT
      VF50=D50*D50*(S50-SF)/1800./VK
      RF50=VF50*D50/10./VK
      RS50=VS*D50/10./VK
      VC50=(2.5/(ALOG10(RS50)-0.06)+0.66)*VF50
      IF(RS50.LT.1.2)VC50=150.*VF50
      IF(RS50.GE.70.)VC50=2.05*VF50
   80 CONTINUE
      C50=10.**(5.435-0.286*ALOG10(RF50)-0.457*ALOG10(VS/VF5
     X0)+(1.799-0.409*ALOG10(RF50)-0.314*ALOG10(VS/VF50))*(A
     XLOG10((V-VC50)*80/VF50)))
      Q50=C50*Q*60./1000.*SF
      QSLEFT=Q50
C
C*** ITERATE THROUGH TOTAL NUMBER OF SEDIMENT TYPES,
C*** DISTRIBUTING THE TRANSPORT CAPACITY BASED UPON
C*** CONCENTRATION RATIOS AND LIMIT TRANSPORT BY DETACHMENT
C*** AND DELIVERED SEDIMENT LOAD
C
      DO 90 II=1,10
      I=ICE(II)
      C(I)=CE(I)/CTOT*C50
      QT(I)=Q*C(I)*SF*60./1000.
      QS(I)=QT(I)
      IF(QT(I).GT.QST(I))QS(I)=QST(I)
      IF(QSLEFT.EQ.0.0)QS(I)=0.0
      IF(QSLEFT.LT.QS(I))GOTO140
      QSLEFT=QSLEFT-QS(I)
      GOTO90
  140 QS(I)=QSLEFT
      QSLEFT=0.0
   90 CONTINUE
      GOTO110
  100 WRITE(6,1)
```

```
  1 FORMAT(' **** NO SEDIMENT IN FLOW ****')
    DO 105 I=1,10
    QS(I)=0.0
105 CONTINUE
110 CONTINUE
    RETURN
    END
```